

**REPUBLIC OF TURKEY
MUĞLA SITKI KOÇMAN UNIVERSITY
GRADUATE SCHOOL OF
NATURAL AND APPLIED SCIENCES**

DEPARTMENT OF GEOLOGICAL ENGINEERING



**TECTONIC GEOMORPHOLOGY OF
MUĞLA-YATAĞAN REGION**

MASTER OF SCIENCE

ORKUN TÜRE

MAY 2017

MUĞLA

**REPUBLIC OF TURKEY
MUĞLA SITKI KOÇMAN UNIVERSITY
GRADUATE SCHOOL OF
NATURAL AND APPLIED SCIENCES**

DEPARTMENT OF GEOLOGICAL ENGINEERING



**TECTONIC GEOMORPHOLOGY OF
MUĞLA-YATAĞAN REGION**

MASTER OF SCIENCE

ORKUN TÜRE

**MAY 2017
MUĞLA**

MUGLA SITKI KOÇMAN UNIVERSITY
Graduate School of Natural and Applied Sciences

APPROVAL OF THE THESIS

The thesis submitted by **ORKUN TÜRE** with the title of “**TECTONIC GEOMORPHOLOGY OF MUĞLA-YATAĞAN REGION**” has been unanimously accepted by jury members on the 16th of May, 2017 to fulfil the requirements for degree of Master of Science in the Department of Geological Engineering.

THESIS JURY MEMBERS

Prof. Dr. Murat GÜL (**Head of Jury**)
Department of Geological Engineering,
Muğla Sıtkı Koçman University, Muğla

Signature:



Assist. Prof. Dr. Murat Ersen AKSOY (**Supervisor**)
Department of Geological Engineering,
Muğla Sıtkı Koçman University, Muğla

Signature:



Assist. Prof. Dr. Gülsen Uçarkuş (**Member**)
Department of Geological Engineering,
İstanbul Technical University, İstanbul

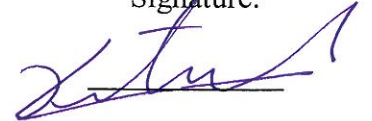
Signature:



APPROVAL OF THE HEAD OF THE DEPARTMENT

Assist. Prof. Dr. Bedri KURTULUŞ
Head of Department, Geological Engineering,
Muğla Sıtkı Koçman University, Muğla

Signature:



Assist. Prof. Dr. Murat Ersen AKSOY

Signature:

Supervisor, Department of Geological Engineering,
Muğla Sıtkı Koçman University, Muğla



Date of Defence: 16/05/2017

I hereby declare that all information in this document has been obtained and presented in accordance with academic rules and ethical conduct. I also declare that as required by these rules and conduct. I declare that I have fully cited and referenced all material and results that are not original to this work.

Orkun TÜRE

16/05/2017



ABSTRACT
TECTONIC GEOMORPHOLOGY OF MUĞLA-YATAĞAN REGION

Orkun TÜRE

Master of Science (M.Sc.)

Graduate School of Natural and Applied Sciences

Department of Geological Engineering

Supervisor: Assist. Prof. Dr. M. Ersen AKSOY

May 2017, 132 pages

South Western Anatolia is seismically one of the most active regions in the world. While the Anatolian plate migrates westwards due to the collision of the Arabian plate with Anatolia, the western part of Anatolia experiences N-S extension caused by the pulling effect of the Hellenic subduction zone. Several E-W trending grabens are formed within this extensional tectonic setting. The Muğla-Yatağan region is located at the southern part of SW Anatolia between Menderes graben and Gökova graben.

The seismic history of the region marks several damaging earthquakes with destructive intensities. The study area consists of two large basins; The Yatağan basin and the Muğla basin. Both basins show different geomorphic characteristics at their southern and northern boundaries. While the one side exposes a well-developed old morphology; the opposite side is significantly higher and forms distinct steep slopes indicating young morphology typical of half graben systems. The normal faults are exposed along the slopes and form iron flats. Stream channels show wine glass channel profiles indicating recent tectonic uplift. The hanging valleys and iron flats are clear markers of recent tectonic movement. Despite the numerous amount of Quaternary outcrops only two localities showed evidence of recent faulting.

The analysis of four geomorphic indices yield results that signify the ongoing tectonic activity in the region. The low Vf values (< 0.4) mark V-shaped valleys at proximal to the faults which turn to U-shape valleys away from the fault. Hypsometric curves point moderate to young drainage basins that are influenced of tectonic uplift. The peaks in the SL indices are directly linked with fault escarpments observed in the field. AF analysis yield no specific pattern of tectonic tilting in the area.

Using the seismic moment and moment magnitude scale of Hanks and Kanamori (1979) it has been calculated that the Muğla-Yatağan region prone to earthquakes M

5.7 to 6.6 assuming 6 km fault width, 25-55 km fault length and 10-80 cm average displacement.

As a result of these observations Muğla-Yatağan fault zone is an active fault zone. It controls the morphology of SW margin of Yatağan Basin and NE margin of Muğla Basin. Yatağan coal power plant, quarries, other industrial activities and settlements are located close to the fault, therefore further analysis on the seismic hazard are essential.

Key words: Morphometric Analyses, Morphology, Muğla-Yatağan Fault Zone.



ÖZET

MUĞLA-YATAĞAN CİVARININ TEKTONİK JEOMORFOLOJİSİ

Orkun TÜRE

Yüksek Lisans Tezi

Fen Bilimleri Enstitüsü

Jeoloji Mühendisliği Anabilim Dalı

Danışman: Yrd. Doç. Dr. M. Ersen AKSOY

Mayıs 2017, 132 sayfa

Güneybatı Anadolu tektonizma bakımından dünyanın en aktif bölgelerinden biridir. Anadolu plakası, Arap ve Anadolu plakalarının çarpışması sonucu batıya hareket ederken, Helenik yayın çekmesinden dolayı Batı Anadolu Kuzey – Güney yönlü gerilmeye maruz kalmaktadır. Bu bölgede gerilmeye dayalı olarak birçok Doğu – Batı doğrultulu grabenler oluşmuştur. Muğla – Yatağan bölgesi Güneybatı Anadolu'nun Güneyinde, Menderes Grabeni ile Gökova Grabeni arasında kalmaktadır.

Bölgenin tarihsel deprem geçmişi bölgede birçok hasara yol açan şiddetli depremlerin varlığını göstermektedir. Bölge Yatağan ve Muğla olmak üzere 2 büyük havzadan oluşmaktadır. Her iki havza da kuzey ve güney sınırlarında farklı özellikler göstermektedir. Havzaların bir tarafı iyi gelişmiş, yaşlı morfolojiye sahipken, diğer sınırı daha genç morfolojiyi gösteren sarplıklardan oluşmaktadır ve yarı-graben özelliği taşımaktadır. Sınırlar boyunca yüzeylenen faylar üçgen yapıları oluşturmaktadır. Dereler güncel tektonizmaya işaret eden şarap kadehi şekillerini göstermektedir. Asılı vadiler ve ütü altı yapıları güncel tektonizmanın işaretçileridir. Birçok Kuvaterner çökel olmasına rağmen bu güncel çökeller içinde sadece iki bölgede güncel faylanmanın izleri gözlemlenebilmiştir. Dört jeomorfik indis analizlerinin sonuçları devam eden bir tektonik aktiviteye işaret etmektedir. $V_f < 0.4$ değerleri faya yakın yerlerde V-şekilli, ve faydan uzaklaştıkça U-şekilli vadiye dönen vadilere işaret etmektedir. Hipsometrik eğriler tektonizmadan etkilenen olgun-geç havzalar olduğunu işaret etmektedir. SL değerlerindeki ani artışlar doğrudan arazide tespit edilmiş fay sarplıklarına karşılık gelmektedir. AF değerleri herhangi bir tektonik eğimlenme belirtisi göstermemektedir.

Muğla – Yatağan fayının bölgede $M=5.7$ ile 6.6 büyüklüğünde depremler üretebileceği hesaplanmıştır. Bu sonuca Hank ve Kanamori (1979)'a sismik moment ve moment büyüklük hesabı kullanarak varılmıştır ve fay parametreleri fay derinliği 6 km, fay uzunluğu 25-55 km ve ortalama atım 10 – 80 cm olarak alınmıştır.

Sonuç olarak Muğla-Yatağan fay zonu aktif bir fay zonudur. Yatağan Havzasının Güneybatı sınırının ve Muğla Havzasının Kuzeydoğu sınırının morfolojisini kontrol

etmektedir. Yatađan termik santrali, kmr iřletmesi, maden ocakları ve diđer endriyel aktivitelerin ve yerleřim yerlerinin faya yakın olmalarından dolayı blgenin deprem tehlikesinin daha fazla arařtırılması gerekmektedir.

Anahtar Kelimeler: Morfometrik Analiz, Morfoloji, Muđla-Yatađan Fay Zonu





To My Family

ACKNOWLEDGEMENT

I wish to express my sincere gratitude to my supervisor Assistant Prof. Dr. Murat Ersen AKSOY for providing me the opportunity to complete my Master of Science and his supports with endless patients.

I should not forget to mention the help and guidance of my friends Özlem YILMAZ, and Mehmet ÇAM.

I am also grateful to my father Mevlüt, mother Hülya and brother Onurhan who patiently helped me during my bad and good times while I was preparing my MSc. Thesis.



TABLE OF CONTENTS

1. INTRODUCTION	23
1.1. Previous Studies	24
2. METHODOLOGY	32
2.1. The Physics of Earthquake	32
2.1.1. The rupture process and earthquake occurrence	32
2.1.2. Magnitude of an earthquake that normal faults produce; seismic moment and magnitude.....	34
2.2. Active Faulting, Fault Geometry, Faulting Behaviour and Segmentation ..	34
2.2.1. Active faulting.....	34
2.2.2. Faulting behavior, fault geometry and segmentation.....	35
2.3. Geomorphic Approach	37
2.3.1. Hypsometric curve and hypsometric integral (HI).....	37
2.3.2. Drainage basin asymmetry (AF)	38
2.3.3. Stream length-gradient index (SL index).....	39
2.3.4. Mountain front sinuosity (S_{mf})	39
2.3.5. Valley floor width to height ratio (V_f)	40
2.4. Case Studies	41
3. SEISMOTECTONIC BACKGROUND OF THE REGION	45
3.1. Historical Seismicity of Muğla region	49
3.2. Recent Seismicity of SW Anatolian and Muğla Region.	52
4. ACTIVE TECTONICS, GEOMORPHOLOGY OF THE MUĞLA – YATAĞAN REGION	57
4.1. Introduction	57
4.2. Geological Overview.....	57
4.2.1. Regional geology of Southwestern Anatolia.....	57
4.2.2. Local geology.....	58
4.2.2.1. <i>Kavaklıdere group</i>	58
4.2.2.2. <i>Marçal group</i>	58
4.2.2.3. <i>Ören unit</i>	58
4.2.2.4. <i>Akçay Group</i>	59

4.2.2.5. <i>Muğla Group</i>	59
4.3. Morphologic Framework of the Muğla–Yatağan Region	62
5. MORPHOMETRIC ANALYSIS	76
6. CONCLUSION	121



LIST OF TABLES

Table 2.1. Active fault classification of California State Mining and Geology Board (1973).....	35
Table 2.2. Fault segment types and their characteristics (McCalpin, 1996; Aksoy, 2009)	36
Table 2.3. Summary of the morphometric analyses with schematic, verbal explanations and mathematical formulas.....	43
Table 3.1. List of historical earthquakes at the Muğla region (study area). (Compiled from Tan et. al., 2008). There are 22 records of earthquakes. (Before the establishment of World Wide Standard Seismographic Network (WWSSN)	50

LIST OF FIGURES

Figure 1.1. Schematic illustration of the locations and orientations of some of the Grabens. Yatağan and Ören Grabens formed as cross Grabens (Gürer&Yılmaz, 2002).....	26
Figure 1.2. Active fault map of the area (Karabacak, 2015) with instrumental earthquakes. He has concluded that the Muğla Fault has dextral component according to the fault parallel profiles.....	29
Figure 1.3. Active fault map of MTA. (Obtained from Geoscience Map Viewer and Drawing Editor)	29
Figure 1.4. a) Earthquake occurrence number-time graphic shows anomaly between 08:00 and 15:00 because of blasting operations and b) magnitude-earthquake occurrence graphic shows anomaly at M=3.	30
Figure 2.2. Principle stress directions for normal faults. The maximum principle stress σ_1 is linked with gravity. Normal faults generally dip with 60° (Anderson, 1942).....	33
Figure 2. 3. Illustration of normal faulting and geometric features of normal faults (Peacock et. al., 2000).....	36
Figure 2. 4. Point based calculation of hypsometric curve. Hypsometric curve is plot of relative area to relative height. (Keller & Pinter, 1996).	38
Figure 2. 5. Block diagram showing left tilted (downstream left) basin (Keller&Pinter, 1996). Right side of basin is elevated much more relative to the left side of the basin.	38
Figure 2. 6. Stream length-gradient index (Hack's index) measurement. Index is defined in terms of the slope and length as their multiplication. Length is the distance of the mid point of the portion that is going to measured to the source of the drainage.	39
Figure 2. 7. Components of the mountain front sinuosity index. Lmf is the true length of the mountain front and Ls is the straight length of the mountain front.40	40
Figure 2. 8. Schematic illustration showing the calculation of valley floor width to height ration values.	41
Figure 3. 1. Seismic hazard potentials of European countries are compared in terms of Peak Ground Acceleration (PGA). Areas with comparatively low PGA values and so low seismic hazard values are coloured with green. Yellow coloured areas have moderate and red coloured areas have high seismic	

hazard values. Turkey has high PGA and so high seismic hazard values. The highest values are observed along active plate boundaries including North Anatolian Fault Zone and Eastern Anatolian Fault Zone. These are followed by Western Anatolian Extensional Province (Giardini, D., et al., 2013).	45
Figure 3. 2. Active plate boundaries of Turkey. Northward motion of Arabian plate and its subduction beneath Anatolian plate is resulted in the westward extrusion (counterclockwise rotation) of Anatolian plate along East Anatolian Fault and North Anatolian Fault, (Okay et. al., 1999).	46
Figure 3. 3. Location map of the study area with active faults of SW Anatolia. Study area is located obliquely to major large E-W trending Büyük Menderes Graben and Gökova Fault Zone.	47
Figure 3. 4. Local map of the study area. Muğla-Yatağan Fault Zone is oblique to Gökova Fault Zone. Muğla-Yatağan Fault zone extending from Yatağan to Yaraş, bounding Yatağan basin from its SW margin and Muğla basin from its NE margin and Muğla Fault Zone is highly segmented. Yatağan Fault is close to Yatağan coal power plant. Fault data from (Gen. Dir. of Min. Res. and Exp.)	48
Figure 3. 5. GPS horizontal velocity field of Turkey and surrounding regions in a Eurasia-fixed frame (Reilinger et. al., 2006).....	49
Figure 3. 6. Historical seismicity map of the study area. 22 Earthquakes have been recorded in this period. Four of them have magnitudes greater than M=6. Earthquakes M=6 have been located as red stars. There is no earthquake record linked with Yatağan Fault because these data are collected before the establishment of World Wide Standard Seismographic Network (WWSSN).	51
Figure 3. 7. Spatial distribution of earthquake records in SW Anatolia after 1963AD with seismic stations.	52
Figure 3. 8. Histogram of earthquake events for 24 hours time interval in a day. Between 06:00 and 16:00 number of events show peaks.	53
Figure 3. 9. Earthquake distributions below M=3.5.	53
Figure 3. 10. After earthquake crack on the road of Kavakçalı village.	54
Figure 3. 11. Seismicity map of Kavakçalı region with earthquake records, focal mechanism of M=5 Kavakçalı earthquake and entry table of focal mechanism solution. Earthquake records comprise the latest 30 days and this implies that there is high seismic activity in the region.	55

- Figure 3.12. Recent seismicity map of the study area. Number of earthquake records have been increased dramatically after 1963 after the establishment of World Wide Standard Seismographic Network (WWSSN). 5 Large earthquakes have been recorded after 1963. These large earthquakes have been shown on the map as red stars. Blue circle indicates the cluster of earthquake records in front of Bahçeyaka fault after the elimination of data. Black circle is the cluster of records behind the Bahçeyaka fault which are related with blasting in the quarry. 56
- Figure 4. 1. Generalized columnar section of the study area (modified from Gürer et. al., 2011)..... 60
- Figure 4. 2. Geological map of the study area (Modified from Gürer&Yılmaz, 2002). 61
- Figure 4. 3. Schematic illustration of the Muğla plain with satellite image basemap. Muğla basin is a triangular shaped plain which is bounded by NW-SE, E-W trending S dipping normal faults to the Yılanlıdağ straight. Northern margin is characterized by steep slopes, topographic limestone escarpments and fault related alluvial fan deposits transported via large streams flowing N to S which covers the alluvium of Muğla plain. Blue lines with arrows indicate the drainage network with flow direction, black lines indicate transportation of sediments via drainages forming alluvial fan coverin the alluvium of Muğla basin. Red lines indicate the active normal faults of the area..... 63
- Figure 4. 4. Faulting is traced by the change in topography-small hills near Gölcük village..... 63
- Figure 4. 5. Schematic illustration of the Yaraş section with satellite image basemap. Northern margin is characterized by steep slopes, topographic limestone escarpments and fault related alluvial fan deposits transported via large streams flowing N to S which covers the alluvium of Muğla plain. Blue lines with arrows indicate the drainage network with flow direction, black lines indicate transportation of sediments via drainages forming alluvial fan coverin the alluvium of Muğla basin. Red lines indicate the active normal faults of the area. Black rectangle shows the location of Figure 4.6. 64
- Figure 4. 6. The lowermost segment of Muğla Fault Zone near Yaraş village. Fault strikes with 130° and dips with 50° South. Fault plane is limestone and flow marks are observed on the fault plane. Slickenlines are not observable. 65

- Figure 4. 7. Schematic illustration of Muğla basin where it bounds to Yılanlıdağ straight from its Northern margin. Triangular shaped flat-iron is observed in the limestone fault plane formed by the progressive effects of both erosion and tectonic uplift. Fault related alluvial fans are observed in front of the basin margin fault. 65
- Figure 4. 8. Schematic illustration of Düğerek region with satellite image basemap. Düğerek is located on alluvial fan which is formed because of tectonic uplift in the area. Fault is covered by colluviums at the western part of region and covered fault is showed with dashed line 66
- Figure 4. 9. Fault planes of Muğla Fault near Düğerek village are shown in this Figure. Slikenlines and ondulations are clear in Figure 4.16 a and b. Figure 4.16 a. fault breccias are seen..... 67
- Figure 4. 10. Düğerek basin margin fault is not completely linear fault and its strike changes. Different slip directions measured for two different strike values. Red lines indicating the Düğerek fault..... 67
- Figure 4. 11. Schematic illustration of the hanging valleys and iron flats (dashed surfaces) near Düğerek district. Tectonic processes prevail against the surface processes and the morphology is shaped by tectonic processes... 68
- Figure 4. 12. Schematic illustration of Muğla plain. Muğla plain is fed by large streams at the Northern margin of the basin and because of tectonic uplift sediments deposited as alluvial fan. There is a fault controlled single limestone hill in the middle of the basin. 68
- Figure 4. 13. Menteşe region is a highly-segmented part of Muğla fault zone. In the parts of segmentation relay ramps formed. Black boxes with the 1 and 2 numbers are relay ramps. Black line indicates the line of cross section... 69
- Figure 4. 14. a) Bird view satellite image with geological units (Satellite image obtained from Bing maps). Locations of the photographs have been shown in Figure 4.6 a. b) Hanging valley is observed at the Major Menteşe fault. This indicates that tectonic processes prevail against the surface processes in this region. c) Young deposits have been tilted towards the fault. d) 50cm downthrown observed in the colluviums. This is a normal fault which is seen as reverse fault because of the direction of trench's wall. Gray shaded parts in Figure 4.6 c. and d. are waste deposits and the soil cover..... 70
- Figure 4. 15. Cross section of the Menteşe region. There are lots of fault sets in the area. Menteşe part of the cross section is the location mentioned in Figure 4.6 c and d. 70

- Figure 4. 16. Photograph of one of the faults mentioned in the Figure 4.7. a) Whole view of the fault b) photograph of the fault surface..... 71
- Figure 4. 17. Schematic illustration of Paşapınarı fault and related flat-irons, hanging valleys and fault controlled alluvial fan. Older long stream at the right side forms a windgap. Flat-irons are either in the form of triangular or trapezoidal shapes. Basin margin fault bounds recrystallized limestone of Menderes Massif and alluviums of Paşapınarı basin. 72
- Figure 4. 18. Schematic illustration of the Paşapınarı part of Yatağan fault. SW margin of the basin is bounded by faults and resulted in the formation of hanging valleys and alluvial fan deposits. No deformation has been observed on the colluvium and alluvial fan deposits at this region. 72
- Figure 4. 19. Bahçeyaka fault plane. Narrow and high colluvial fan and hanging valleys are the indicator of a continuous uplift in the area. Ondulations on the fault plane showing a right lateral component. 73
- Figure 4. 20. Şahinler region of the Yatağan fault. Fault plane is not observable but the faulting morphology is covered..... 74
- Figure 5. 1. Overall view of the drainage basins and calculated asymmetries at the fault generated mountain fronts at the Muğla Polje. Muğla region is simply characterized by NW-SE trending Muğla-Yaraş and Yılanlıdağ segments. Green colored arrows indicate the basins in which there is no observed asymmetry. Yellow arrow indicate downstream right side asymmetry and white arrow used for downstream left side asymmetry..... 76
- Figure 5. 2. Morphometric analyses results of basin M1. Vf values indicate V-shaped valleys. Hypsometric curve indicates young a basin morphology influenced by tectonic processes. Hack's stream gradient index indicates that faults are active. AF values do not show any asymmetry in the overall of the basin. Middle block shows asymmetry individually. 77
- Figure 5. 3. Morphometric analyses of basin M2. Decreasing Vf values from source to mouth indicate increase in the effect of tectonic activity towards mouth. Hypsometric curve indicates that basin is young and is influenced by tectonic processes. Hack's stream gradient index indicates that faults are active. AF value shows asymmetry towards the downstream left side that may be related with tectonic tilting..... 79
- Figure 5. 4. Morphometric analyses of basin M3. Moderate Vf values indicate transition from young phase to old phase. Hypsometric curve shows transition from young-phase to old-phase. Hack's stream gradient index indicates that faults are active. AF value does not show asymmetry..... 81

- Figure 5. 5. Morphometric analyses of basin M4. Moderate and high Vf values indicate transition from V-shaped valley to U-shaped valley from mouth to source. Hypsometric curve shows transition from young-phase to mature-phase. Hack's stream gradient index indicates that faults are active. AF value shows asymmetry towards downstream right side of the basin. 83
- Figure 5. 6. Morphometric analyses of basin M5. Low Vf values indicate that valley is V-shaped. Hypsometric curve shows a perfect mature basin. Hack's stream gradient index indicates that the fault is active. AF value does not show asymmetry but the middle block shows asymmetry towards downstream left side of the basin individually. 85
- Figure 5. 7. Morphometric analyses of basin M6. Low Vf values indicate that valley is V-shaped. Hypsometric curve shows transition from young phase to mature phase. Hack's stream gradient index indicates that the fault is active. AF value does not show asymmetry but the lowermost block shows asymmetry towards downstream left side of the basin individually which may be the sign of tilting. 87
- Figure 5. 8. Morphometric analyses of basin M7. Low Vf values indicate valley is V-shaped. Hypsometric curve reflects young basin. Hack's stream gradient index indicates that the faults are active. AF value does not show asymmetry in the overall but the uppermost block shows asymmetry towards downstream right side and the bottom 3 blocks show asymmetry towards downstream left side of the basin because faults collect all small drainages to a single branch. 89
- Figure 5. 9. Morphometric analyses of basin M8. Low Vf values indicate valley is V-shaped through the mouth of the basin. Hypsometric curve reflects mature basin. Hack's stream gradient index indicates that the fault is active. AF value does not show asymmetry in the basin. 91
- Figure 5. 10. Morphometric analyses of basin M9. Low Vf values indicate valley is V-shaped through the mouth of the basin and U-shaped through the source. Hypsometric curve reflects young basin. Hack's stream gradient index indicates that the faults are active. AF value shows asymmetry towards downstream left side of the basin. 92
- Figure 5. 11. Morphometric analyses of basin M10. Low Vf value at the mouth indicate V-shaped profile and high Vf values through the top reflects U-shaped profile. Hypsometric curve reflects mature basin. Hack's stream gradient index indicates that the fault is active. AF value does not show asymmetry. 94

Figure 5. 12. Overall view of the basins in Yatağan depression. Green arrows are used for basins which do not show asymmetry, red arrows are used for basins show downstream right side asymmetry and yellow arrows are used to describe basin with downstream left side asymmetry.....	95
Figure 5. 13. Morphometric analysis of basin Y1. AF value does not show asymmetry. Vf values indicate valley is U-shaped. Hypsometric curve shows a mature basin. Hack's stream gradient index indicate that fault is active.	96
Figure 5. 14. Morphometric analysis of basin Y2. AF value does not show asymmetry. Vf values indicate that valley is V-shaped. Hypsometric curve shows that basin is young. Hack's stream gradient index indicate that fault is active.	97
Figure 5. 15. Morphometric analysis of basin Y3. AF value shows asymmetry towards downstream right side of the basin. Vf values indicate that valley is V-shaped. Hypsometric curve shows that basin is young. Hack's stream gradient index indicate that fault is active.	99
Figure 5. 16. Morphometric analysis of basin Y4. AF value shows asymmetry towards downstream right side of the basin. Vf values indicate that valley is V-shaped. Hypsometric curve shows that basin is young. Hack's stream gradient index indicate that faults are active.....	100
Figure 5. 17. Vf values indicate that valley is V-shaped. AF value shows asymmetry towards downstream left side of the basin. Hypsometric curve indicates that basin is young. Hack's stream gradient index implies that the fault is active.	102
Figure 5. 18. Vf values indicate that valley is V-shaped. AF value shows asymmetry towards downstream left side of the basin. Hypsometric curve indicates that basin is old.	103
Figure 5. 19. Vf values indicate that valley is V-shaped. AF value shows asymmetry towards downstream left side of the basin. Hypsometric curve indicates that basin is young. Hack's stream gradient index implies that the fault is active.	104
Figure 5. 20. Vf values indicate that valley is V-shaped. AF value does not show asymmetry. Hypsometric curve indicates that basin is young. Hack's stream gradient index implies that the fault is active.....	106
Figure 5. 21. Vf values indicate that valley is V-shaped. AF value does not show asymmetry. Hypsometric curve indicates that basin is mature. Hack's stream gradient index implies that the fault is active.....	107

Figure 5. 22. Vf values indicate that valley is V-shaped. AF value does not show asymmetry. Hypsometric curve indicates that basin is mature.	109
Figure 5. 23. Vf values indicate that valley is V-shaped. AF value does not show asymmetry. Hypsometric curve indicates that basin is old.	110
Figure 5. 24. Vf values indicate that valley is V-shaped. AF value does not show asymmetry. Hypsometric curve indicates that basin is mature.	111
Figure 5. 25. Vf value indicate that valley is in the transition from V-shaped to U-shaped. AF value shows asymmetry towards downstream right side of the basin. Hypsometric curve indicates that basin is mature.	112
Figure 5. 26. Chart of the distribution of asymmetry factors of both Muğla and Yatağan drainage basins. Two horizontal black lines represent $\pm 10\%$ symmetry buffer. AF values exceeding this zone are considered to be assymmetric. A total of 9 basins are assymmetric.	114
Figure 5. 27. Distribution of Vf values of the stream channel of Muğla section. In general Vf values in the study area show low Vf that indicate V-shaped valleys.	115
Figure 5. 28. Distribution of Vf values of the stream channel of Yatağan section. In general Vf values in the study area show low Vf that indicate V-shaped valleys.	115
Figure 5. 29. Hypsometric curves of drainage basins in the Muğla section. Convex to sigmoidal shaped curves are observed in the drainage basins.	116
Figure 5. 30. Hypsometric curves of drainage basins in the Yatağan section. Sigmoidal to concave shaped curves are observed in the drainage basins.	117
Figure 5. 31. Hack's index analyses in the Muğla region are characterized by peaks with high magnitudes on the basin margin faults and peaks with low magnitudes on the second branch.	118
Figure 5. 32. In the Yatağan region all of the peaks are above the basin margin fault except Y4. This second peak in the basin Y4 may be related with another escarpment, however this finding has not been verified in the field.	119

LIST OF ABBREVIATIONS

NAFZ	North Anatolian Fault Zone
EAFZ	Eastern Anatolian Fault Zone
N	North
S	South
E	East
W	West
NE	Northeast
NW	Northwest
AD	Anno Domini
BC	Before Christ
Ø	Grain size
σ	Stress
M_o	Seismic moment
μ	Shear modulus
A	Rupture area
D	Displacement of rupture
M_w	Moment magnitude
V_f	Valley floor width to height ratio
AF	Asymmetry Factor
SL	Hack's stream gradient index
Smf	Mountain front sinuosity
HI	Hypsometric integral
WWSSN	Worldwide standard seismographic network

1. INTRODUCTION

Tectonic geomorphology is the study of tectonic processes that produce unique landforms and these unique landforms are used in the identification of active faults. In tectonic geomorphology, active fault is described as fractures that have moved and modified the landscape in Quaternary (Keller and Pinter, 1996). Active faults are the source of most recent earthquakes which are occurred in a time scale significant for humanity. These earthquakes cause secondary effects such as strong ground motion, landslides, liquefactions, tsunamis. Deformations on nuclear generators, dams, etc. also threat humanity. Because of these reasons, it is important to determine active faults in a region.

Muğla-Yatağan region is a fault zone obliquely situated to Büyük Menderes Graben and Gökova fault zone. Despite there are lots of studies about these major fault zones and they are well known, active tectonics of Muğla-Yatağan fault zone is not studied in detail. There are many active fault maps of the area. But there are missing faults in these maps. Morphometric analyses have never been done for the area before.

The Muğla region is a growing residential area with high population. Muğla-Yatağan fault zone passes through several villages and towns of Muğla region where important factories run and there is Yatağan coal power plant. Several touristic settlements are located close to Muğla-Yatağan fault zone. Any destructive earthquake that will occur on this fault zone will be critical because of great risk to population. So, determination of the activity of the faults and the magnitudes of earthquakes that these faults can generate at this fault zone will be crucial for seismic risk assessment of the region and this study will remedy the deficiency in the literature.

In this purpose 1:25.000 scale topographic maps were used during the field studies. These maps have been scanned and imported to ArcMap and digitized. Digital Elevation Model of the area has been created and morphometric analyses (Hack's

stream gradient index, valley floor width to height ratio, mountain front sinuosity and etc.) have been performed. During the field studies Muğla-Yatağan Fault Zone have been mapped and markers of the tectonic activity on the morphology have been examined. By using the equation by Kanamori (1977) probable magnitudes of earthquakes that these faults may generate are calculated.

1.1. Previous Studies

Yilmaz (1993), Bozkurt (2001) has discussed the tectonics of the Western Anatolian region. Because of Western Anatolia is one of the most active regions of Turkey most scientists are interested in the area (Bozkurt, 2001).

Kayan (1979) has studied the geomorphology of the Muğla-Yatağan Neogene basins within the context of script no TBAG-189 TUBITAK project and said that tectonic units at the Muğla-Yatağan region have controlled the development of the landforms. According to his study geomorphologic evolution of the area is divided into four periods as 1) Erosion of the area between Late Oligocene and Middle Miocene. 2) Formation of Turgut, Yatağan and Muğla basins due to tectonic processes. 3) Processing of Middle Pliocene Pedi plain by the rivers and 4) Quaternary tectonic deformation of the complete area.

Şaroğlu et. al. (1987) has stated that the faults that have ruptured since Quaternary is called active and they are the first who defined the Muğla-Yatağan Fault as active. They have stated that the fault is a right lateral strike-slip fault.

Aktimur et. al. (1996) have studied the field usage potential of Muğla province central town. They have summarized the geology of Muğla surrounding they have stated that even if there are thrusts, nappes, folds, normal faults etc. area has been shaped in the Neotectonic period and they have divided the faults that have potential to generate earthquake as Yatağan Fault, Ula-Ören Faults, and Karova-Milas Faults. They have indicated that these faults are highly segmented and comprising 4-20 km long segments. Aktimur et. al. (1996) also stated that the faults near Muğla has a right lateral component. They have suggested that these faults have produced many

earthquakes in the past and still may produce in the future. According to Aktimur et. al. (1996), potential urbanization area should be the piedmonts of Karadağ mountain due to lower the destructive effects of potential earthquakes that should be generated by NW-SE trending normal active fault passing from the Muğla city.

Barka et. al. (1996) has stated that the Muğla-Yatağan Fault Zone is E-W trending normal fault through the eastern part of Muğla and the fault disappears through east. They have stated that, according to the observations on the fault scarps that bound the Northern part of Düğerek, these faults are older relative to the others and have not ruptured for a long time.

Eyidoğan et. al. (1996) has investigated historical earthquake catalogues for the region. According to these catalogues, they have stated that there are major earthquakes in the area. According to the earthquake distributions Eyidoğan et. al. (1996) have stated that the area is active.

Alçıçek (2010) has compared and correlated basin fill successions with regard to sedimentary facies, fossil content, and paleoenvironment concepts; and synthesized paleogeographic, paleoclimatic and tectonic events. According to her study, Yatağan basin was strongly controlled by climate. Alçıçek (2010) has described Yatağan basin as depression located on the Southern flank of Menderes Massif.

Gürer&Yılmaz (2002) has discussed the evolution of the grabens near Muğla-Yatağan region. He has stated that the oldest basin in the region is Kale-Tavas basin (Early Miocene) and the youngest one is Gökova Graben (Late Miocene). He has stated that the Yatağan basin formed as cross graben (Figure 1.1). Tectonic evolution of the area is discussed in detail in the next chapters.

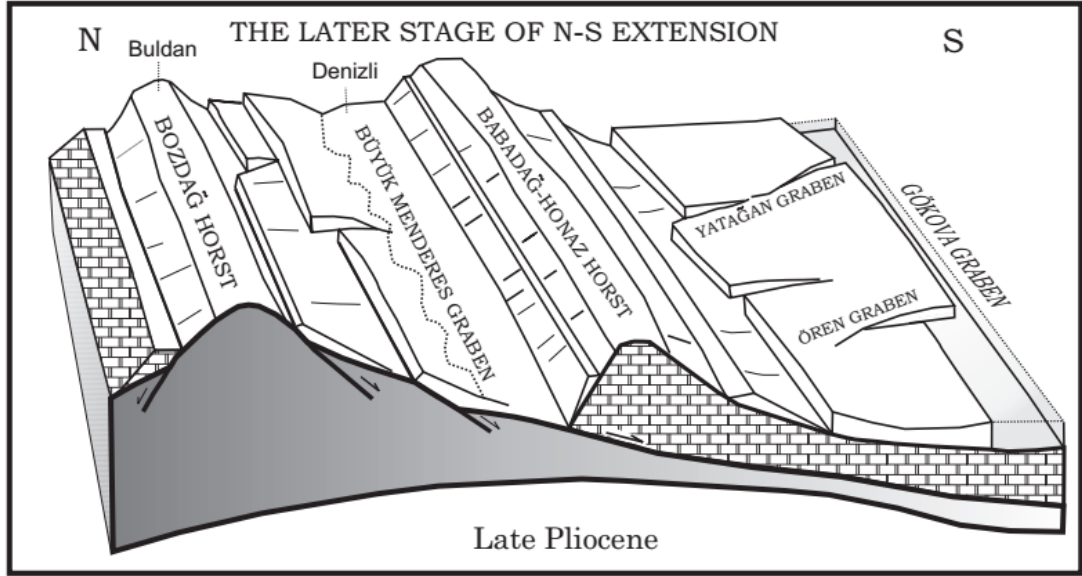


Figure 1.1. Schematic illustration of the locations and orientations of some of the Grabens. Yatağan and Ören Grabens formed as cross Grabens (Gürer&Yılmaz, 2002).

Gürer et. al. (2011) have concentrated on the investigation of the neotectonics of the surrounding of Muğla-Yatağan basin. In this study, they have studied Kale-Tavas basin, Eskihisar-Tınaz basins, Yatağan basin, Muğla-Gökova basin and its surrounding and Plio-Quaternary basins. According to their investigation, they have agreed that there are 4 distinctive basins of different age. These are:

NE-trending Kale-Tavas basin, which is filled by Late Oligocene- Early Miocene terrigenous and shallow marine deposits.

NE-NW trending structural depressions (Eskihisar-Tınaz basins), which are filled by Middle Miocene terrigenous deposits.

NW-SE trending Yatağan basin, which is filled by Upper Miocene-Pliocene deposits.

Plio-Quaternary Paşapınarı, Muğla, Yeşilyurt, Ula and Gökova basins crossing the first three groups of basins. These tectonically controlled basins are filled by Plio-Quaternary terrigenous and marine.

According to Gürer et. al. (2011), the evolution of these four basins is controlled by 2 different tectonic regimes. While the region is under the control of N-S compressional regime during the Late Cretaceous-Pliocene, beginning from the Late Pliocene N-S extensional regime is controlling the regime. Middle Miocene-Pliocene

interval is tectonically inactive. Researchers mentioned that during the Late Tertiary two basins have evolved during the N-S compressional regime and five basins have evolved during the N-S extensional regime. And the transition from the compressional regime to extensional one has occurred during Plio-Quaternary.

Kahraman et. al. (2011) has stated that the Yatağan-Eskihisar basin is composed of Palaeozoic schist and marble bedrock with Neogene cover deposits. N-S, E-W and NW-SE controls the tectonic evolution of the Yatağan-Eskihisar surrounding. According to Kahraman et. al. (2011) Şahinler and Turgut Faults, which are the product of NE-SW extensional regime, cut N-S trending graben, formed by Aldağ and Yeşilbağcılar Faults. E-W and NW-SE striking normal faults along the SW margin of Yatağan basin are syn-extensional structures and are the product of recent tectonic regime.

According to Kaya et al. (2012), Becker-Platen (1970) is the first study that describes sedimentary succession in the Yatağan basin and considered it a single formation, which divided into Turgut, Sekköy, Yatağan and Milet members. According to Kaya et al. (2012), Atalay (1980) has revised this model by distinguishing three units comprising Eskihisar Formation, Yatağan Formation and Milet Formation.

Gül et. al. (2013) has studied the geological and engineering geology properties of Muğla and surroundings for land use potential of the region. They have studied geology and geomorphology of the study area and have stated that the active normal faults and related secondary active faults threat settlements around Muğla. Small and high magnitude earthquakes point out the occurrence of normal faults covered by alluviums.

Gürer (2013) has entitled the faults as Paşapınarı Fault, Aksivri fault.and Muğla Fault. Gürer (2013) has differentiated Muğla fault zone as Muğla Fault 1 Muğla Fault 2 for its different branches according to the different evolutionary stages. Karabacak (2015) has considered the two faults as a single Muğla Fault; extending from Gölcük to Turgut. In this study these faults will be called as Yatağan Fault for Yatağan to Akçaova, Muğla Fault for Menteşe to Yaraş, Aksivri Fault for the Northern branch of Muğla Fault zone and Kavakçalı Fault. In this study Muğla and

Yatağan faults have been separated and evaluated individually because they have different geometries (dip directions).

Gül (2015) has studied the properties and importance of Quaternary colluviums of SW grabens of Turkey. Colluviums in Muğla are controlled by tectonic activity, climate, gravitational forces and host rock characteristics. Colluviums, overlying Liassic age limestones, laterally passes into alluvial sediments in the down dip direction. They are characterized by their angular-sub angular, poorly sorted properties Gül et. al. (2013). During the study, he has collected fourteen samples for sieve analyses and presented frequency (%) versus grain size (\emptyset) graph, cumulative retaining percentage (%) versus grain size (\emptyset) graph, cumulative passing percentage (%) versus grain size (mm) graph, and the classification of the colluviums based on Folk (1974). He has concluded his research that colluviums of the Muğla are composed of gravel (AF, BF, and CF) and muddy gravel (DF), as well as breccia. BF– CF, BF–CF–DF, BF–DF and CF–DF-type facies associations are the fining upward sequences and may indicate evolution during tectonically stable periods, while coarsening upward sequence indicates evolution during tectonically active periods (Fidolini et. al., 2013).

Karabacak (2015) has studied the activity of the Muğla-Yatağan fault by tracing the markers of the activity on the morphology and geology. He mapped active faults of the area from the East of Gölcük through the West of Yatağan (Figure 1.2). He made interpretations on the historical earthquakes according to the deformations on the Lagina ancient city. According to Karabacak (2015), deformations of alluvial and colluvial deposits indicate the late Quaternary tectonic activity of the area. According to rake angles on the fault surfaces, faults have strike-slip component. He prepared parallel topographic profiles from the sides of fault branches around the Stratonikeia ancient city and determined offset streams. Offset streams are also the indicator of the tectonic activity of the region (Figure 1).

At last Karabacak (2015) has stated in his study that, deformations of the buildings of Lagina ancient city including tilting, rotation, falling etc. are markers of historical earthquake that caused damage to Lagina during 4th Century AD.

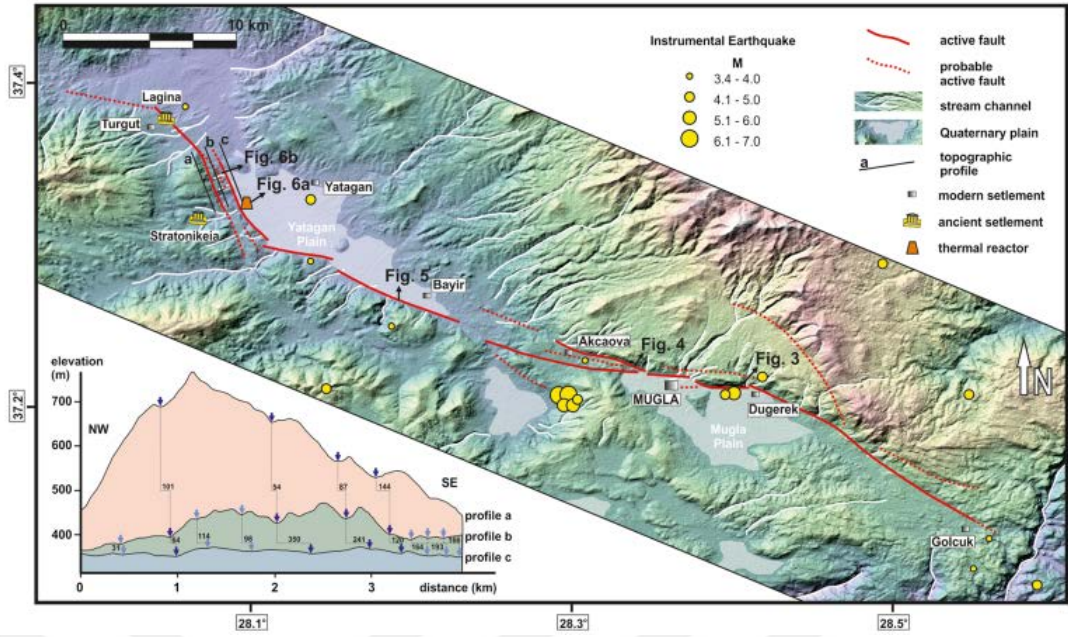


Figure 1.2. Active fault map of the area (Karabacak, 2015) with instrumental earthquakes. He has concluded that the Muğla Fault has dextral component according to the fault parallel profiles.

MTA has mapped the active faults of the area (Figure 1.3). Active fault map prepared by MTA has some missing faults in the area e.g. Kavakçalı Fault. MTA has also not mapped the faults on the colluviums near Menteşe district.



Figure 1.3. Active fault map of MTA. (Obtained from Geoscience Map Viewer and Drawing Editor)

Kalafat (2016) has analysed the seismic events within the time period of 1900-2015 (KOERI data) in two aspects as time dependent variation and compliance for different regions. He has generated depth-time, magnitude-time, magnitude-earthquake occurrence number, earthquake occurrence number-depth and earthquake occurrence number-time graphics (Figure 1.4). Between 08:00 and 15:00 time interval, number of seismic events shows huge anomaly because of blasting operations in the regions. He has separated natural and artificial seismic events by declustering (Reasenberg, 1985) and dequarry (Wiemer and Baer, 2000) methods.

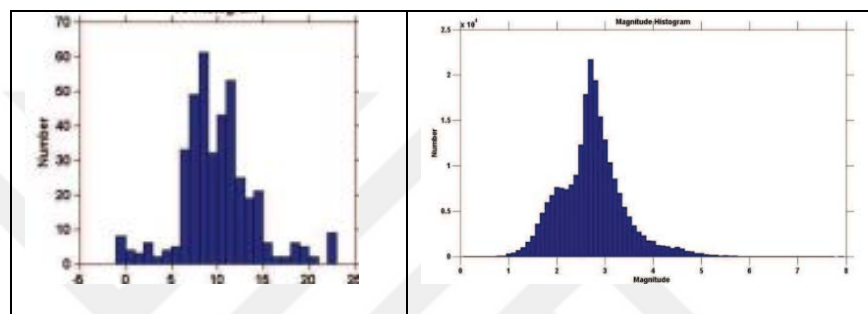


Figure 1.4. a) Earthquake occurrence number-time graphic shows anomaly between 08:00 and 15:00 because of blasting operations and b) magnitude-earthquake occurrence graphic shows anomaly at M=3.

This thesis consists of seven (7) chapters:

Chapter 1 (Introduction and previous studies): In this chapter objective of the study is discussed. Some basic information about the study area is given and previous studies about the study area are summarized.

Chapter 2 (Methodology): In this chapter, it is focused on the methods used during the study. Theoretical and applied aspects including tectonic geomorphology and quantitative morphometric analyses are discussed in this chapter.

Chapter 3 (Seismotectonic background): This chapter includes the topics of tectonic setting and seismotectonic background of the study area. Evolution of Anatolian plate, Western Anatolian Extensional Province and historical and recent seismicity maps of the study area are given in this chapter.

Chapter 4 (Tectonic geomorphology – field studies): Information about the geology and geomorphology of the area is given in this chapter. Long- and short-term deformation properties of the study area are explained in detail. Markers of the tectonic activity on morphology, geology are discussed.

Chapter 5 (Morphometric analyses): This chapter concerns all of the stages of quantitative morphometric analyses.

Chapter 6 and 7 (Results and conclusions) These chapters concludes the thesis.



2. METHODOLOGY

Even if the large earthquakes in Turkey are linked particularly with strike-slip faults, normal faults may produce large and destructive earthquakes.

Muğla-Yatağan fault zone is a seismic source, which has generated and still does large earthquakes. Characteristics of large fault zones such as Büyük Menderes Graben and Gediz Graben in the Aegean Region are studied in detail. However, Muğla-Yatağan Fault zone has to be studied detailly to understand the characteristics of the faults.

2.1. The Physics of Earthquake

2.1.1. The rupture process and earthquake occurrence

Elastic rebound theory is the explanation of the occurrences of earthquakes based on the sudden release of elastic strain energy which is stored during the motion of the blocks relative to each other along locked fault (Figure 2.1 time-1 and time-2) (Reid, 1910). When stored energy exceeds the strength of the rocks, it releases the stored energy while blocks pass each other and earthquake occurs (Figure 2.1 time-3).

For dip-slip normal faults, maximum stress (σ_1), and so the principle direction of movement is vertical (downward) due to gravity (Figure 2.2). Under the effect of gravity, thinning and stretching crust stores energy. It releases its stored energy when the gravity exceeds the strength of crust and blocks in each side of fault. During the release of this energy earthquake occurs.

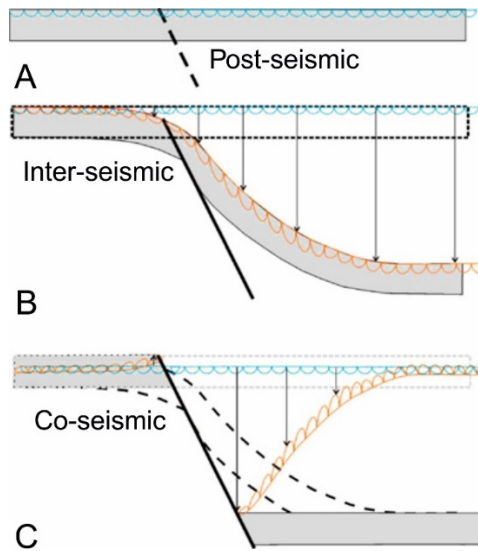


Figure 2.1. Elastic rebound theory put forward by Reid (1910). Three phases of an earthquake cycle is represented. In a) post seismic stage there is no crustal displacement. b) In interseismic stage fault is locked and crust is bent. c) Post seismic stage where the fault is no more locked and the energy is released. Fault ruptures and earthquake occurs. Blue wavy line is the initial stage of blocks and the orange wavy line in the configuration of the blocks (McCalpin, 1996).

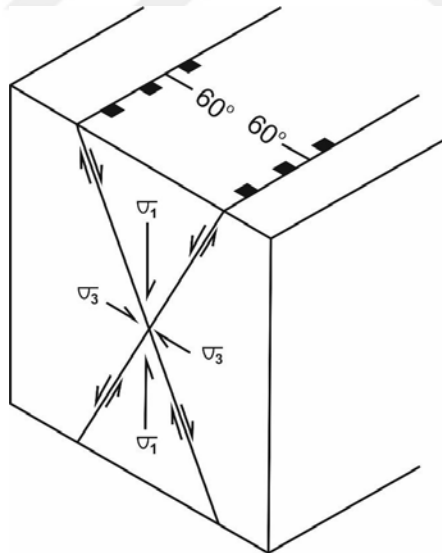


Figure 2.2. Principle stress directions for normal faults. The maximum principle stress σ_1 is linked with gravity. Normal faults generally dip with 60° (Anderson, 1942).

2.1.2. Magnitude of an earthquake that normal faults produce; seismic moment and magnitude.

Wyss, M. (1979) has stated that normal fault related earthquakes are generally less than magnitude 7. According to Schorlemmer et. al. (2005) and Doglioni et. al. (2015), differential stress is necessary to generate rock failure in extensional environments is 5–6 times smaller than that required in contractional environment. So, normal fault-related earthquakes do not reach the magnitudes $>M_w$ 8.5 recorded in strike-slip and contractional settings.

Moment magnitude (M_w), by Kanamori (1977), is the measure of the released energy, and is expressed using seismic moment defined as given in the Equation 1.

Eq. 2. $M_w = \frac{2}{3} \log M_o - 10.7$

2.2. Active Faulting, Fault Geometry, Faulting Behaviour and Segmentation

2.2.1. Active faulting

Active faulting is a geologic hazard, which causes earthquakes and earthquake related strong ground motion, landslides, liquefaction and tsunamis which are linked with the loss of life and properties. Active faulting is expressed with the terms probability and recency. So, designation of active faults is vital in terms of seismic hazard assessment. Many features help us to determine the active faults. Prominent markers used in the determination of the activity of faults are geologic, geomorphic, geodetic and seismologic indicators (Slemmons and Depolo, 1986).

California State Mining and Geology Board has classified active fault as fault that has ruptured since Holocene (10,000 years ago) and potentially active if it has last ruptured in Pleistocene (1,650,000 years ago) (Table 2.1). General Directorate of Mineral Research and Exploration has classified active faults as earthquake surface rupture which ruptured since 1900, Holocene fault which produced surface rupture in Holocene (11,000 years) and Quaternary fault which produced surface rupture in Pleistocene (1,600,000 years) and which is suspicious for Holocene activity.

McCalpin (2009) and Keller and Pinter (2002) have defined active fault as faults that generates tectonic movements that occur in a time range that concerns society. In this study classification of California State Mining and Geology Board is used for active fault classification in order to better classify the degree of activity of the faults in detail.

Table 2. 1. Active fault classification of California State Mining and Geology Board (1973)

Geologic Age			Years Before Present	Fault Activity		
Era	Period	Epoch				
Cenozoic	Quaternary	Historic (Calif.) Holocene	—200—	Active	Potentially active	
		Pleistocene	—10,000—			
	Tertiary	Pre-Pleistocene	—1,650,000—	Inactive		
	Pre-Cenozoic time		—65,000,000—			
Age of the earth			—4,500,000,000—			

2.2.2. Faulting behavior, fault geometry and segmentation

Faulting behaviour involves slip along a fault. Geometry of an active fault trace at the surface is linked with the fault's nature at depth (Schwartz and Sibson, 1989). Not all faults rupture completely at one go, they may be broken up to segments whose boundaries are controlled by anomalies which act as barrier that ends the rupture of faults (Schwartz and Sibson, 1989; Zhang et. al., 1999). If surface rupture evidences are low, faults may be divided into branches according to geometric or geologic properties. "Fault segment" is a general term for branches of the fault. Type of these segments may be different (Table 2.2) (McCalpin, 2009). The term segment boundary is a part of a fault in which minimum two rupture zones have ends (Wheeler, 1989). If a branch of fault has ruptured several times in a time-scale individually it is named as earthquake segment (dePolo et al., 1989, 1991). There have been records of documented earthquakes for a single segment (McCalpin, 2009).

2.3. Geomorphic Approach

Tectonic geomorphology studies comprise investigation of geomorphic and tectonic processes, geological units and it tries to understand how the landscape evolves since its formation. Cycle of erosion has been put forward by William Morris Davis in the late 1980's. He assumed that period of tectonic activity is followed by erosion and tectonic inactivity. During the cycle landscape is modified continuously and characterized by special features such as V-shaped valleys, wine glass morphology at the valleys, flat-irons, hanging valleys and etc. (Keller and Pinter, 1996).

Morphometry is the quantitative measurement of the shape of landscape including the parameters such as size, elevation and slope of the landforms to identify the particular characteristics of an area. These geomorphic indices are hypsometric integral, drainage basin asymmetry, stream length-gradient index (Hack's gradient index) mountain front sinuosity and ratio of valley floor width to height ratio (Keller and Pinter, 1996).

2.3.1. Hypsometric curve and hypsometric integral (HI)

Hypsometric curve is the description of the distribution of elevations of an area and convex curves are the marker of young weakly eroded regions (Keller and Pinter, 1996; Özkaymak, 2014). Shape of the curve for a drainage basin is characterized by calculating the hypsometric integral which is the area under the curve (Figure 2.4). High values of integral indicate that most of the topography is high relative to the mean and low values indicate most of the topography is low relative to the mean (Keller and Pinter, 1996).

Eq. 2. $HI = (h_{\text{mean}} - h_{\text{min}}) / (h_{\text{max}} - h_{\text{min}})$

Where h_{mean} is the mean height, h_{min} is the minimum height and h_{max} is the maximum height.

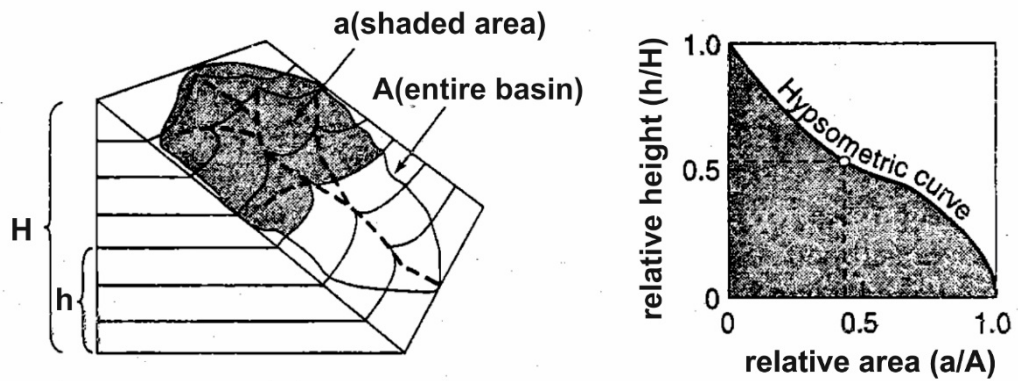


Figure 2. 4. Point based calculation of hypsometric curve. Hypsometric curve is plot of relative area to relative height. (Keller & Pinter, 1996).

2.3.2. Drainage basin asymmetry (AF)

In the areas of tectonic activity drainage network is also affected and tilted toward one side of the basin. Asymmetry factor is the measure of the tectonic tilting ($AF \neq 50\%$) (Keller&Pinter, 1996) (Figure 2.5).

Eq. 3. $AF = 100 (A_{\text{right}} / A_{\text{total}})$

Where A_{right} is the area of right side of basin and A_{total} is the total area.

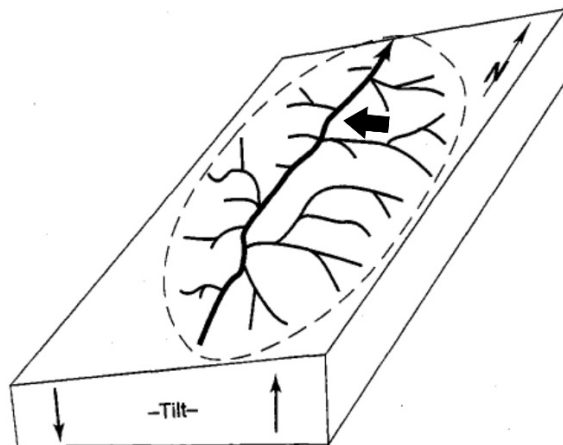


Figure 2. 5. Block diagram showing left tilted (downstream left) basin (Keller&Pinter, 1996). Right side of basin is elevated much more relative to the left side of the basin.

2.3.3. Stream length-gradient index (SL index)

Stream length gradient index is hypersensitive in the determination of active faults and the degree of this activity because it is directly related with the change in the slope of drainage (Show a great increase where elevation changes rapidly). SL index, known as Hack's index, is written in terms of slope of the portion of drainage and length of the drainage from the point of interest as (Figure 2.6); (Keller and Pinter, 1996; Yıldırım, 2014)

Eq. 4. $SL = (\Delta H / \Delta L) L$

Where $\Delta H / \Delta L$ is the slope and L is the length.

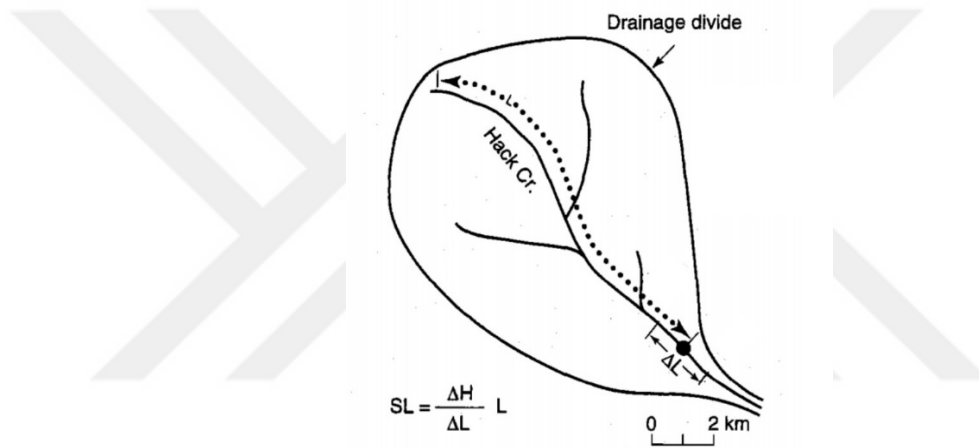


Figure 2. 6. Stream length-gradient index (Hack's index) measurement. Index is defined in terms of the slope and length as their multiplication. Length is the distance of the mid point of the portion that is going to measured to the source of the drainage.

2.3.4. Mountain front sinuosity (S_{mf})

Mountain front sinuosity is a term related with the equilibrium between tectonic processes and erosional processes. If the area is under the control of an ongoing tectonic activity, uplift will lead to the erosional processes and will produce straight mountain fronts. However, if erosional processes are active at the area, drainages incises and generates sinuous mountain fronts. S_{mf} is expressed in terms of the ratio of true length of mountain front to the straight length of the mountain front as (Figure 2.7); (Keller and Pinter, 1996; Özkaymak, 2014)

Eq. 5. $S_{mf} = L_{mf} / L_s$

where L_{mf} is the true length of mountain front and L_s is the straight length of the mountain front.

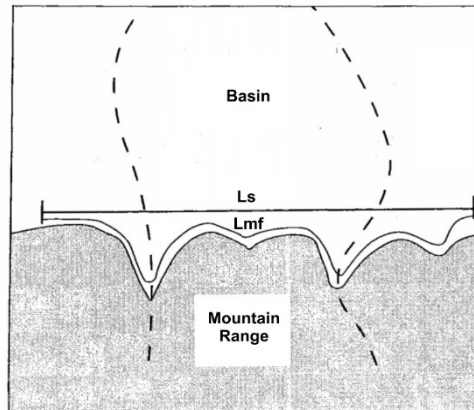


Figure 2. 7. Components of the mountain front sinuosity index. L_{mf} is the true length of the mountain front and L_s is the straight length of the mountain front.

2.3.5. Valley floor width to height ratio (V_f)

Drainages at the tectonically active regions tend to form deeply incised V-shaped valleys. Valley floor width to height ratio is expressed in terms of the elevation of the right-side divide, elevation of left side divide, base height and the valley floor width of drainage as (Figure 2.8); (Keller and Pinter,1996; Özkaymak, 2014)

Eq. 6. $V_f = 2V_{fw} / [(E_{ld} - E_{sc}) + (E_{rd} - E_{sc})]$

Where V_{fw} is the valley floor width, E_{ld} and E_{rd} are the right and left side divides and E_{sc} is the elevation of valley floor.

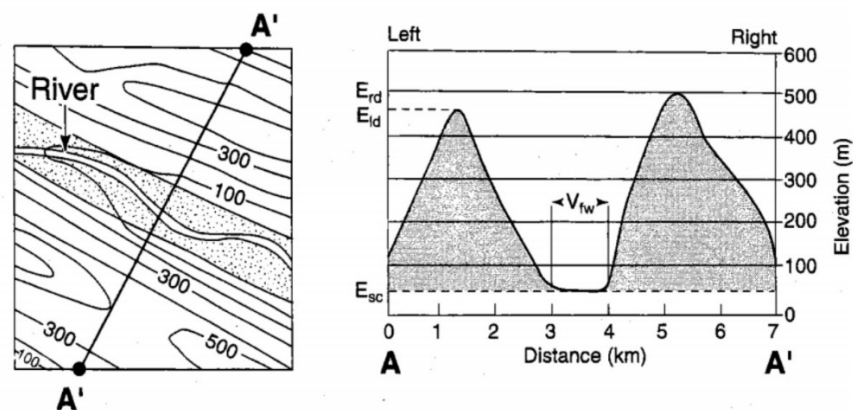


Figure 2. 8. Schematic illustration showing the calculation of valley floor width to height ration values.

2.4. Case Studies

Raj (2012) has stated that shape of the landscape is modified by the combination of tectonic and climatic forces, and he said that tectonic and geomorphic processes are interrelated and tightly coupled. He has performed morphometric analysis in his study and combined their results with field evidence. According to his studies, he has stated that the N-S and NE-SW tectonic trends were active until very recent times.

Özkaymak and Sözbilir (2012) has studied the Spildağı high ranges. They have conducted quantitative morphometric analysis including channel sinuosity, valley floor width-to-height ratio, asymmetry factor, hypsometric integral etc. and results indicate high degree tectonic activity. According to kinematic analyses along three sectors of the Manisa Fault Zone, they were discrete strike-slip faults during the Early-Middle Pliocene, and they have been reactivated as dip-slip normal faults during the Plio-Quaternary.

Yıldırım (2014) has performed mountain front sinuosity (Smf), valley floor width to valley height ratio (Vf) and stream channel gradient analysis on the Tuz Gölü Fault Zone in order to correlate the results with the tectonic activity of the fault. According to the study he has correlated SL values with the activity of the fault zone and the Smf and Vf values with the degree of activity. According to the results he has stated that the fault is moderately active.

Özkaymak (2015) has studied Honaz Fault using geomorphic indices including axial river patterns, valley floor-width-to-height ratios, longitudinal valley profiles, asymmetry factors, hypsometric curves and hypsometric integrals; regional implications and they have conducted stress field orientations. In his study, Özkaymak suggested that normal fault segments of the Honaz Fault are highly active and are possible to generate earthquakes of magnitude 6.7. In his study, he divided asymmetry factors as $45 \leq AF \leq 55$ (symmetric basins), $AF > 55$ (asymmetric westward-tilting basins) and $AF < 45$ (none of these basins show a trend of tilting to

the east). Deviation from 50 in the AF indicates tectonic tilting. Hypsometric integral values are divided into 3 groups as ($.73 > HI > .61$) with convex hypsometric curves, HI values ranging from .40 to .43 with straight hypsometric curves and .43 to .63 that have convex hypsometric curves. Because Honaz Mt. has mostly convex hypsometric curves, the area is tectonically active. Özkaymak (2015) has stated that Vf values lower than 1 indicate the valleys are associated with active down cutting.

Topal et. al. (2016) has studied the geomorphology of Akşehir Normal Fault at SW Turkey in order to evaluate the activity of the fault and seismic hazard. They have used mountain front sinuosity, valley floor width to height ratio, facet slope to height ratio, asymmetry factor, facet drainage density, channel steepness and hypsometric integral. According to the analysis of 32 drainage basins and mountain front facets they have concluded that northern and central part of the fault have high slip rates and the southern segment has low slip rate.

Table 2. 3. Summary of the morphometric analyses with schematic, verbal explanations and mathematical formulas.

Mathematical Formula	Schematic illustration	Explanation
$\frac{h_{mean} - h_{min}}{h_{max} - h_{min}}$		<p>Hypsometric curve may be convex, sigmoidal or concave in shape. Convex hypsometric curve indicates young basin whose shape is modified by tectonic processes, sigmoidal curve indicates a mature basin and concave curve indicates old basin whose shape is modified by erosional processes.</p>
$\left(\frac{A_{left}}{A_{total}}\right) \times 100$ $\left(\frac{A_{right}}{A_{total}}\right) \times 100$ <p>Asymmetry factor is described as percentage.</p>		<p>Asymmetry Factor is a mathematical explanation of the tectonic tilting of the basin in a fault zone. Measured by the ratio of the one side area of the basin to total area of the basin. Right tilting and left tilting terms are used according to the downstream direction the basin.</p>
$(\Delta h / \Delta L) \times L$		<p>Hack's stream gradient index is directly proportional with tectonic activity and rock strength and shows high values at the areas with high tectonic activity. Differentiation of the reason of the high values must be done in detail to determine tectonic activity.</p>
$S_{mf} = L_{mf} / L_s$		<p>Mountain front sinuosity is the measure of the ratio of straight length of mountain front to the true length of mountain front. Linear mountain fronts are linked with tectonically uplifting and active margins. Measured from the margins between quaternary deposits and plane.</p>

Table 2.3 (Continues)

$V_f = 2V_{fw} / [(E_{ld} - E_{sc}) + (E_{rd} - E_{sc})]$		<p>Valley floor width to height ratio is an important parameter used in the description of tectonic activity. Drainage network is sensitive to tectonic activity. Valleys at the active tectonic margins are tend to incise deeper and form V-shape valleys otherwise they will be U-shaped.</p>
---	--	---



3. SEISMOTECTONIC BACKGROUND OF THE REGION

According to Bozkurt (2001), Western Anatolia is one of the most seismically active extensional regions in the world (Figure 3.1) where numerous large earthquakes have been recorded at the region (e.g. 16 July 1956 M=7.1 Söke and 28 March 1970 M=7.2 Gediz earthquakes)

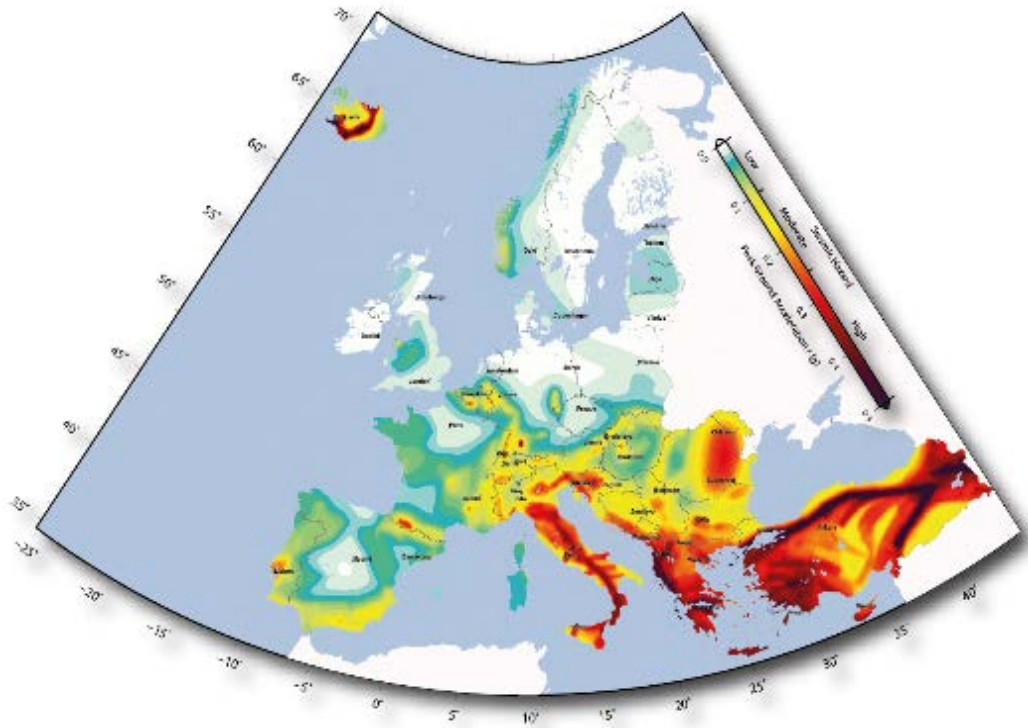


Figure 3. 1. Seismic hazard potentials of European countries are compared in terms of Peak Ground Acceleration (PGA). Areas with comparatively low PGA values and so low seismic hazard values are coloured with green. Yellow coloured areas have moderate and red coloured areas have high seismic hazard values. Turkey has high PGA and so high seismic hazard values. The highest values are observed along active plate boundaries including North Anatolian Fault Zone and Eastern Anatolian Fault Zone. These are followed by Western Anatolian Extensional Province (Giardini, D., et al., 2013).

The place where now Anatolia is situated was a large ocean called as Tethys which contained many continental fragments. The Tethys Ocean was located between two large continents called Laurasia and Gondwana. Collision of these two megacontinents and closure of Tethys Ocean and its fragments in Oligocene resulted in the formation of Anatolia (Okay&Tüysüz, 1999; Okay, 2008). Neo-Tethys stayed open until the end of Oligocene (Okay, 2008) and it closed completely in Miocene after the collision of the Arabian and Anatolian blocks. This collision resulted in the formation of crustal shortening in the Eastern Anatolia. In Early Pliocene, because of the collision of Arabian and Anatolian plates, the Anatolian plate started to migrate Westward along East Anatolian Fault and North Anatolian Fault (Figure 3.2) (Şengör and Yılmaz, 1981; Şengör et. al., 1985; Bozkurt, 2001 and references therein).

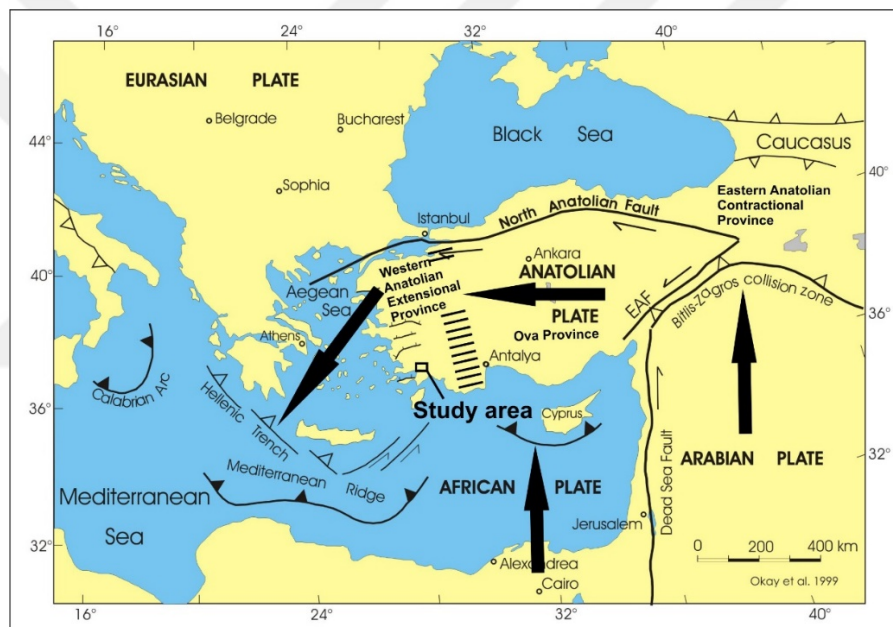


Figure 3. 2. Active plate boundaries of Turkey. Northward motion of Arabian plate and its subduction beneath Anatolian plate is resulted in the westward extrusion (counterclockwise rotation) of Anatolian plate along East Anatolian Fault and North Anatolian Fault, (Okay et. al., 1999).

The accompanied back-arc spreading in the Aegean Sea due to the subduction along Hellenic-Trench causes currently a pulling effect in the Aegean region and is the main force for extensional tectonic regime in the SW Anatolia. The combined result of westward propagation of the Anatolian block and the pulling effect of the Hellenic trench causes a counter clockwise rotation in Western Anatolia. This extension forms

large and small graben systems and fault zones in the Aegean region. Büyük Menderes Graben, Gediz Graben and Gökova Graben are large active graben systems of SW Anatolia (Figure 3.3a). The Muğla-Yatağan fault zone is an active fault zone located in SW Anatolia.

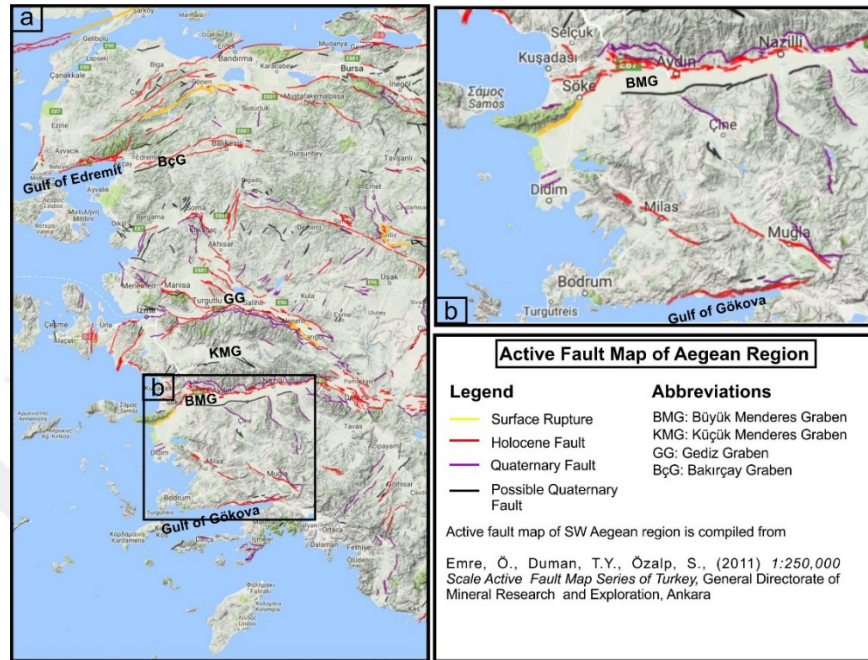


Figure 3. 3. Location map of the study area with active faults of SW Anatolia. Study area is located obliquely to major large E-W trending Büyük Menderes Graben and Gökova Fault Zone.

During the Late Miocene time, N-S extension began and E-W trending Bozdağ horst was elevated. The horst is located between the Gediz Graben in the north and the Küçük Menderes Graben in the south (Figs 1, 2) (Gürer&Yılmaz, 2002) as a typical continental ribbon which is bounded by conjugate normal faults both dipping north and south (Bozkurt and Rojay, 2005).

Low angle detachment faults are observed on both the southern and northern side of the Bozdağ Horst (Yılmaz et al., 2000). N-S trending accommodation faults began to form on detachment faults (Gürer&Yılmaz, 2002).

N-S trending Yatağan and Ören basins probably developed in N-S compressional stress field. These basins are bounded by oblique-slip faults (Yılmaz & Polat 1998; Yılmaz et al. 2000; Robertson 2000 and Gürer&Yılmaz, 2002). N-S

trending accommodation faults began to develop on the upper plates of the detachment faults (Gürer&Yılmaz, 2002). According to Barut&Gürpınar (2005), grabens and rifts in the Gökova region are divided into 2 groups as Muğla-Yatağan and Milas-Ören rifts and these rifts are formed of NW-SE trending Middle-Late Miocene deposits and Plio-Quaternary rocks respectively. Görür et al. (1995) has stated that the origin of the Muğla-Yatağan rift was N-S trending and has gained its recent orientation because of its counter-clockwise rotation in the Late Miocene. After all the modern Gökova Graben formed along E-W trending normal faults during Late Miocene. These normal faults cut older units and related structures (Gürer&Yılmaz, 2002). Schematic illustration of the E-W and N-S trending grabens is given in the Figure 1.1. Local map of the study is given in Figure 3.4.

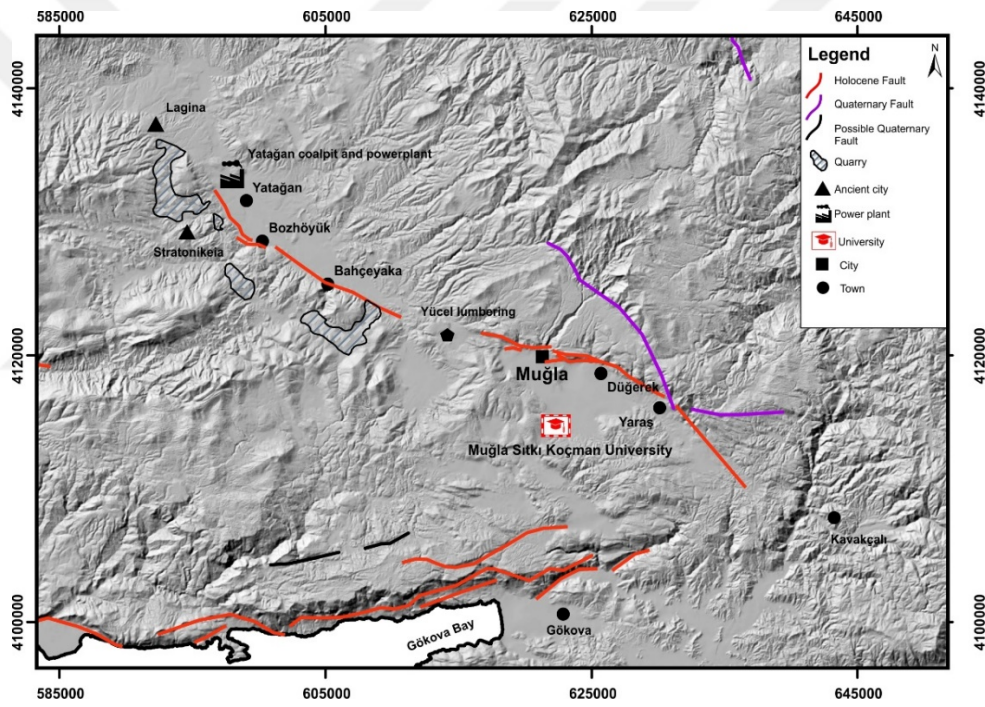


Figure 3. 4. Local map of the study area. Muğla-Yatağan Fault Zone is oblique to Gökova Fault Zone. Muğla-Yatağan Fault zone extending from Yatağan to Yaraş, bounding Yatağan basin from its SW margin and Muğla basin from its NE margin and Muğla Fault Zone is highly segmented. Yatağan Fault is close to Yatağan coal power plant. Fault data from (Gen. Dir. of Min. Res. and Exp.)

According to the present-day kinematics, the Arabian plate is moving in N-NW direction at a rate of about 20-30 mm/yr. (Reilinger et. al., 2006) while the African plate is moving North at a rate of 10 mm/yr. (Oral et. Al., 1995). Recent GPS data

imply that the present rate of motion of EAFZ is 11 ± 2 mm/yrs. NAFZ is about 15-25 mm/yrs. according to, (Oral et. Al., 1995). Western Anatolia is now extending in the direction of N-S at a rate of 30-40 mm/yr. (Oral et. al., 1995). GPS velocity field map of Turkey (Figure 3.5) is characterized by short arrows in the Eastern Anatolia and Long Arrows in the Western Anatolian Extensional Province. Small arrows indicate low velocities while the long arrows indicate high velocities of motion. In Eastern Anatolia, crustal thickening-shortening is followed by crustal extension in Western Anatolia.

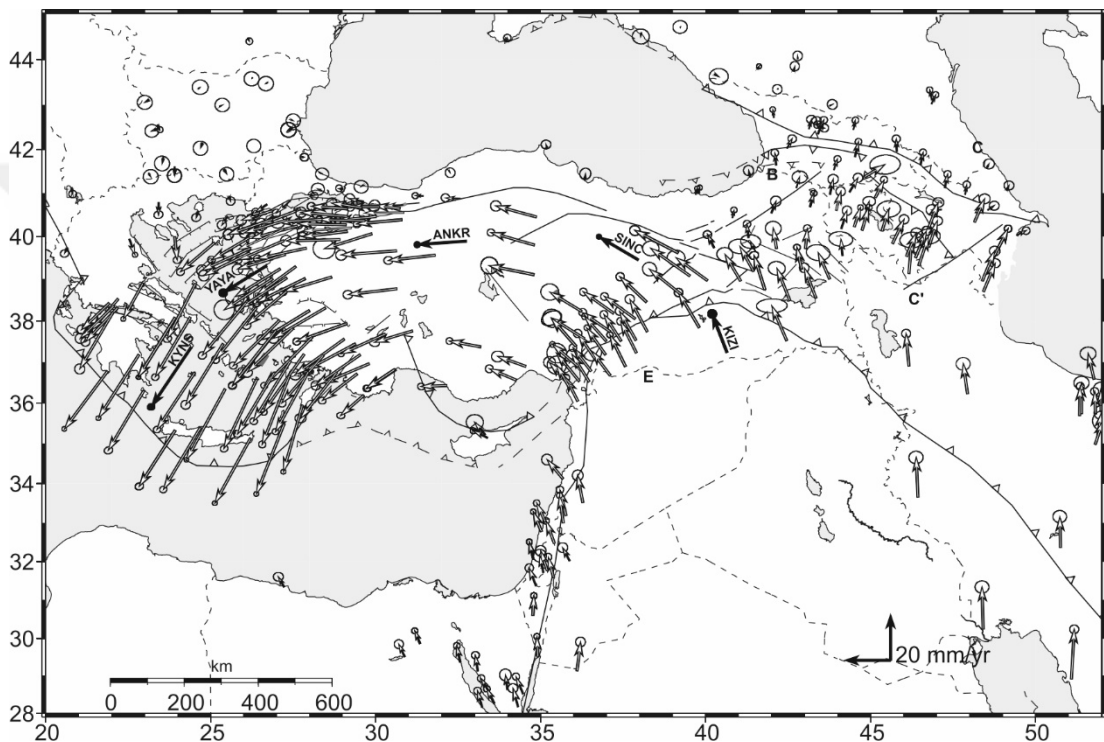


Figure 3. 5. GPS horizontal velocity field of Turkey and surrounding regions in a Eurasia-fixed frame (Reilinger et. al., 2006).

3.1. Historical Seismicity of Muğla region

There are records of several historical earthquakes (2300BC to 1963AD) in the Muğla region. Historical earthquake data compiled from Tan et. al., (2008) (Table 3.1).

There are clusters of earthquakes in 1941 in the Muğla region. 4 of them have $M \geq 6$. There is a record of destructive in 1941, which caused great damage on the village resulted in the complete destruction of the Bayır village. After that earthquake, Bayır has been reconstructed again and has had its recent configuration. There are two $M \geq 6$ earthquake records which may potentially be the reason of this disaster in 1941.

Table 3. 1. List of historical earthquakes at the Muğla region (study area). (Compiled from Tan et. al., 2008). There are 22 records of earthquakes. (Before the establishment of World Wide Standard Seismographic Network (WWSSN))

No	Latitude	Longitude	Magnitude	Depth(km)	Year	Month	Day
1	37,21	28,55	4,59		1900	7	
2	37,21	28,4	4,59		1931	5	
3	37,21	28,4	4,59		1931	12	28
4	37,21	28,4	5,18		1938	5	1
5	37,2	28,3			1939	7	24
6	37,21	28,4	5,18		1941	2	20
7	37,2	28,3	6	100	1941	5	23
8	37,2	28,3			1941	5	23
9	37,2	28,3	5,3	60	1941	5	23
10	37,2	28,2			1941	5	23
11	37,21	28,4			1941	5	26
12	37,2	28,3			1941	6	23
13	37,2	28,3			1941	9	21
14	37,21	28,4	5,18		1941	10	14
15	37	28	6	100	1941	12	13
16	37,21	28,4	5,18		1943	1	1
17	37	28	5,18		1943	1	8
18	37,2	28,3	5,18		1943	1	11
19	37,21	28,4	4,59		1944	3	16
20	37,2	28,3	6,25	100	1944	5	27
21	37	28,5	6,3		1959	4	25
22	37	28,5	5,6		1959	4	25

One of the $M \geq 6$ earthquakes, which is in the Menteşe region, is probably generated by the E-W trending Menteşe fault where current Menteşe residential area is constructed and may be responsible for the 50 cm offset in the Quaternary deposits in front of the Menteşe fault. Earthquakes between $M=5$ and $M=6$ in 1941 are cumulated at the Düğerek region.

Yatağan basin is characterized by the lack of seismic record. This is why World Wide Standard Seismographic Network (WWSSN) has been established after 1963 and activity of faults could not be recorded before 1963.

These earthquake data indicate that the Muğla Fault has ruptured many times during last 1000 years. Karabacak (2015) has mentioned about several earthquake records in historical times. These earthquakes occurred in 227 BC, 199–198 BC, 142–144 AD, and 365 AD. Historical seismicity map Muğla region is given in the Figure 3.6 below.

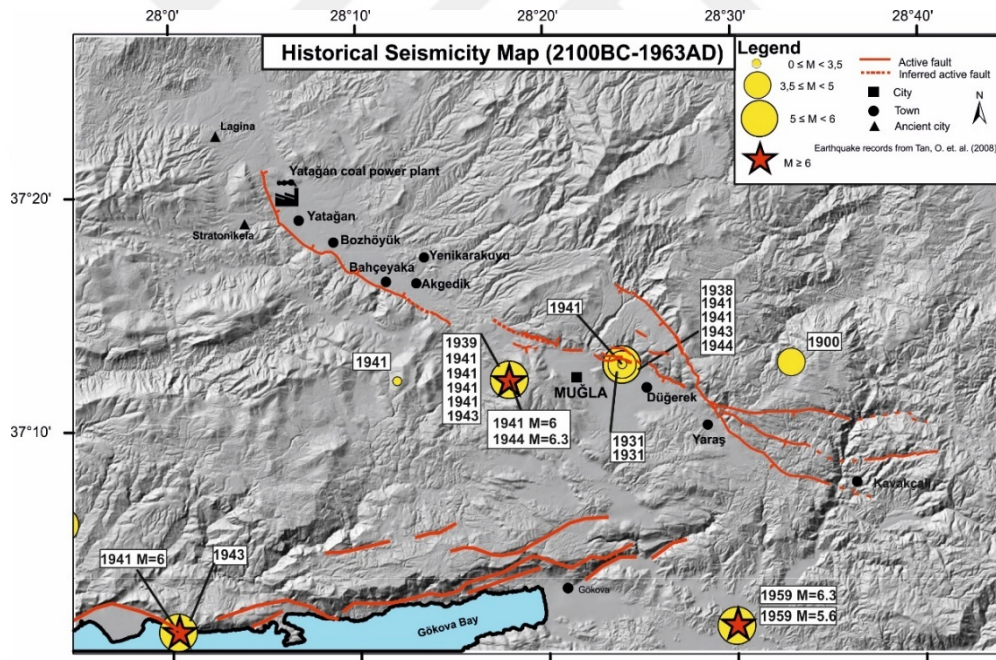


Figure 3. 6. Historical seismicity map of the study area. 22 Earthquakes have been recorded in this period. Four of them have magnitudes greater than $M=6$. Earthquakes $M=6$ have been located as red stars. There is no earthquake record linked with Yatağan Fault because these data are collected before the establishment of World Wide Standard Seismographic Network (WWSSN).

3.2. Recent Seismicity of SW Anatolian and Muğla Region.

There are clusters of earthquake records in the SW region. These are accumulated along the major important graben systems and fault zones which are Büyük Menderes Graben and Gökova Graben (Figure 3.7). 4 Earthquakes with $M \geq 6$ have been recorded after 1963 AD. 3 of 4 $M \geq 6$ earthquakes are submarine.

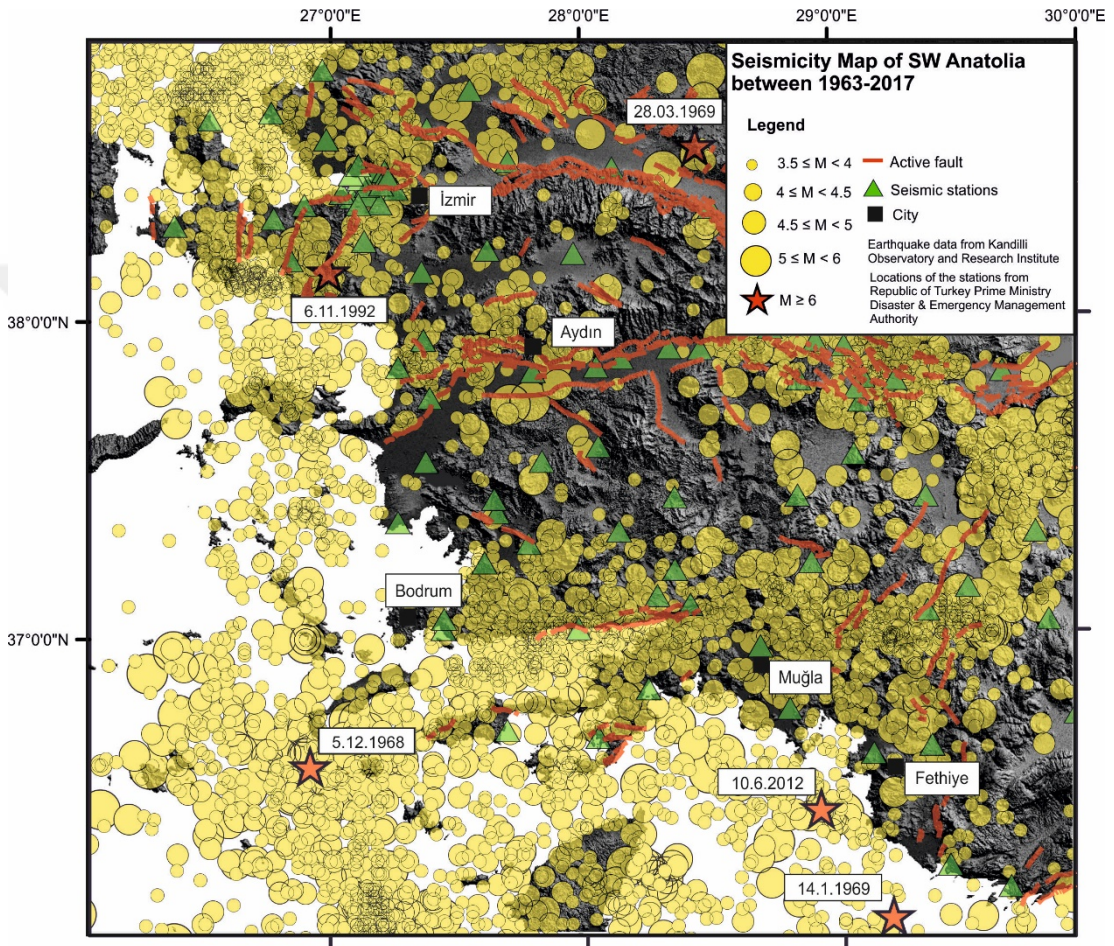


Figure 3. 7. Spatial distribution of earthquake records in SW Anatolia after 1963AD with seismic stations.

There are quarries in the area where blasting operations are carried out. Quake records which has $M < 3.5$ and between 6AM and 4PM are eliminated from data because they are the most possible data of the shaking due to blasting. Histogram showing the earthquake records for 24 hours interval is given in the Figure 3.8 below and magnitude distributions below $M=3.5$ (Figure 3.9). Even if there is still an

accumulation in the records at area of quarry (SE of Bahçeyaka), it is obvious that earthquake records in front of the Bahçeyaka fault is highly active.

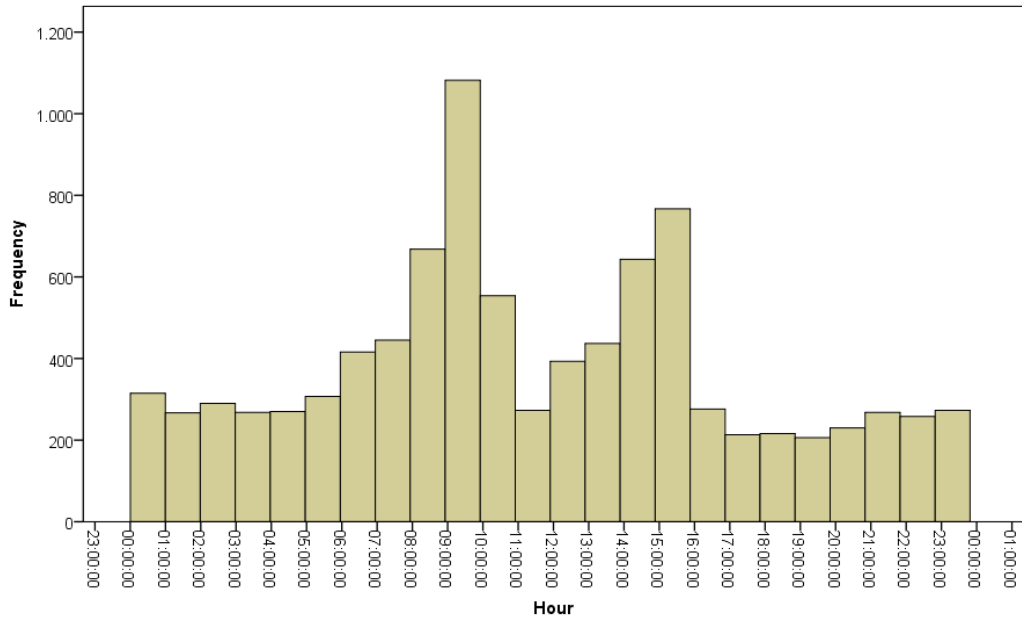


Figure 3. 8. Histogram of earthquake events for 24 hours time interval in a day. Between 06:00 and 16:00 number of events show peaks.

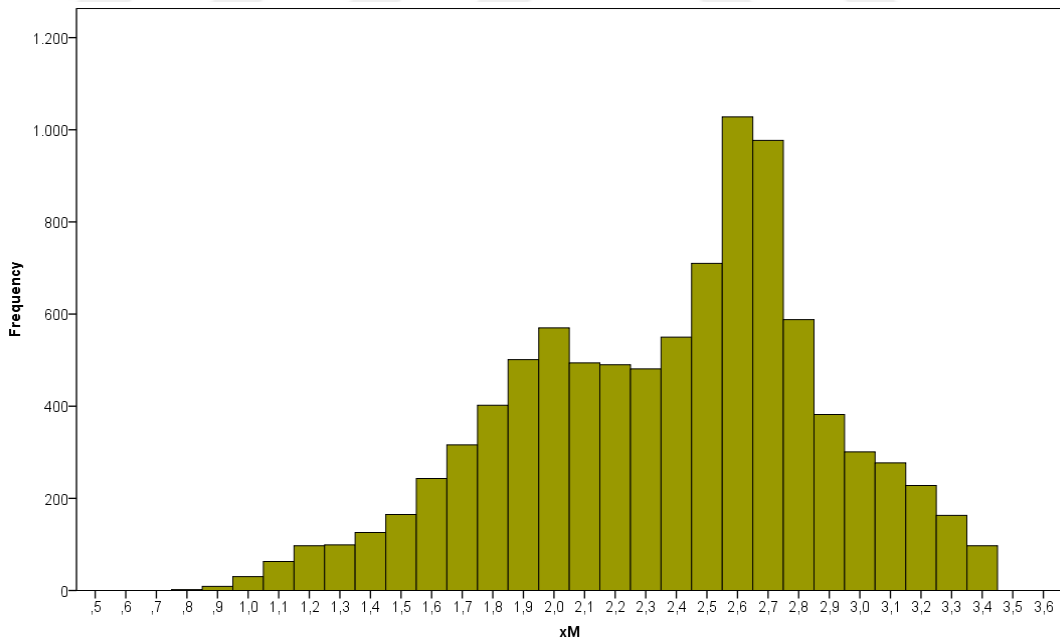


Figure 3. 9. Earthquake distributions below M=3.5.

In 13.04.2017 M=5 Ula Kavakçalı earthquake has occurred at 28.647E / 37.1533N. Focal mechanism solutions of the faults indicate that the earthquake may be created either by E-W striking N dipping low angle normal faults or E-W trending S dipping high angle normal faults.

Our field observations have shown that the source of earthquake is E-W trending (90 °), S dipping, high angle normal fault with 70° dip angle with pure normal to small amount of strike slip component. Focal mechanism solution indicates that earthquake has been generated by a fault with 18 ° dip amount and S dip direction. Difference in the dip amounts of field observations and focal mechanism solutions is why fault is listric. Change in the dip amount of fault in 5km depth means our fault is a shallow fault. M=5 Earthquake has not created surface rupture but there have been observed cracks on the road which have about 40m long, max 3 cm width and small deformations on the buildings at the Kavakçalı village. Kavakçalı fault and related damage caused by earthquake is illustrated in Figure 3.10. Distribution of the earthquake in the Kavakçalı region and focal mechanism of M=5 Kavakçalı earthquake is given in Figure 3.11.

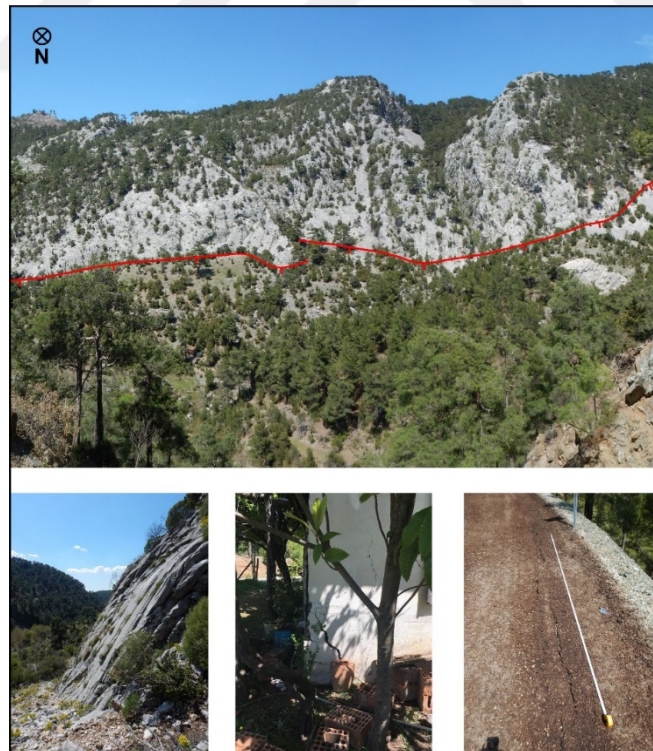


Figure 3. 10. After earthquake crack on the road of Kavakçalı village.

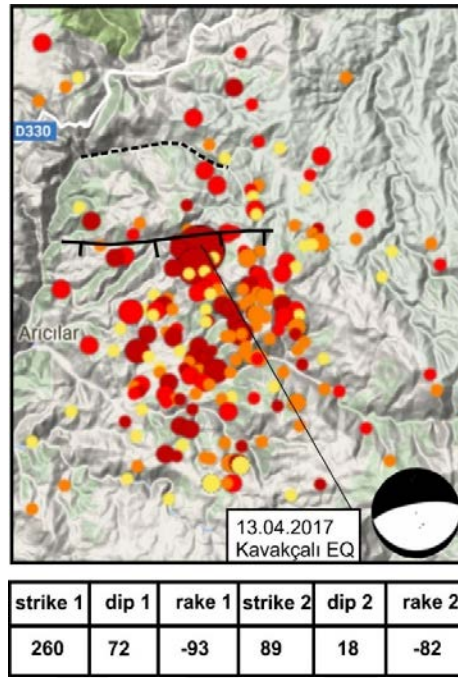


Figure 3. 11. Seismicity map of Kavakçalı region with earthquake records, focal mechanism of M=5 Kavakçalı earthquake and entry table of focal mechanism solution. Earthquake records comprise the latest 30 days and this implies that there is high seismic activity in the region.

So, if M=5 earthquake can create this deformations at the area, earthquakes with magnitudes higher than 6 will result in severe effects at the area. So, identification of the geometric features of these faults and their potential to produce large and destructive earthquakes are important in terms of seismic risk assessment and for future studies.

After 1963, there is a great increase in the earthquake records in the study area (Figure 3.12). There are quarries in the area and there are blasting operations in the field. Quake records which has $M < 3.5$ which are between 6AM and 4PM are eliminated from data because they are the most possible data of the shaking due to blasting. Even if there is still an accumulation in the records at area of quarry (SE of Bahçeyaka), it is obvious that earthquake records in front of the Bahçeyaka fault is highly active.

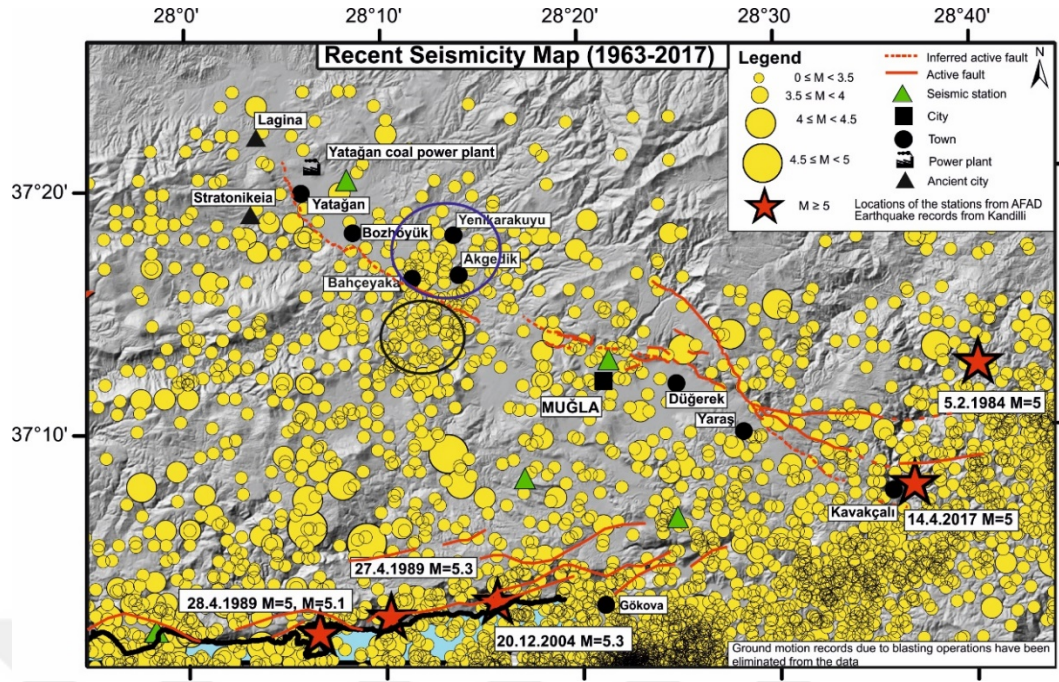


Figure 3.12. Recent seismicity map of the study area. Number of earthquake records have been increased dramatically after 1963 after the establishment of World Wide Standard Seismographic Network (WWSSN). 5 Large earthquakes have been recorded after 1963. These large earthquakes have been shown on the map as red stars. Blue circle indicates the cluster of earthquake records in front of Bahçeyaka fault after the elimination of data. Black circle is the cluster of records behind the Bahçeyaka fault which are related with blasting in the quarry.

4. ACTIVE TECTONICS, GEOMORPHOLOGY OF THE MUĞLA – YATAĞAN REGION

4.1. Introduction

In this chapter, general geology, regional geology and markers of the tectonic activity on the morphology will be discussed.

4.2. Geological Overview

4.2.1. Regional geology of Southwestern Anatolia

Menderes Massif is located in the Western Anatolia (Okay, 2008). Şengör et. al. (1984) divided the Menderes Massif as Northern and Southern sections which are bounded by Büyük Menderes Graben. Menderes Massif is divided into two subgroups as core complex and cover units (Schuiling, 1962; vanHinsbergen., 2010; Akbay, 2011; Gürer at. al., 2011). Core of Menderes Massif is formed of augen gneisses, migmatites, gabbros, medium to high grade metamorphic rocks etc.; cover units include Paleozoic schists, Mesozoic-Cenozoic marble, Triassic age conglomerate bearing quartzite which are overlain by Upper Triassic-Liassic marble, Jurassic-Lower Cretaceous dolomitic marbles (Okay, 2008; Akbay, 2011).

Menderes Massif is tectonically overlain by Lycian Nappes (Akbay, 2011; Gürer at. al., 2011) and Lycian Nappes are differentiated into five main tectonic units, which are Tavas, Bodrum, Domuzdağ, Gülbahar and Marmaris ophiolitic nappe (Şenel,2007). Nappes comprise carbonate rocks, clastic rocks, mélangé and ophiolites. Collins and Robertson (1997, 1998, 1999) has differentiated Lycian Nappes into 3 subgroups as Lycian Thrust Sheets, Lycian Mélangé and Lycian

Peridotite Thrust Sheet. Lycian Thrust sheets comprises Upper Paleozoic-Tertiary sedimentary rocks. Lycian Peridotite Thrust Sheets tectonically overlay the Lycian Mélange (Akbay,2011 and references in it).

SW Turkey composed of many dynamic graben systems, which are filled with Neogene and Quaternary deposits (Gül et. al., 2013). Upper Tertiary (Neogene) units composed of Pliocene and Miocene conglomerates, sandstones and mudstones. Quaternary deposits are composed of colluviums, alluvial fans and alluvial deposits unconformably overlying older units (Aktimur et. al., 1996; Gül et. al., 2013 and references in them).

4.2.2. Local geology

4.2.2.1. Kavaklıdere group

1000m thick Kavaklıdere group formed during Permo-Carboniferous and located at the bottom of the stratigraphic sequence of the study area. Kavaklıdere group crops out at the Western side of Dirgeme. Composed of metaclaystone, quartz, quartz schist, garnet schist and phyllite (Aktimur et. al., 1996; Akbay, 2011; Gül, 2013 and references in them).

4.2.2.2. Marçal group

Kavaklıdere Group is unconformably overlain by the Mesozoic-Lower Tertiary Marçal Group which is composed of red conglomerate, metasandstone, metasilstone, dolomite-dolomitic limestone, and rudist bearing limestone (Aktimur et. al., 1996; Akbay, 2011; Gül, 2013).

4.2.2.3. Ören unit

Ören unit is formed of 1500m thick Lower-Middle Triassic Karaova formation. Karaova formation comprises conglomerate–metasandstone-shale alternation. 300-1700m thick Middle Triassic-Liassic-Upper Cretaceous Gereme formation is composed of dolomitic limestone-dolomite alternation. Upper Cretaceous-Paleocene

Karabörtlen formation includes conglomerate, sandstone and siltstone. Peridotites cover all of these units at the top (Aktimur et. al., 1996; Akbay, 2011).

4.2.2.4. *Akçay Group*

Oligocene-Aquitania age Akçay group is formed of Oligocene age Mortuma formation comprising sandstone – conglomerate alternation, Aquitania age Yenidere formation comprising conglomerate, mudstone, sandstone siltstone, claystone and Kerme formation which is Aquitania and comprises alternation of conglomerate, sandstone, siltstone, claystone, clayey limestone (Aktimur et. al., 1996; Akbay, 2011 and references in it). (Aktimur et. al., 1996 and Gül, 2013) or conglomerate, sandstone, siltstone and limestone intercalation (Akbay, 2011 and references in it)

4.2.2.5. *Muğla Group*

Muğla group is composed of Milet, Yatağan, Sekköy and Turgut formations. Conglomerate-sandstone alternation of Çardaklı member and sandstone-siltstone-conglomerate-claystone alternations of Dokuzçam member are the rock types of Turgut formation. Sekköy formation overlies Turgut formation. Limestone, siltstone and tuff are found in 50-150m thick Middle Miocene age Sekköy formation. 75-140m thick Pliocene age Milet formation is formed of conglomerate-sandstone at the bottom and clayey limestone at the top. Yatağan formation is formed of medium to thin bedded white marl and claystone and thickly bedded red coloured claystone, siltstone (Gül et. al., 2013). Upper Miocene age Yatağan formation has 150-400m thickness and passes to Milet formation (Aktimur, 1996; Akbay, 2011; Gül 2013).

Generalized columnar section of the study area is given in the Figure 4.1 and geological map of the study area is given in the Figure 4.2 below (Aktimur, 1996).

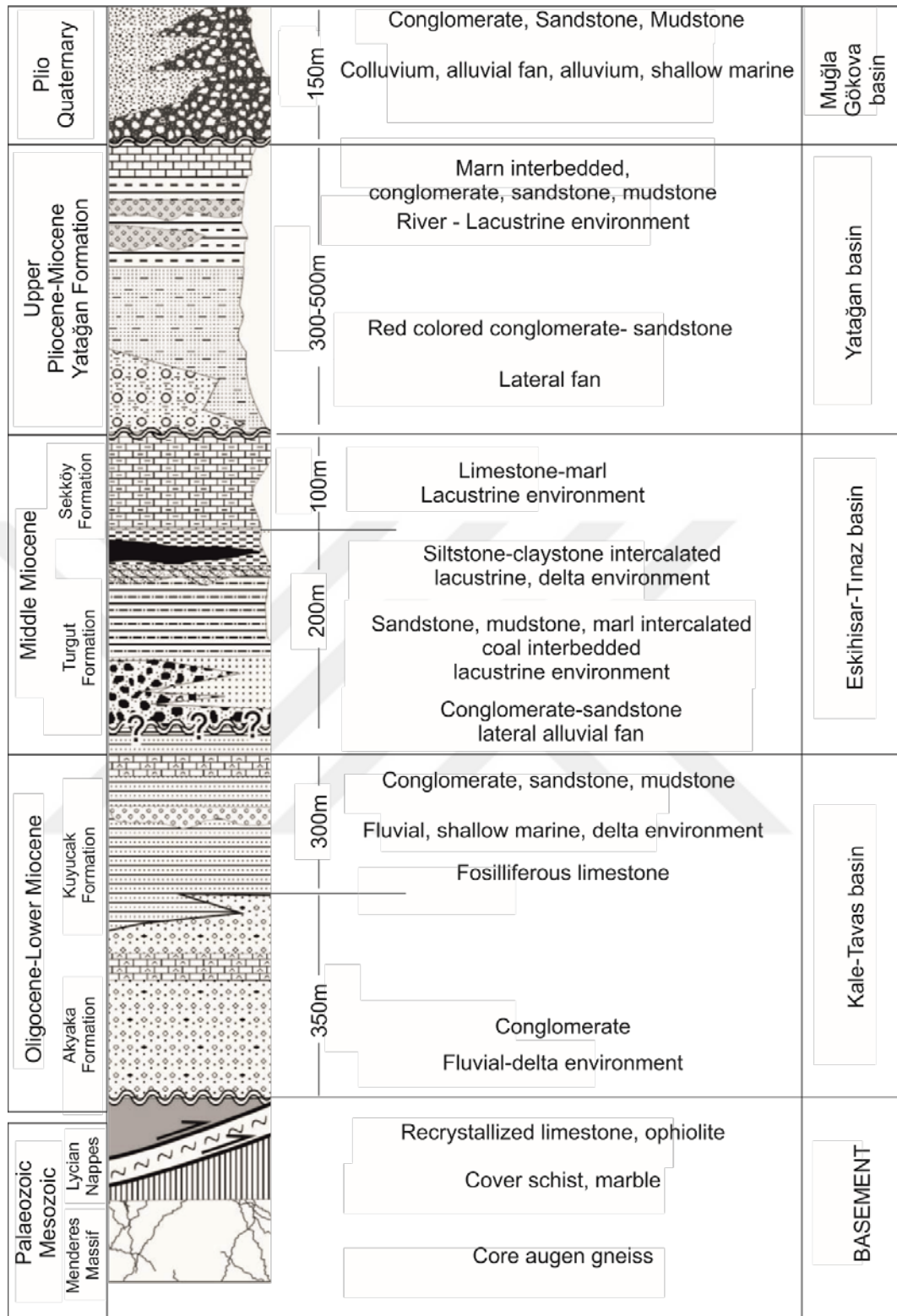


Figure 4. 1. Generalized columnar section of the study area (modified from Gürer et. al., 2011)

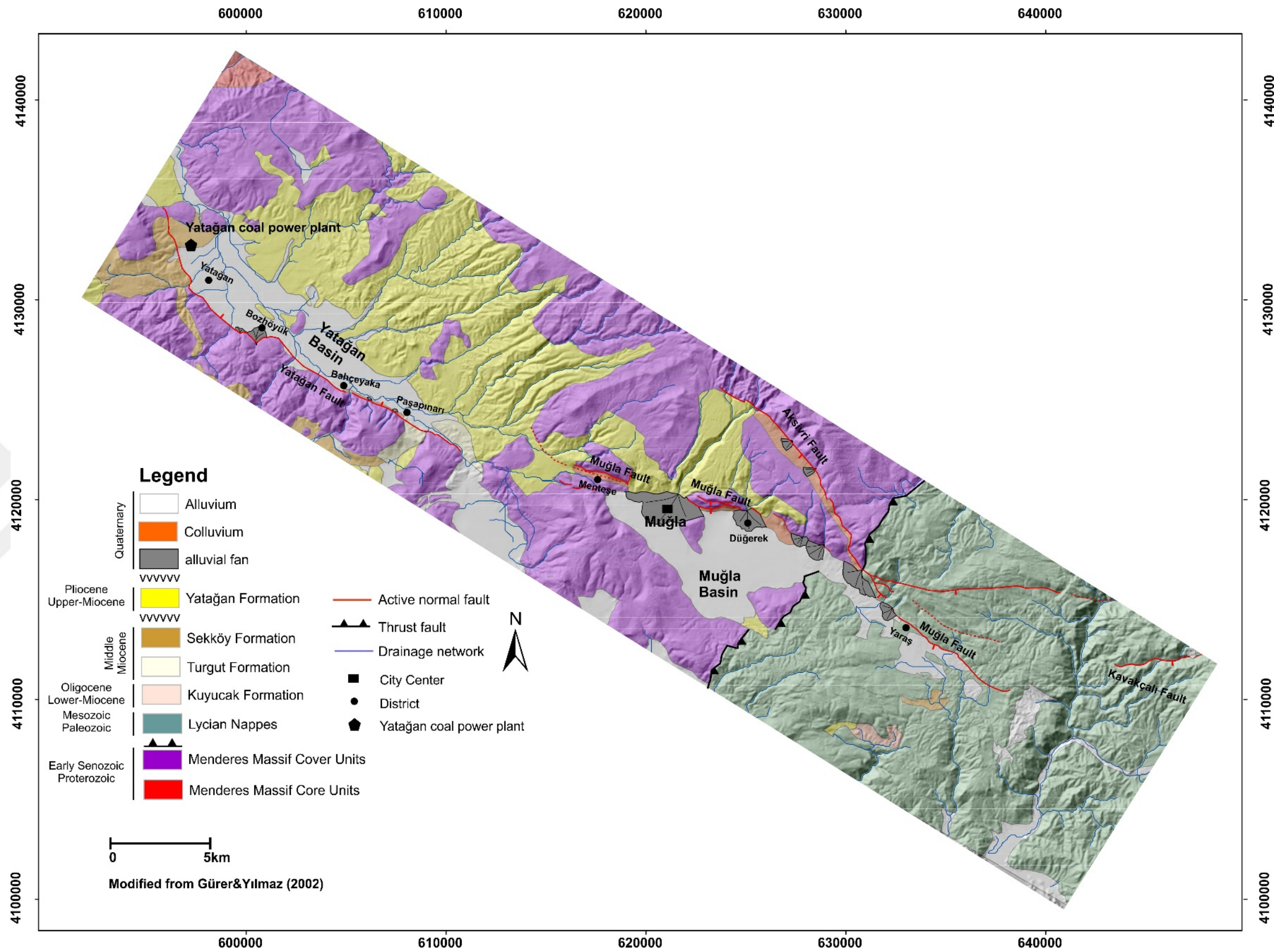


Figure 4. 2. Geological map of the study area (Modified from Gürer&Yılmaz, 2002).

4.3. Morphologic Framework of the Muğla–Yatağan Region

Study area is located in the SW Anatolia, given in the Figure 3.3, which is under a primarily N-S extensional tectonic regime (Şengör et. al., 1985; Bozkurt, 2001 and Karabacak, 2015). Both tectonic processes and erosional processes modifies the morphology. While the tectonic processes are constructive, erosional processes are destructive. So, different morphological features are seen together because of the effects of both tectonic and erosional processes in the area.

Surrounding of Muğla-Yatağan region is characterized by the topographic highs and lows. The most prominent geomorphic structures in the surrounding of Muğla-Yatağan region are the Yatağan basin, Turgut basin, Eskihisar basin, Muğla Polje, Yeşilyurt depression with topographic highs bounding them (Kayan, 1979).

Study area comprises Yatağan and Muğla basins which form the lowlands of the study area. These two depressions situated obliquely to Gökova normal fault system and Büyük Menderes Graben (Karabacak, 2015). Both depressions are formed by the margin bounding normal faults. Yatağan, Bahçeyaka, Paşapınarı, Muğla, Düğerek and Yaraş are the main settlements in the study area.

Muğla Polje is situated at the Eastern part of Menteşe region and has a triangular shape. It bounds to Yaraş village with a narrow corridor. Northern part of the Muğla depression is bounded by E-W and NW-SE trending S-SW dipping normal faults and characterized by steep slopes (given in the Figure 4.3). Basin is fed by large streams coming from the hills of Yılanlıdağ Mountain.



Figure 4. 3. Schematic illustration of the Muğla plain with satellite image basemap. Muğla basin is a triangular shaped plain which is bounded by NW-SE, E-W trending S dipping normal faults to the Yılanlıdağ straight. Northern margin is characterized by steep slopes, topographic limestone escarpments and fault related alluvial fan deposits transported via large streams flowing N to S which covers the alluvium of Muğla plain. Blue lines with arrows indicate the drainage network with flow direction, black lines indicate transportation of sediments via drainages forming alluvial fan covering the alluvium of Muğla basin. Red lines indicate the active normal faults of the area.

At the Eastern part of Muğla basin Yarış village is located. There is no observable fault plane but markers of faulting is traced on the morphology with steep slopes at the Eastern part of Muğla Fault Zone near Gölçük (Figure 4.4).



Figure 4. 4. Faulting is traced by the change in topography-small hills near Gölçük village.

Northern margin of the Yaraş village is formed of different segments of Muğla fault zone. Stream is cut by different fault segments, hanging vallys are observed and because of faulting sediments deposited as alluvial fan. Altitude of the basin is about 710m above sea level and the highest point of the escarpments is about 1420m (Figure 4.5).

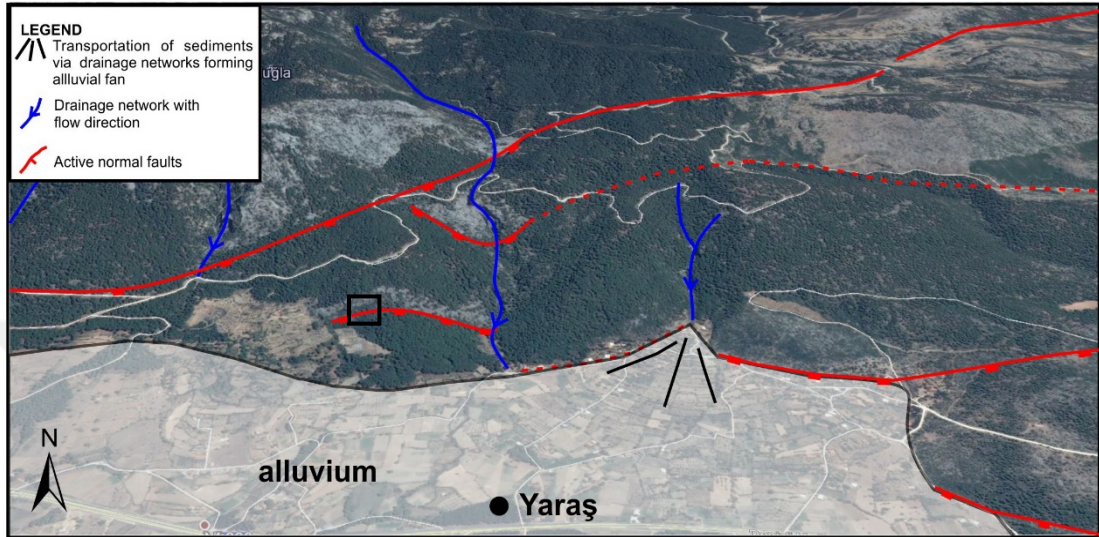


Figure 4. 5. Schematic illustration of the Yaraş section with satellite image basemap. Northern margin is characterized by steep slopes, topographic limestone escarpments and fault related alluvial fan deposits transported via large streams flowing N to S which covers the alluvium of Muğla plain. Blue lines with arrows indicate the drainage network with flow direction, black lines indicate transportation of sediments via drainages forming alluvial fan coverin the alluvium of Muğla basin. Red lines indicate the active normal faults of the area. Black rectangle shows the location of Figure 4.6.



Figure 4. 6. The lowermost segment of Muğla Fault Zone near Yaraş village. Fault strikes with 130° and dips with 50° South. Fault plane is limestone and flow marks are observed on the fault plane. Slickenlines are not observable.

Western part of Yaraş is characterized by a fault segment whose tip is about 1100m above sea level corresponding to the base height of Yılanlıdağ straight. This segment is separated from the Yaraş segment by NW-SE trending Aksivri-Yılanlıdağ fault (Figure 4.7).

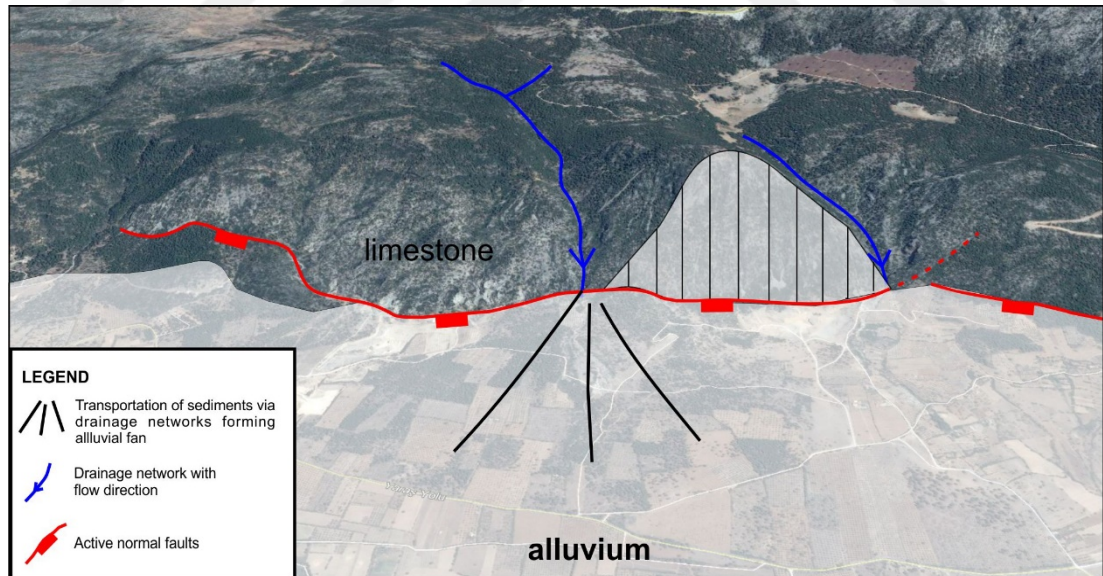


Figure 4. 7. Schematic illustration of Muğla basin where it bounds to Yılanlıdağ straight from its Northern margin. Triangular shaped flat-iron is observed in the limestone fault plane formed by the progressive effects of both erosion and tectonic uplift. Fault related alluvial fans are observed in front of the basin margin fault.

Düğerek village is located in the Western part of this locality and settled on alluvial fan deposit. Northern margin is controlled by normal faults and streams cut by these faults are resulted in the formation of alluvial fan. Lowermost segment of Düğerek fault is covered by colluviums at its western part and exposes in the Düğerek village (Figure 4.8).

Fault planes are highly fresh in the Düğerek region (Figure 4.9), slickenlines and ondulations are covered. Slickenlines and ondulations indicate that motion of the fault is normal with strike-slip component. Different slip directions are observed on the same fault plane according to the slickenlines and ondulations. Schematic representation of the change in slip directions is given in the Figure 4.10. Hanging valley and flat irons are observed in this region (Figure 4.11).

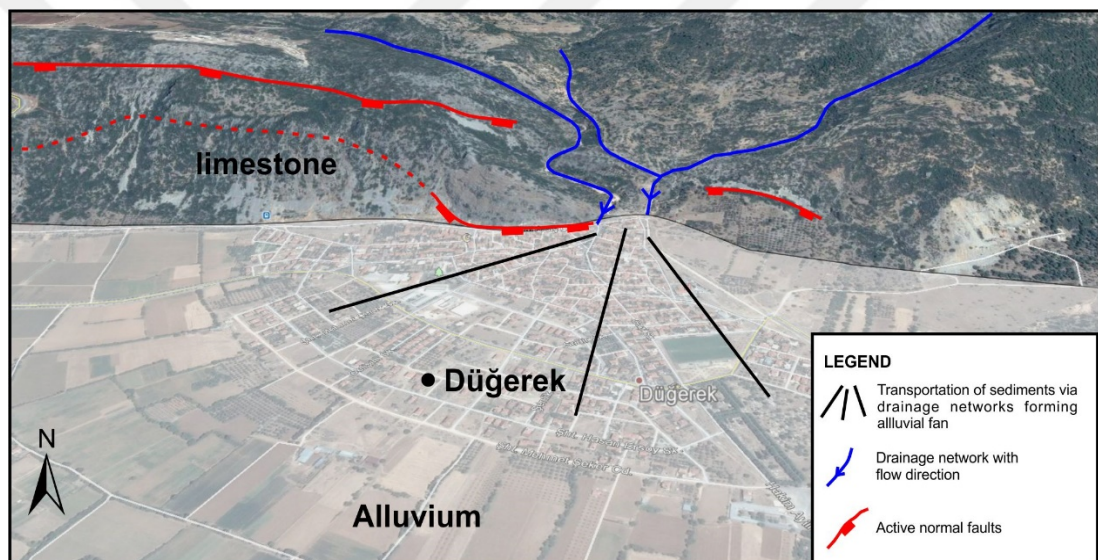


Figure 4. 8. Schematic illustration of Düğerek region with satellite image basemap. Düğerek is located on alluvial fan which is formed because of tectonic uplift in the area. Fault is covered by colluviums at the western part of region and covered fault is showed with dashed line .

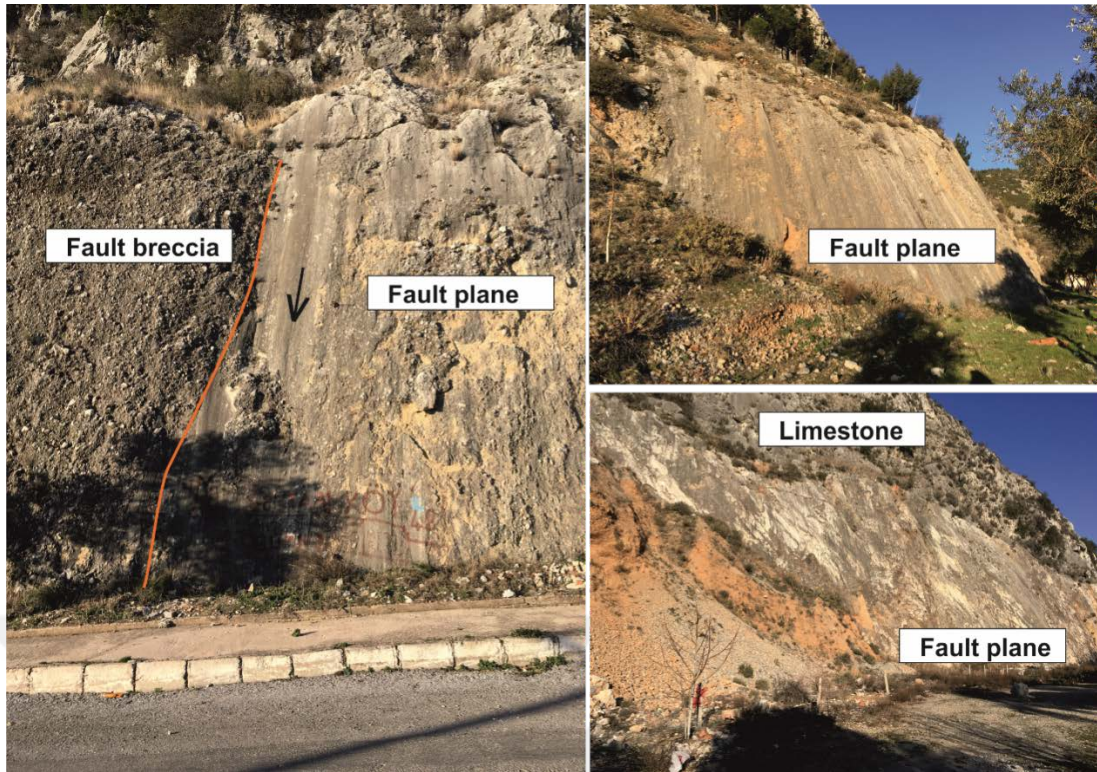


Figure 4. 9. Fault planes of Muğla Fault near Düğerek village are shown in this Figure. Slikenlines and ondulations are clear in Figure 4.16 a and b. Figure 4.16 a. fault breccias are seen.

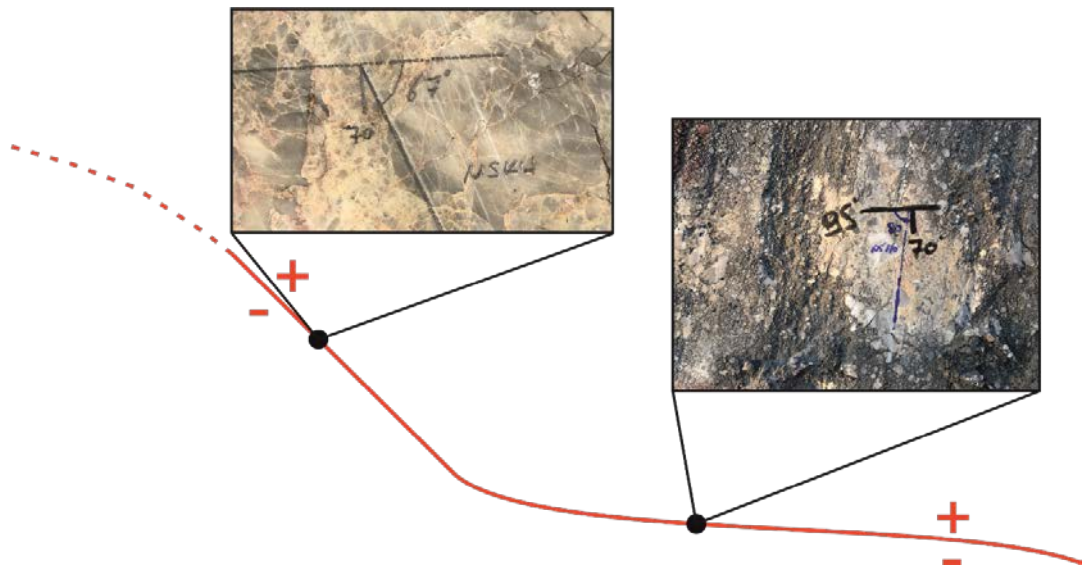


Figure 4. 10. Düğerek basin margin fault is not completely linear fault and its strike changes. Different slip directions measured for two different strike values. Red lines indicating the Düğerek fault.

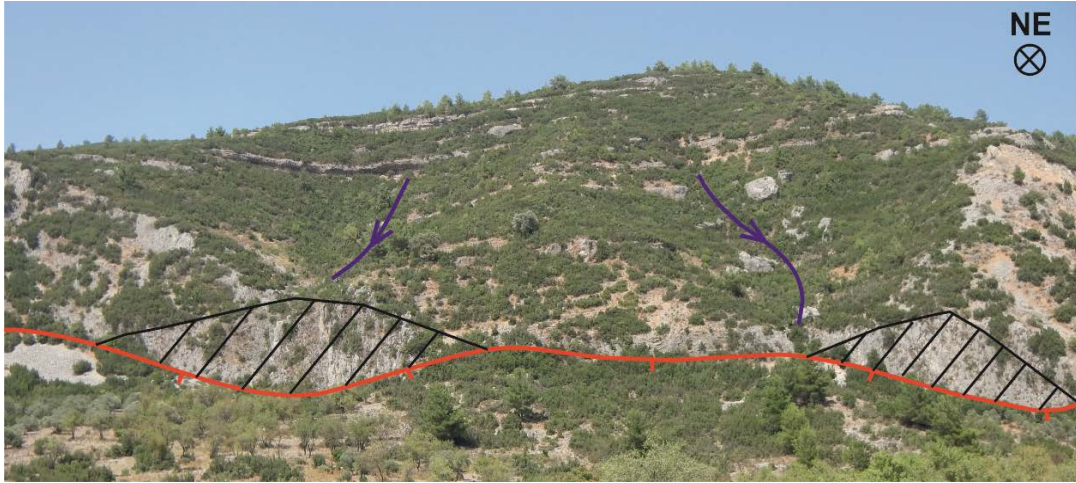


Figure 4. 11. Schematic illustration of the hanging valleys and iron flats (dashed surfaces) near Düğerek district. Tectonic processes prevail against the surface processes and the morphology is shaped by tectonic processes.

Düğerek is attached to Muğla with a single limestone hill within the basin. Muğla is located on a huge alluvial fan formed by tectonic uplift. Muğla plain is fed by large drainages incising limestone hills at the Northern margin (Figure 4.12).

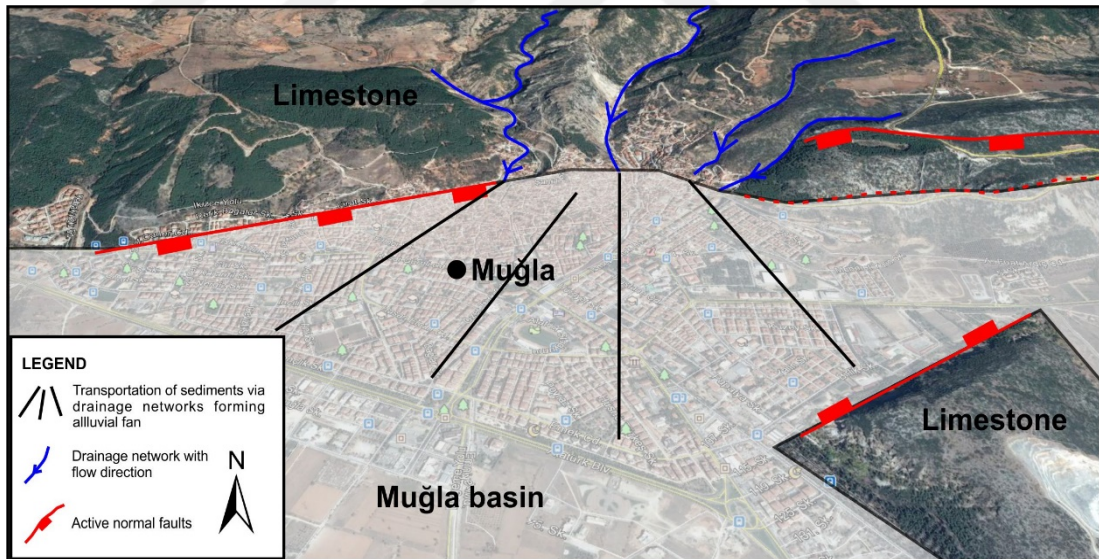


Figure 4. 12. Schematic illustration of Muğla plain. Muğla plain is fed by large streams at the Northern margin of the basin and because of tectonic uplift sediments deposited as alluvial fan. There is a fault controlled single limestone hill in the middle of the basin.

Muğla plain is attached to Yatağan plain (Paşapınarı basin) with a belt at its Western side which is called Menteşe district. Menteşe district is highly segmented from

North to South and because of the segmentation relay ramps are observed. Mentese district is a key location in the determination Holocene activity of the faults in the region because 50cm offset is observed in the colluviums deposited in front of the faults (Figure 4.13 and Figure 4.14). Hanging valley is also observed in this location (Figure 4.13b). Geological cross section of the area is given in Figure 4.15.

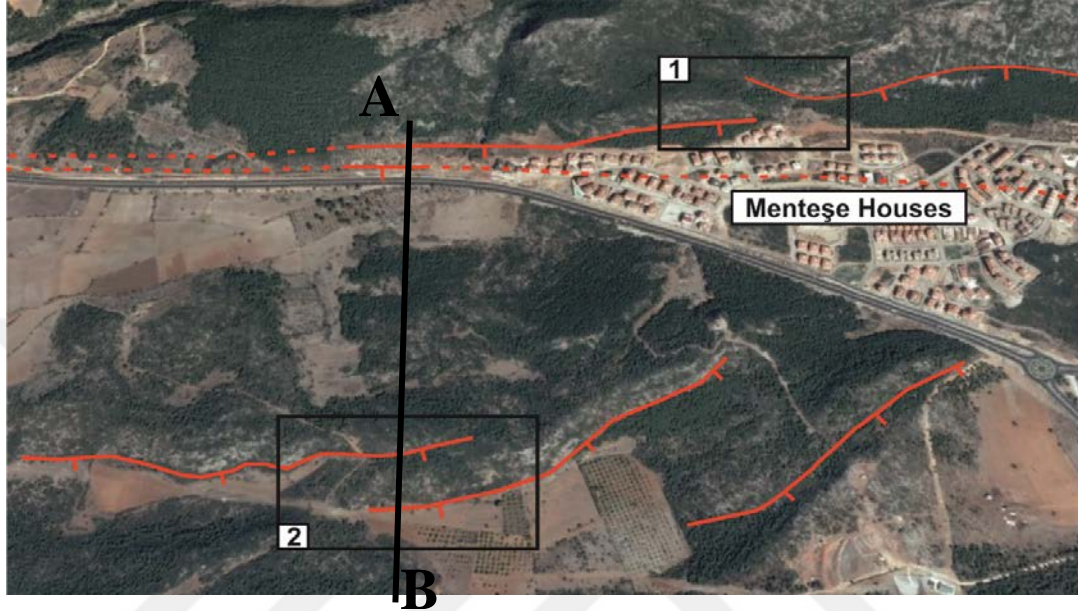


Figure 4. 13. Mentese region is a highly-segmented part of Muğla fault zone. In the parts of segmentation relay ramps formed. Black boxes with the 1 and 2 numbers are relay ramps. Black line indicates the line of cross section.

Fault at the southernmost segment of Mentese district is given in the Figure 4.16. Region shows topographic escarpment and fresh fault planes. Slickenlines or undulations are not observable on the fault planes.

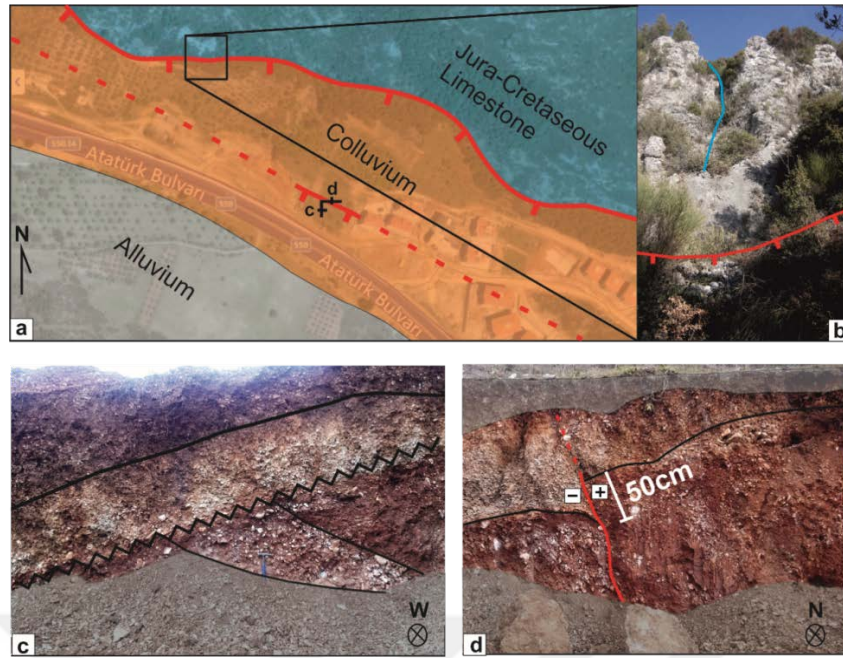


Figure 4. 14. a) Bird view satellite image with geological units (Satellite image obtained from Bing maps). Locations of the photographs have been shown in Figure 4.6 a. b) Hanging valley is observed at the Major Mentese fault. This indicates that tectonic processes prevail against the surface processes in this region. c) Young deposits have been tilted towards the fault. d) 50cm downthrown observed in the colluviums. This is a normal fault which is seen as reverse fault because of the direction of trench's wall. Gray shaded parts in Figure 4.6 c. and d. are waste deposits and the soil cover.

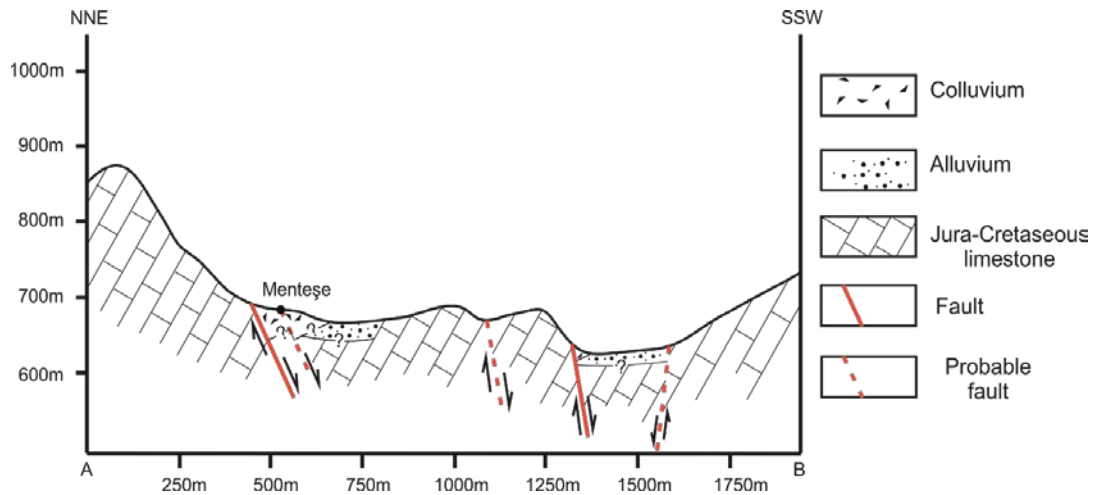


Figure 4. 15. Cross section of the Mentese region. There are lots of fault sets in the area. Mentese part of the cross section is the location mentioned in Figure 4.6 c and d.

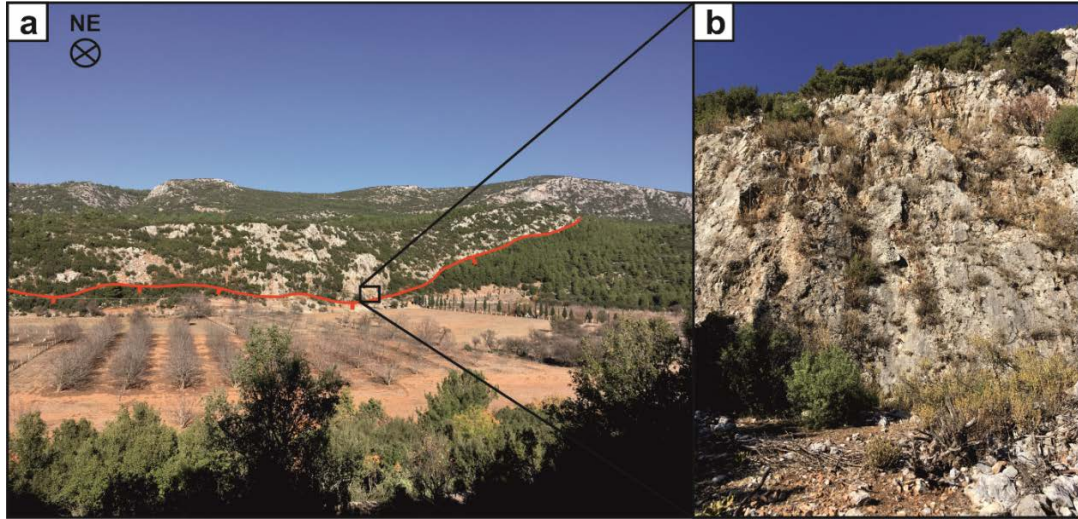


Figure 4. 16. Photograph of one of the faults mentioned in the Figure 4.7. a) Whole view of the fault b) photograph of the fault surface.

Yatağan basin extends NW to SE beginning from Yatağan at the NW to Salihpaşalar village in the SE . NW-SE trending Yatağan basin is separated from the topographic highs from its SW margin by NE dipping high angle normal faults and has a narrow but long shape. It is located between Western Menteşe Highs and Eastern Menteşe Highs (Gürer et. al., 2011).

Aldağ hill, Ayıalan hill, Bakacak hill, Aladağ hill, Kırtaş hill, Kocadüz hill and Karakuyu hill are the names of these important topographic highs. Base height of the basin is about 350-400m and tilted towards the fault. Kamış stream (Kayan, 1979) flows next to the Yatağan fault and is resulted because of the tilting of the basin.

Topography changes abruptly at the SW side of the basin. This abrupt change has resulted in the formation of hanging valleys and alluvial fan deposits. Fault planes are observed at the several parts of Yatağan fault between Paşapınarı and Bahçeyaka villages. Fresh fault planes are suitable for strike-dip and rake angle measurements. Schematic illustration of Yatağan basin and photograph of the Yatağan fault just next to the Paşapınarı village are given in the Figure 4.17 and 4.18 respectively.

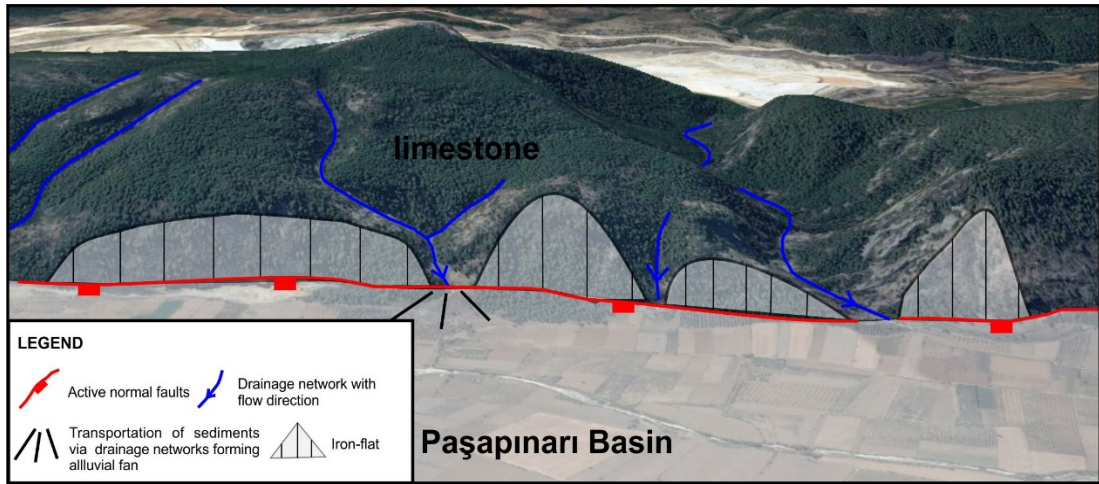


Figure 4. 17. Schematic illustration of Paşapınarı fault and related flat-irons, hanging valleys and fault controlled alluvial fan. Older long stream at the right side forms a windgap. Flat-irons are either in the form of triangular or trapezoidal shapes. Basin margin fault bounds recrystallized limestone of Menderes Massif and alluviums of Paşapınarı basin.



Figure 4. 18. Schematic illustration of the Paşapınarı part of Yatağan fault. SW margin of the basin is bounded by faults and resulted in the formation of hanging valleys and alluvial fan deposits. No deformation has been observed on the colluvium and alluvial fan deposits at this region.

Paşapınarı section of the Yatağan fault is separated from Bahçeyaka section. Bahçeyaka fault plane is more deformed and slickenlines are not clear. Instead of slickenlines, ondulations on the fault surface are observable and indicate right lateral component on the movement with the slickenlines on the Paşapınarı section. In the

Paşapınarı region there are several deformations on the footwall. Photograph of the fault of Bahçeyaka section is given in the Figure 4.19.



Figure 4. 19. Bahçeyaka fault plane. Narrow and high colluvial fan and hanging valleys are the indicator of a continuous uplift in the area. Ondulations on the fault plane showing a right lateral component.

Western part of the Bahçeyaka shows more sinuous form and streams cross with the basin. Recrystallized limestone near the Paşapınarı region turns into phyllite near Bahçeyaka village. Fault morphology shows itself as instant topographic changes through west of Bahçeyaka.

However, NE margin of the basin is characterized by U shaped and wide valleys. SW Margin is linear while the NE margin is sinuous indicating the power of surface processes is high in the NE part of basin. So, SW-NE cross section of the area shows asymmetric profile.

At the western part of the basin, near Şahinler village, uplift on the morphology can be easily traced along the whole mountain. But, the surfaces are highly deformed and slickenlines and undulations can't be observed. The middle area of this region has a flat area which indicates an erosional area. Photograph of the morphology near Şahinler village is given in the Figure 4.20.



Figure 4. 20. Şahinler region of the Yatağan fault. Fault plane is not observable but the faulting morphology is covered.

Geomorphology map of the study area is given in the Figure 4.21 below.

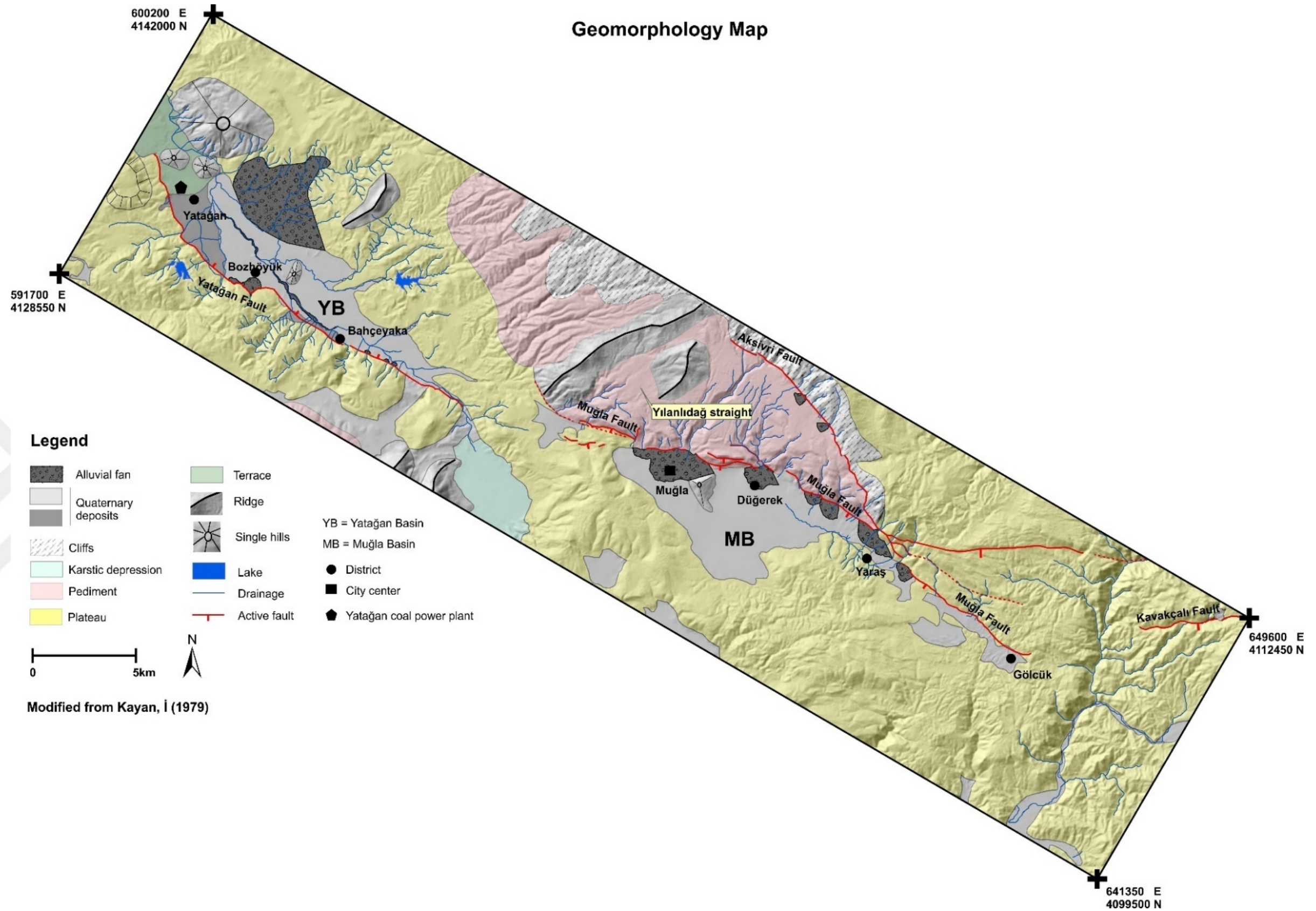


Figure 4. 21. Geomorphology map of the study area (Modified from Kayan, 1979)

5. MORPHOMETRIC ANALYSIS

Morphometry is the measurement of the shape of landscape, quantitatively and landforms are characterized by their sizes, altitudes and slopes. Calculation geomorphic indeces is way to compare different landforms by identifying characteristic of an area (Keller and Pinter, 1996)

In this study, morphometric analyses have been conducted on the fault generated mountain fronts and stream channel gradients. 10 basins and related stream channels in Muğla section and 13 basins and related stream channels in Yatağan section have been studied. Asymmetry factors, hypsometric curves, valley-floor width to height ratios of the basins and Hack's stream gradient index of streams have been calculated. In the calculation of asymmetry factors, downstream left side area is selected as indicator. The study area is divided into 2 sections as Muğla region and Yatağan region and analyses have been evaluated individually for each section.

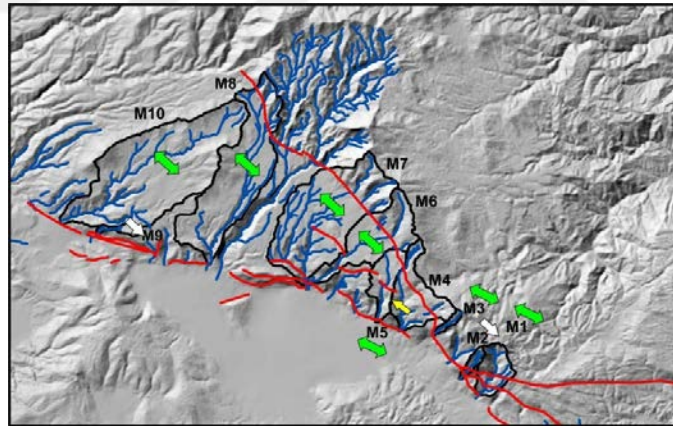


Figure 5. 1. Overall view of the drainage basins and calculated asymmetries at the fault generated mountain fronts at the Muğla Polje. Muğla region is simply characterized by NW-SE trending Muğla-Yaraş and Yılanlıdağ segments. Green colored arrows indicate the basins in which there is no observed asymmetry. Yellow arrow indicate downstream right side asymmetry and white arrow used for downstream left side asymmetry.

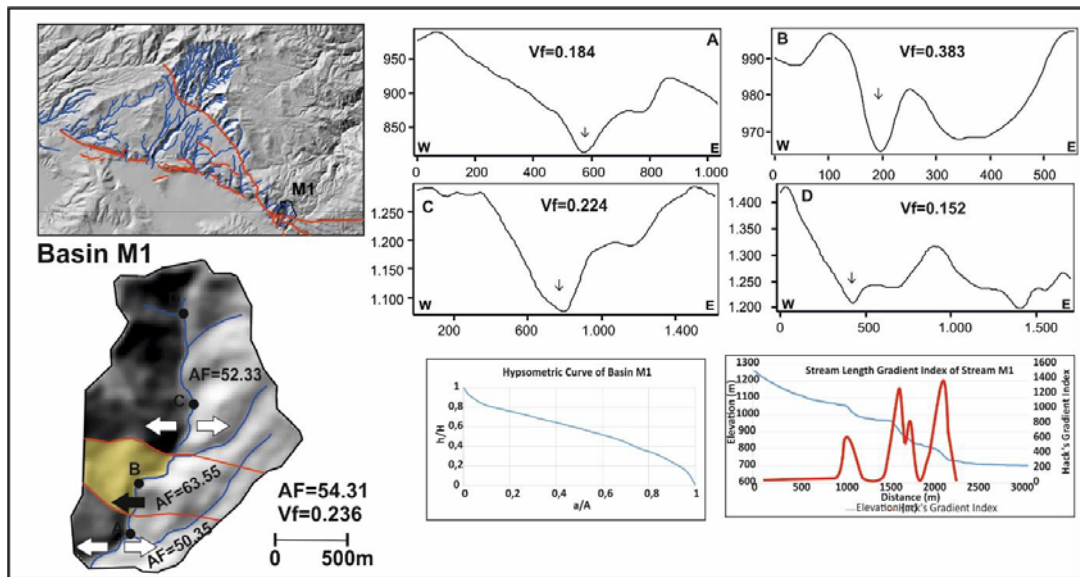


Figure 5. 2. Morphometric analyses results of basin M1. Vf values indicate V-shaped valleys.

Hypsometric curve indicates young a basin morphology influenced by tectonic processes. Hack's stream gradient index indicates that faults are active. AF values do not show any asymmetry in the overall of the basin. Middle block shows asymmetry individually.

Results

Size: The main stream channel of M1 is 2.5 km long and the drainage basin is 2.31 km².

Faults: The basin is cut by two faults therefore can be considered to be consisting of 3 blocks.

Asymmetry factor (AF): Downstream left side area of the basin is 1.25 km², compared to a total basin area of 2.31 km². I applied the AF index for each block to evaluate their individual deformation pattern. From bottom to top the AF index are 50.35%, 63.55% and 52.33% respectively. General AF of the basin is 54.31%. Left side (downstream) area of the basin is a little larger than the right one. The largest difference in the area is observed in the middle block with an AF value of 63.55%.

Geology: A great portion of the basin is composed of dolomite and the drainage flows within this unit. A small portion of the basin is composed of metasandstone-metaconglomerate-metapelite alternations (Fig.Xb).

Hypsometric curve: Hypsometric curve of the basin shows convex to sigmoidal shape.

Valley floor width to height ratio: Vf value of the basin is 0.236. Vf values from mouth to source are between 0.1 and 0.4.

Hack's stream gradient index: SL along the drainage show peaks along downstream where the profile of the stream changes instantly with the distances of 560, 1300 and 1400 m. The magnitude of peaks is increasing towards the mouth of the stream

Evaluation

Drainage of this basin flows close to the middle of the basin with an AF value of 54.31 and it does not show any asymmetry except the middle block. Middle block is showing asymmetry towards downstream right side of the basin.

Hypsometric curve of the basin is typical for young basins which are influenced by tectonic uplift and are less affected from erosional processes.

The sigmoidal shape of the hypsometric curve shows that the basin morphology is relatively young and increasingly influenced by tectonic uplift downstream.

The low values of Vf index identify a high rate of tectonic activity, i.e. uplift.

The three peaks in the Hack's stream gradient index in the increasing order from source to mouth indicates an increasing faulting activity downstream.

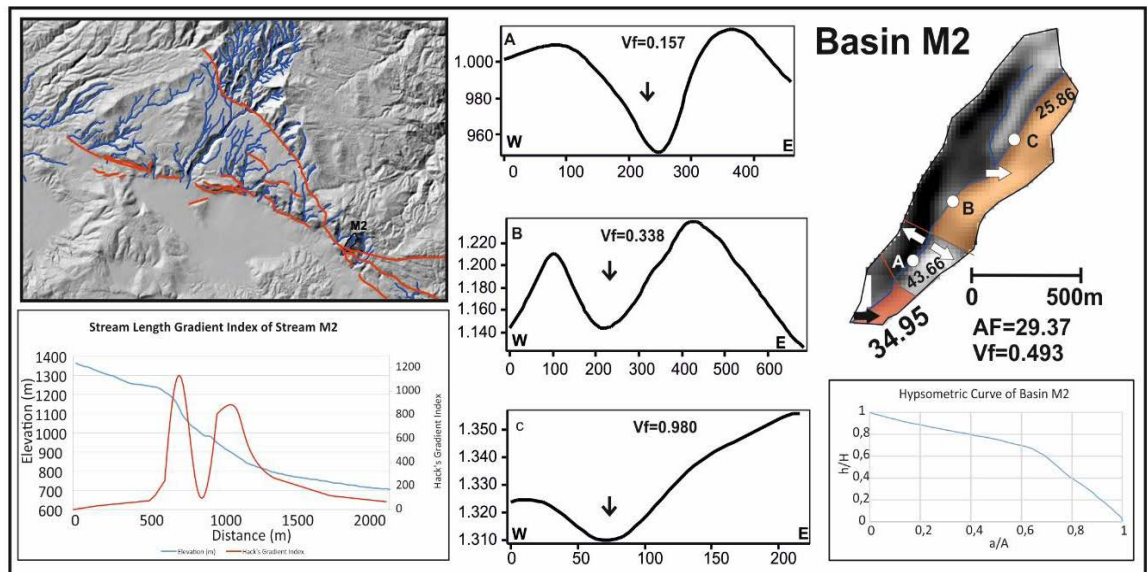


Figure 5. 3. Morphometric analyses of basin M2. Decreasing Vf values from source to mouth indicate increase in the effect of tectonic activity towards mouth. Hypsometric curve indicates that basin is young and is influenced by tectonic processes. Hack's stream gradient index indicates that faults are active. AF value shows asymmetry towards the downstream left side that may be related with tectonic tilting.

Results

Size: The stream channel of M2 is 1.3 km long and the drainage basin has an area of 0.5 km².

Faults: The basin is cut by two faults therefore can be considered to be consisting of 3 blocks. **Asymmetry factor (AF):** Downstream left side area of the basin is 0.14 km², compared to a total size of 0.5km². I applied the AF index for each block to evaluate their individual deformation pattern. AF of each block from bottom to top are 34.95%, 43.66% and 25.86%. General AF of the basin is 29.37%. Left side (downstream) area of the basin is very small compared with the right side of the basin.

Geology: Basin is entirely composed of dolomite.

Hypsometric curve: Hypsometric curve of the basin shows an ideal convex shape.

Valley floor width to height ratio: Vf values of the basin is 0.493. Values of Valley floor width to height ratio (Vf) increases from mouth to source of stream.

Hack's stream gradient index: SL along the drainage shows two peaks downstream where the topographic profile of the channel instantly gets steeper; at values of 1112 and 800 gradient meters.

Evaluation

Drainage of this basin flows next to the left divide (downstream) of the valley and shows a distinct asymmetry towards that might indicate tilting. The middle block of the basin has a higher AF value of 43%, which might be less amount of tilting compared to the other blocks.

Hypsometric curve of the basin is typical for young basins which are influenced by tectonic uplift and are less affected from erosional processes.

Downstream left valley side for all of the 3 profiles of a, b and c are steeper relative to right side. This is because the water incises at the valley side where the basin is tilted and forms steeper slopes.

Values of Valley floor width to height ratio (V_f) is decreasing from source of the stream to the mouth and this is the indicator of increasing effect of faults from top to bottom. At the higher portions of the basin V_f value is 0.9 and indicates that these portions are not affected from the activity of faults too much and is on the state of transition from V shape to U shape. Otherwise, low V_f value near the basin margin fault (the bottom segment) is the indicator of increasing tectonic activity.

Because stream flows on a single geological unit, high Hack's gradient index values are directly linked with active faulting and this supports the activity of these faults. According to the Hack's gradient index, faults in this portion are active and according to the V_f values and shape of Hypsometric curve their degree of activity are high.

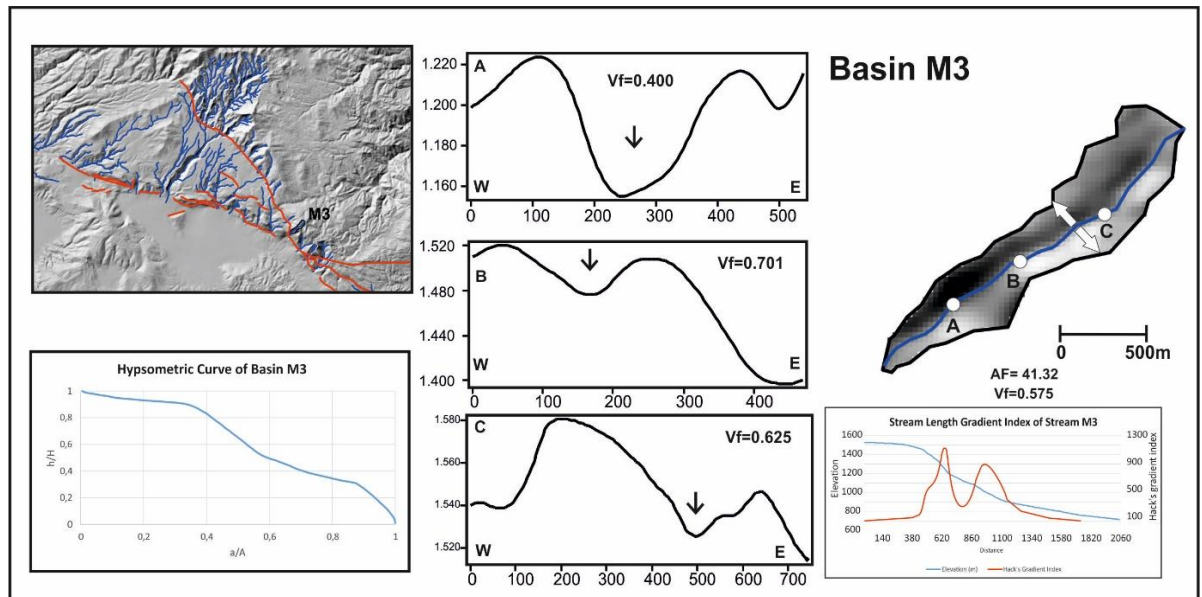


Figure 5. 4. Morphometric analyses of basin M3. Moderate Vf values indicate transition from young phase to old phase. Hypsometric curve shows transition from young-phase to old-phase. Hack's stream gradient index indicates that faults are active. AF value does not show asymmetry.

Results

Size: The main stream channel of M3 is 1.5 km long drainage and has an area of 0.4 km².

Asymmetry factor (AF): Downstream left side area of the basin is 0.14 km², compared to a total size of 0.35 km². AF of the basin is 41.32%. Left side (downstream) area of the basin is quite small compared with the right side of the basin.

Geology: Basin is entirely composed of limestone.

Hypsometric curve: Hypsometric curve of the basin has 2 stage shape beginning with convex shape and turns into sigmoidal shape.

Valley floor width to height ratio: Vf value of the basin is 0.575. Vf values from mouth to source of stream are 0.400, 0.701 and 0.625.

Hack's stream gradient index: SL along the drainage shows two peaks downstream where the topographic profile of the channel instantly gets steeper; at values of 1110 and 859 gradient meters.

Evaluation

Drainage of this basin flows from downstream left side of the basins and shows a small asymmetry. AF value of the basin is not too high to be able to mention about tectonic tilting.

Hypsometric curve of the basin is typical for young basin which are influenced by tectonic uplift and are less affected from the erosional processes in the 1st stage and relatively a mature to old stage in 2nd stage.

Increase of the valley floor width to height ratio (Vf) values from mouth to source of the valley, is the indicator of decreasing effect of faults from bottom to top. Downstream right valley side for all of the 3 profiles of a, b and c are steeper relative to left side but slope amounts are not different from each other. Relatively moderate values of Vf supports the transition from young phase to old phase which is the case in hypsometric curve.

There are two Knick points and 2 peaks in the SL index graph. Because stream flows on a single geological unit, high Hack's gradient index values are directly linked with active faulting.

According to the Hack's gradient index, faults in this portion are active and according to the Vf values and shape of Hypsometric curve their degree of activity is high.

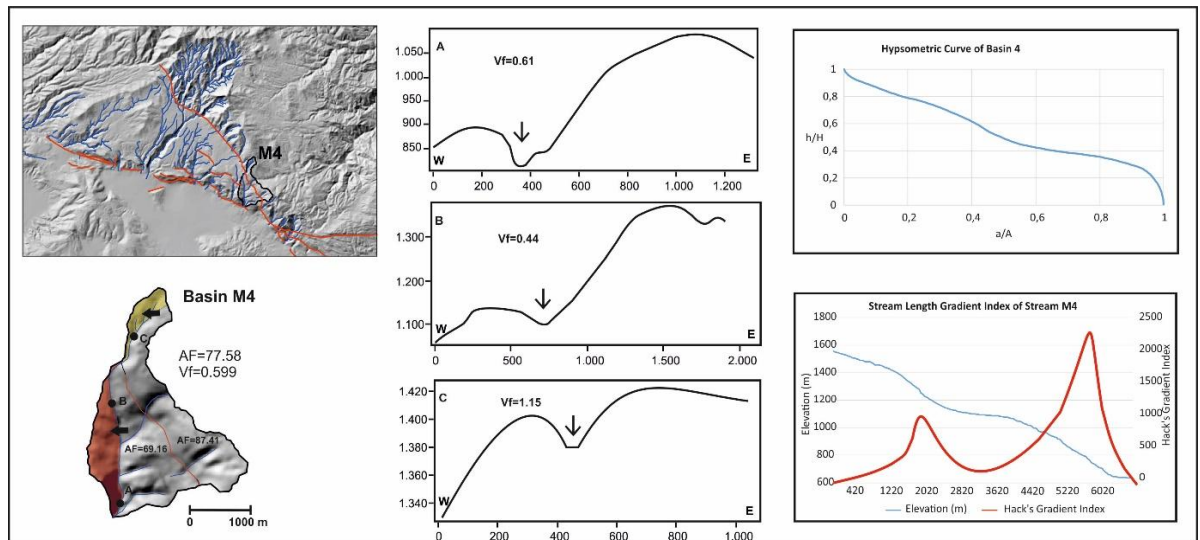


Figure 5.5. Morphometric analyses of basin M4. Moderate and high Vf values indicate transition from V-shaped valley to U-shaped valley from mouth to source. Hypsometric curve shows transition from young-phase to mature-phase. Hack's stream gradient index indicates that faults are active. AF value shows asymmetry towards downstream right side of the basin.

Results

Size: The stream channel of M4 is 3.8 km long and the drainage basin has an area of 4.4 km².

Faults: Basin is cut by a fault and therefore can be considered to be consisting of two blocks.

Asymmetry factor (AF): Downstream left side area of the basin is 3.4 km² compared to a total size of 4.4 km². AF of the basin is 77.58%. Downstream left side area of the basin is too large compared with the right side of the basin.

Geology: Basin is entirely composed of limestone.

Hypsometric curve: Hypsometric curve of the basin shows convex to sigmoidal shape.

Value of Valley floor width to height ratio (Vf): Valley floor width to height ratio of the basin is 0.738. Valley floor width to height ratio values from bottom to top are 0.610, 0.44 and 1.15.

Hack's stream gradient index: SL along the drainage shows peaks downstream where the topographic profile of the channel instantly gets steeper at values of 1000 and 2300 gradient meters.

Evaluation

Drainage of this basin flows next to the right divide (downstream) of the valley and shows a distinct asymmetry towards that might indicate tilting in each block.

Hypsometric curve of the basin has a profile as if there is a transition from young to mature profile.

Moderate values of Valley floor width to height ratio (Vf) at points A and B and high values at the point C identify transition from V shape to U shape valley at the lower elevations and U shape valley at the top of the basin.

The two peaks of Hack's stream gradient index in the increasing order from source to mouth indicates an increasing faulting activity downstream.

Because stream flows on a single geological unit, high Hack's gradient index values are directly linked with active faulting. According to the Hack's gradient index, faults in this portion are active and according to the Vf values and shape of Hypsometric curve, basin margin fault has high to moderate activity and fault on the higher levels of the basin has moderate to low activity.

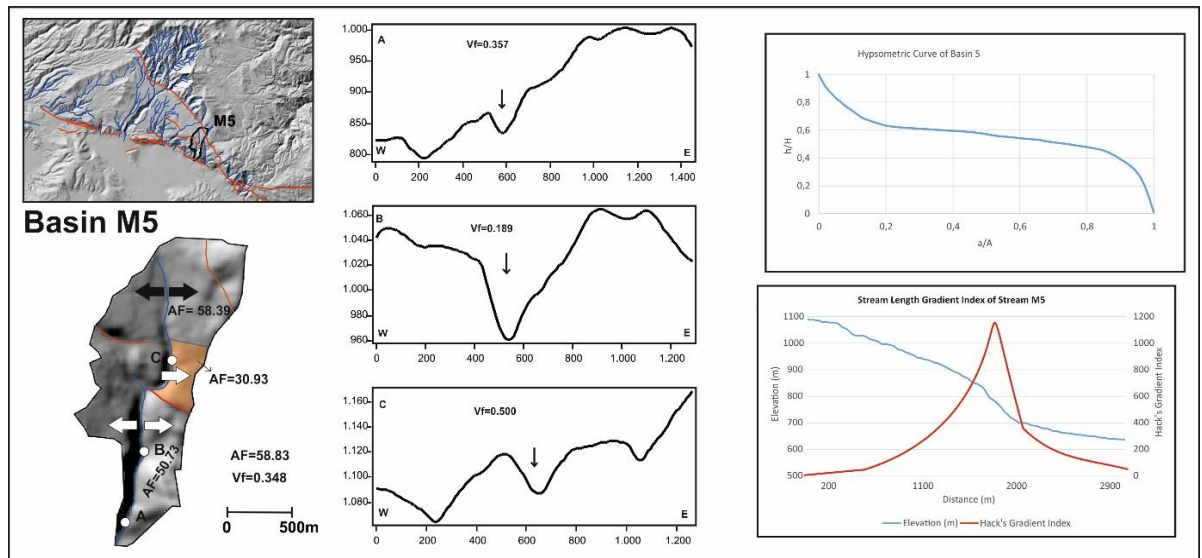


Figure 5. 6. Morphometric analyses of basin M5. Low Vf values indicate that valley is V-shaped. Hypsometric curve shows a perfect mature basin. Hack's stream gradient index indicates that the fault is active. AF value does not show asymmetry but the middle block shows asymmetry towards downstream left side of the basin individually.

Results

Size: The stream channel of M5 is 3 km long and the drainage basin has an area of 2.48 km².

Faults: Basin is formed of 3 blocks each separated from each other by faults.

Asymmetry factor (AF): Downstream left side area of the basin is 1.41 km². I applied the AF index for each block to evaluate their individual deformation pattern. AF of each block from bottom to top are 50.73%, 30.93% and 58.39%. General AF of the basin is 58.39%. Left downstream left side area of the basin is quite larger than the right one. Only middle block of the basin shows asymmetry.

Geology: Great portion of the basin is composed of limestone and small portion of the basin is composed of Pliocene deposits comprising sandstone-conglomerate and limestone alternations.

Hypsometric curve: Hypsometric curve of the basin shows ideal sigmoidal shape.

Valley floor width to height ratio: Vf value of the basin is 0.348. From mouth to source of the channel Vf values are 0.357, 0.189 and 0.500.

Hack's stream gradient index: SL along the drainage shows peak downstream where the topographic profile of the channel instantly gets steeper; at value of 1180 gradient meters.

Evaluation

Drainage of this basin flows from the downstream right divide of the valley and shows a distinct asymmetry towards that might indicate tilting. AF value of the basin may indicate small right tilting when it is evaluated with the adjacent M5 basin.

Hypsometric curve of the basin has ideal sigmoidal shape indicating mature form in which tectonic and erosional processes are in equilibrium.

Valley floor width to height ratio (Vf) values are between 0.1 and 0.6. Low to moderate values of Vf indicates a young to mature basin which is the case in hypsometric curve.

Because stream flows on a single geological unit, high Hack's gradient index value is directly linked with active faulting. According to the Hack's gradient index, fault is active and according to the Vf values and shape of Hypsometric curve their degree of activity is high to moderate.

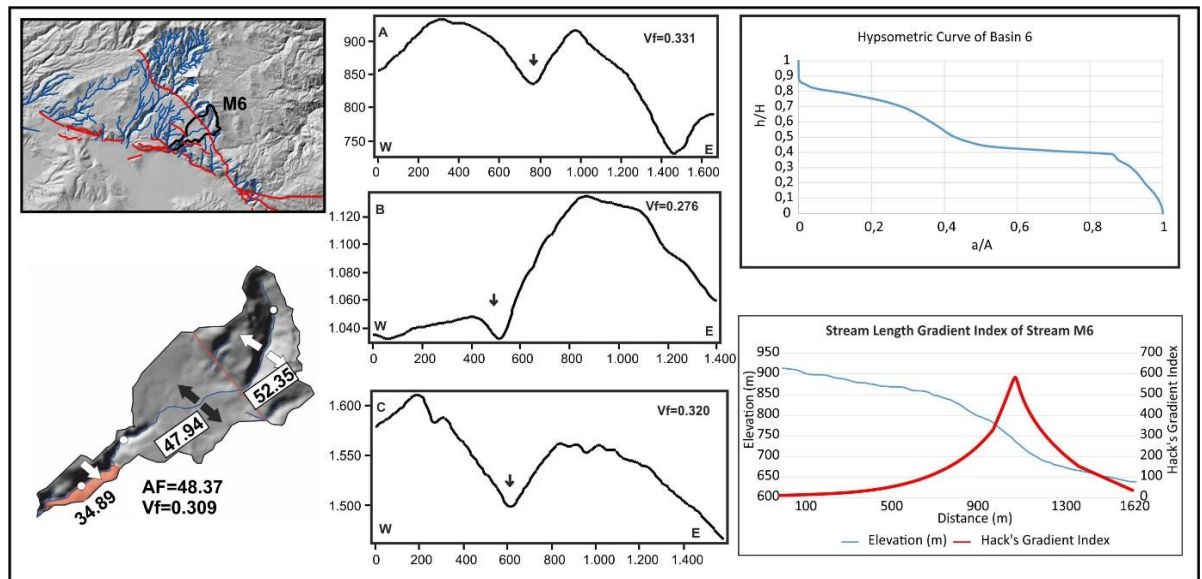


Figure 5. 7. Morphometric analyses of basin M6. Low Vf values indicate that valley is V-shaped. Hypsometric curve shows transition from young phase to mature phase. Hack's stream gradient index indicates that the fault is active. AF value does not show asymmetry but the lowermost block shows asymmetry towards downstream left side of the basin individually which may be the sign of tilting.

Results

Size: The main stream channel of M6 is 6 km long and drainage basin has an area of 6.10 km².

Faults: Basin is formed of 3 blocks each separated from each other by faults.

Asymmetry factor (AF): Downstream left side area of the basin is 2.95 km² compared to a total size of 6.10 km². I applied the AF index for each block to evaluate their individual deformation pattern. AF of each block from bottom to top are 34.89%, 47.94% and 52.35%. General AF of the basin is 48.37% and so close to equilibrium.

Hypsometric curve: Hypsometric curve of the basin shows convex to sigmoidal shape.

Valley floor width to height ratio: Vf value of the basin is 0.309. From mouth to source, Vf values are 0.331, 0.276 and 0.320.

Hack's stream gradient index: SL along the drainage shows peak downstream where the topographic profile of the channel instantly gets steeper; at a value of 590 gradient meters.

Geology: Great portion of the basin is composed of limestone. A small portion of the basin is composed of Pliocene deposits. Stream cuts Pliocene deposits at 970 m elevation.

Evaluation

Stream flows from the middle of the basin at the higher elevations but at the lower levels of the basin it shows asymmetry towards left that might indicate tilting.

Hypsometric curve of the basin has convex shape which implies young basins in which both tectonic and erosional processes modifies the landscape but tectonic processes are a little bit more active.

Low valley floor width to height (V_f) values indicates V-shaped valleys which are the characteristic features of young and tectonically uplifting environment.

Hack's gradient index value isn't affected from change of the formation so it is directly linked with active faulting and this supports the activity of the fault. According to the V_f values and shape of Hypsometric curve basin margin fault has quite high activity. This may be supported by the asymmetry of the basin at the lower levels.

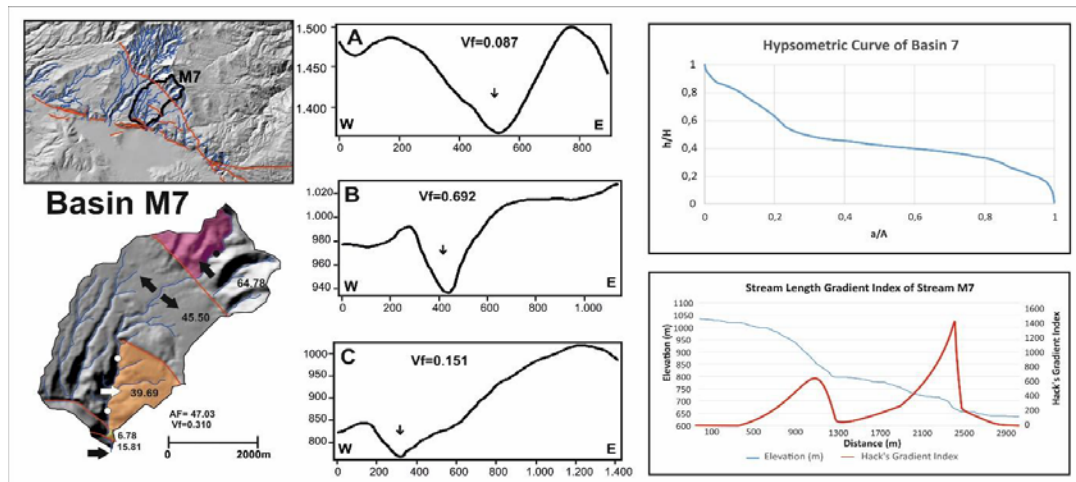


Figure 5. 8. Morphometric analyses of basin M7. Low Vf values indicate valley is V-shaped. Hypsometric curve reflects young basin. Hack's stream gradient index indicates that the faults are active. AF value does not show asymmetry in the overall but the uppermost block shows asymmetry towards downstream right side and the bottom 3 blocks show asymmetry towards downstream left side of the basin because faults collect all small drainages to a single branch.

Results

Size: The stream channel of M7 is 7 km long and drainage basin has an area of 14.2 km².

Faults: Basin is formed of 5 blocks each separated from each other by faults.

Asymmetry factor (AF): Downstream left side area of the basin is 6.7 km². I applied the AF index for each block to evaluate their individual deformation pattern. AF of each block from bottom to top are 15.81%, 6.78%, 39.69%, 45.50% and 64.78%. General AF of the basin is 47.03% and so close to equilibrium. Drainage flows from the right portion of the basin at its source and moves towards the left side towards the mouth.

Geology: Basin is composed of limestone and Pliocene deposits.

Hypsometric curve: Hypsometric curve of the basin shows sigmoidal profile.

Valley floor width to height ratio: Vf value of the basin is 0.310. From mouth to source, Vf values are 0.087, 0.692 and 0.151.

Hack's stream gradient index: SL along the drainage shows two peaks downstream where the topographic profile of the channel instantly gets steeper; at values of 1483 and 697 gradient meters.

Evaluation

Drainage of this basin flows from the right side of the basin at higher elevations and turns to left side at the lower elevations. The top block shows asymmetry towards right and the others show asymmetry towards left except 2nd block from top. Because 2nd fault collects all small drainages to a single branch, it is not a tectonic tilting.

Hypsometric curve of the basin is typical for mature basins which are influenced by both tectonic uplift and from erosional processes.

Downstream left valley side for all of the 3 profiles of a, b and c are steeper relative to right side. This is because the water incises at the valley side where the basin is tilted and forms steeper slopes.

Hack's stream gradient index value isn't affected from change in the formation so it is directly linked with active faulting and this supports the activity of the bottom fault because there is peak above the basin margin fault.

According to the Vf values basin margin fault has quite high activity and according to hypsometric curve basin is under the control of both tectonic and erosional processes. SL value does not show peak above the uppermost fault because this part of the uppermost fault may be inactive.

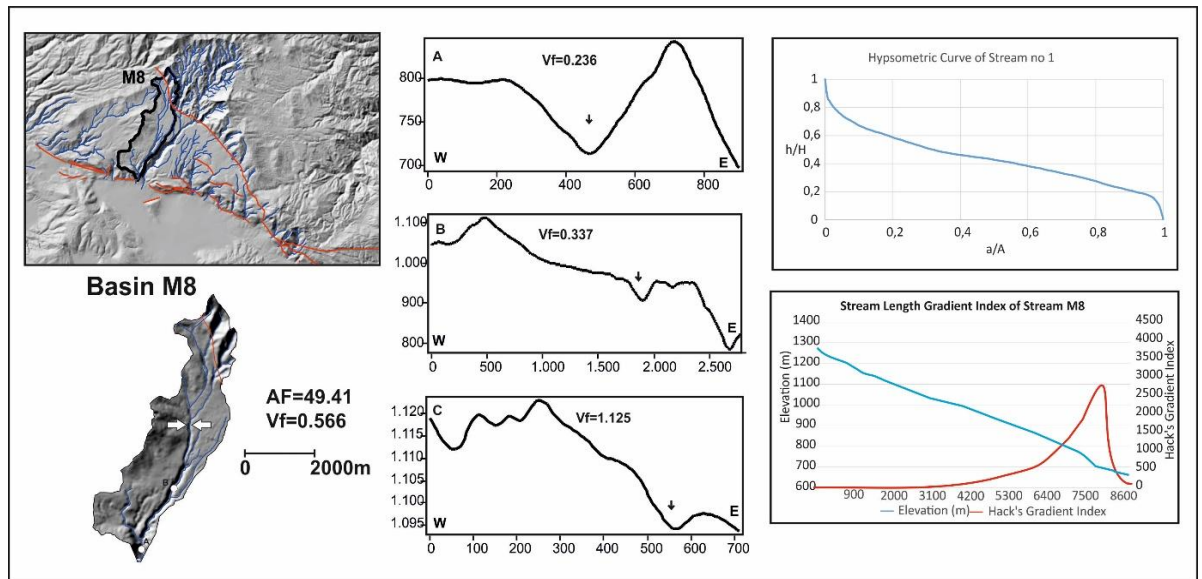


Figure 5. 9. Morphometric analyses of basin M8. Low Vf values indicate valley is V-shaped through the mouth of the basin. Hypsometric curve reflects mature basin. Hack's stream gradient index indicates that the fault is active. AF value does not show asymmetry in the basin.

Results

Size: The stream channel of basin M8 is 8 km long and drainage basin has an area of 12.8 km².

Asymmetry factor (AF): Downstream left side area of the basin is 6.32 km², compared to a total size of 12.8 km². AF of the basin is 49.41% and drainage flows from the middle of the basin.

Geology: Basin is composed of limestone and Pliocene deposits. Stream follows the contact between limestone and Pliocene deposits.

Hypsometric curve: Hypsometric curve of the basin shows sigmoidal profile.

Valley floor width to height ratio: Vf value of the basin is 0.566. From mouth to source, Vf values are 0.236, 0.337 and 1.125 and shows increase from mouth to source.

Hack's stream gradient index: SL along the drainage shows peak downstream where the topographic profile of the channel instantly gets steeper; at value of 2750 gradient meters.

Evaluation

Even if, AF value does not indicate any asymmetry, drainage of this basin flows from the right side of the basin near the source and left side of the basin near the mouth which may be the indicator of a tilting.

Hypsometric curve is typical for mature basin in which tectonic and erosional processes both modify the landscape.

The low values of Vf index identify a high rate of tectonic activity, i.e. uplift. At its mouth and high values of Vf at its source indicate the effects of erosional processes.

Because stream flows on a single geological unit, high Hack's gradient index values are directly linked with active faulting and this supports the activity of the basin margin fault. According to the Vf values and shape of Hypsometric curve basin margin fault has quite high activity and uppermost fault is inactive and indicates U shape valley.

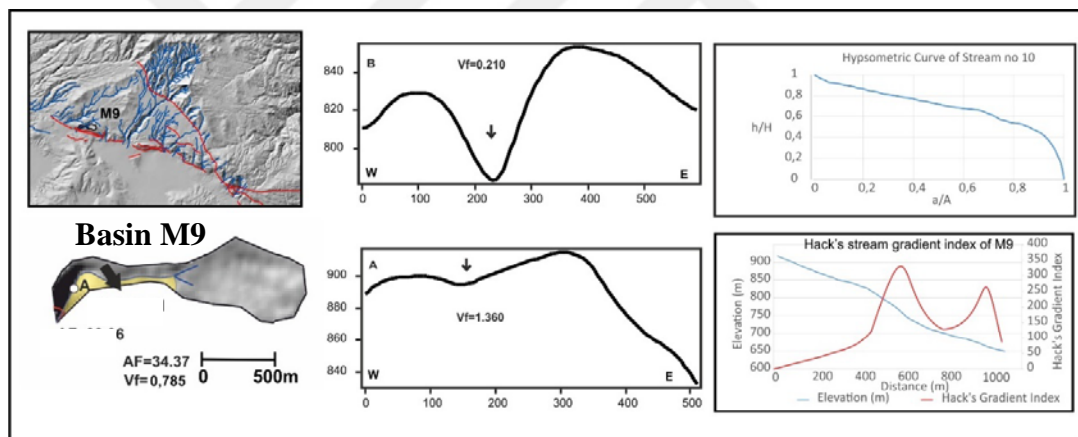


Figure 5. 10. Morphometric analyses of basin M9. Low Vf values indicate valley is V-shaped through the mouth of the basin and U-shaped through the source. Hypsometric curve reflects young basin. Hack's stream gradient index indicates that the faults are active. AF value shows asymmetry towards downstream left side of the basin.

Results

Size: The main stream channel of M9 is 1 km long and drainage basin has an area of 0.17 km².

Asymmetry factors (AF): Downstream left side area of the basin is 0.06 km². I applied the AF index for each block to evaluate their individual deformation pattern. AF of the areas bottom to top are 33.06% and 34.41%. General AF of the basin is 34.37% and drainage flows from the left side of the basin.

Geology: Basin is entirely composed of limestone.

Hypsometric curve: Hypsometric curve of the basin shows ideal convex profile.

Valley floor width to height ratio: Vf of the basin is 0.785. Decrease in the Vf value source to mouth is the indicator of increasing tectonic activity towards the mouth of the channel.

Hack's stream gradient index: SL along the drainage show peaks along downstream where the profile of the stream changes instantly. The magnitudes of peaks are 350 and 275 gradient meters.

Evaluation

Drainage of this basin flows next to the left divide (downstream) of the valley and shows a distinct asymmetry towards that might indicate tilting.

Hypsometric curve of the basin has ideal convex shape and ideal for young basins which are influenced by tectonic uplift and are less affected from erosional processes.

Because stream flows on a single geological unit, SL values are directly linked with the activity of the faults. SL index show peaks on the basin margin fault as two sets.

Vf values of the basin from mouth to source are 0.210 and 1.360 but the Vf value which is closer to the fault is important in evaluation of the degree of tectonic activity. The lower Vf value near the fault is indicator of the high tectonic activity of the fault. This assumption is supported by convex hypsometric curve which indicates that the area of the highlands is more than the average area.

According to SL index this fault is active and according to the hypsometric curve and Vf value our fault is highly active.

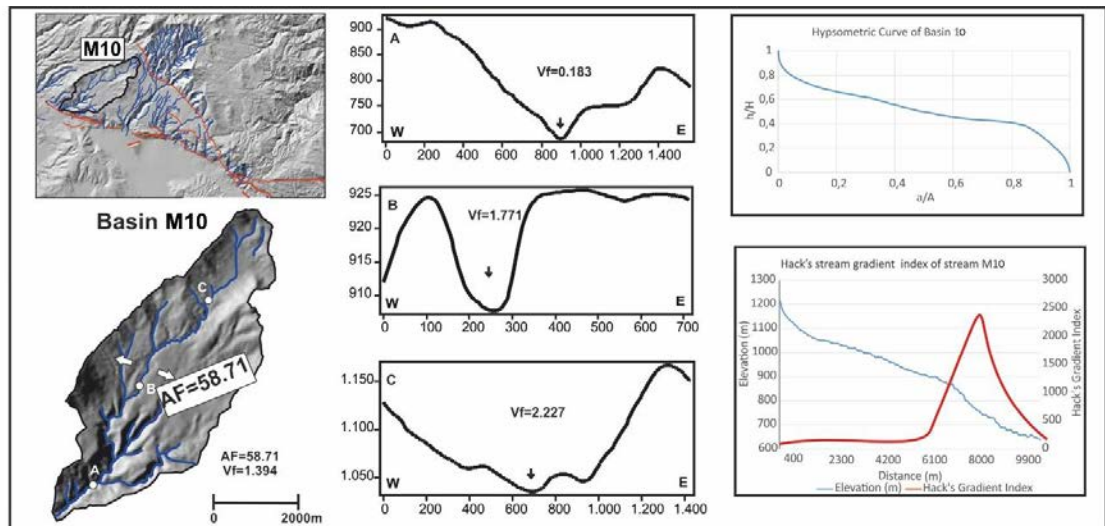


Figure 5. 11. Morphometric analyses of basin M10. Low Vf value at the mouth indicate V-shaped profile and high Vf values through the top reflects U-shaped profile. Hypsometric curve reflects mature basin. Hack's stream gradient index indicates that the fault is active. AF value does not show asymmetry.

Results

Size: The main stream channel of M10 is 9 km long drainage and drainage basin has an area of 19.66 km².

Asymmetry factor (AF): Downstream left side area of the basin is 11.55 km², compared to a total size of 19.66 km². AF of the basin is 58.71% and drainage flows from the right part of the basin.

Geology: Basin is composed of limestone and Pliocene deposits.

Hypsometric curve: Hypsometric curve of the basin shows sigmoidal profile.

Valley floor width to height ratio: Vf of the basin is 1.394. From bottom to top, Vf values are 0.183, 1.771 and 2.227.

Hack's stream gradient index: SL along the drainage show peak downstream where the topographic profile of the channel instantly gets steeper; at value of 2250 gradient meters.

Evaluation

Drainage of this basin flows from the downstream right divide of the valley and does not show important asymmetry that might indicate tilting.

Hypsometric curve is typical for mature basin which is both modified by tectonic and erosional processes in equal degree.

Vf value at point A is so low indicating V shaped valley. Decrease in the Vf values from source to mouth is the indicator of increase in the effect of tectonic activity towards the mouth.

Because drainage flows in a single geologic formation at the bottom of the basin Hack's index is directly linked with tectonic activity. According to Hack's gradient index the fault is active and according to Vf and hypsometric curve degree of activity of the fault is high.

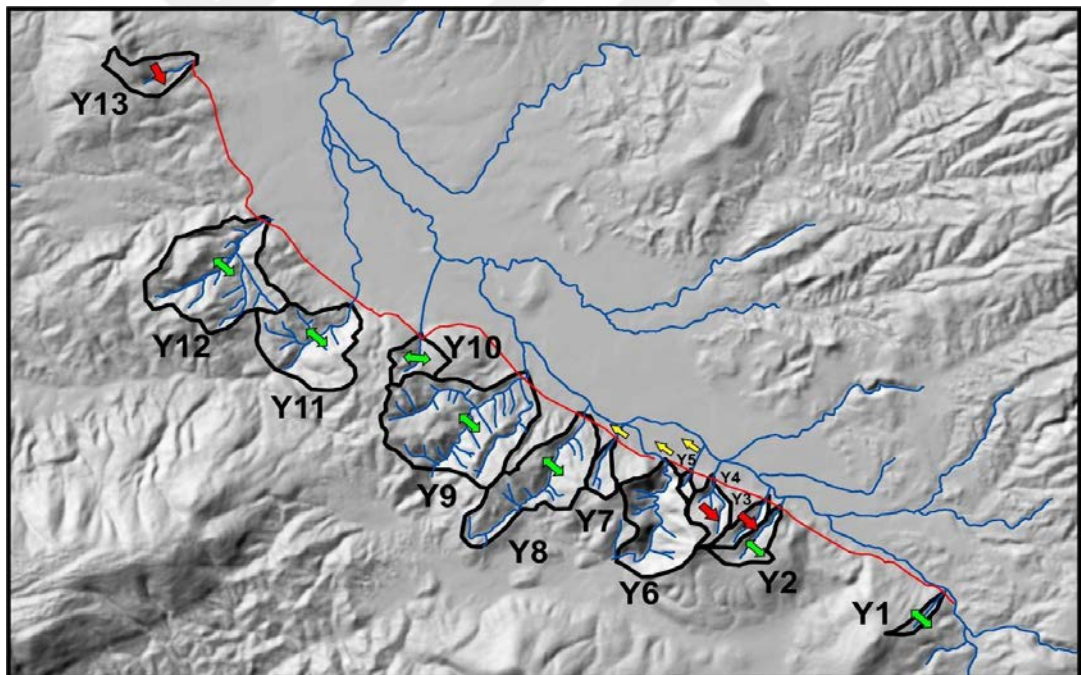


Figure 5. 12. Overall view of the basins in Yatağan depression. Green arrows are used for basins which do not show asymmetry, red arrows are used for basins show downstream right side asymmetry and yellow arrows are used to describe basin with downstream left side asymmetry.

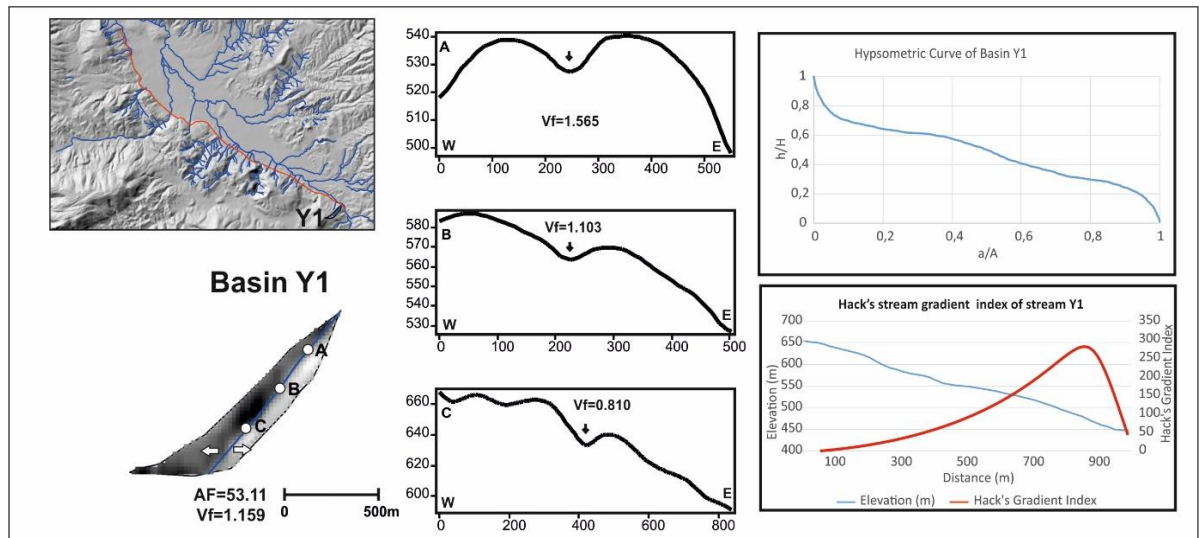


Figure 5. 13. Morphometric analysis of basin Y1. AF value does not show asymmetry. Vf values indicate valley is U-shaped. Hypsometric curve shows a mature basin. Hack's stream gradient index indicate that fault is active.

Results

Size: The main stream channel of Y1 is 875 m long and drainage basin has an area of 0.22 km².

Asymmetry factor (AF): Downstream left side area of the basin is 0.12 km², compared to a total size of 0.22 km². AF of the basin is 53.11% and drainage flows almost from the middle of the basin.

Geology: Basin is entirely formed of limestone.

Hypsometric curve: Hypsometric curve of the basin shows sigmoidal shape.

Valley floor width to height ratio: Vf value of the basin is 1.159. From bottom to top, Vf values are 1.565, 1.103 and 0.810.

Hack's stream gradient index: SL along the drainage shows peak downstream where the topographic profile of the channel instantly gets steeper; at a value of 325 gradient meters.

Evaluation

Drainage flows almost from the middle of the basin which means it does not show a distinct asymmetry towards that might indicate tilting.

Hypsometric curve of the basin is typical for mature basins which are modified both tectonic and erosional processes together.

Vf values are high at the basin and indicating U shaped valley. Because drainage flows in a single geologic formation at the bottom of the basin Hack's index is directly linked with tectonic activity. According to Hack's gradient index the fault is active and according to Vf and hypsometric curve degree of activity of the fault is low. SL values are really low relative to the other streams and this fault may be inactive for a long period.

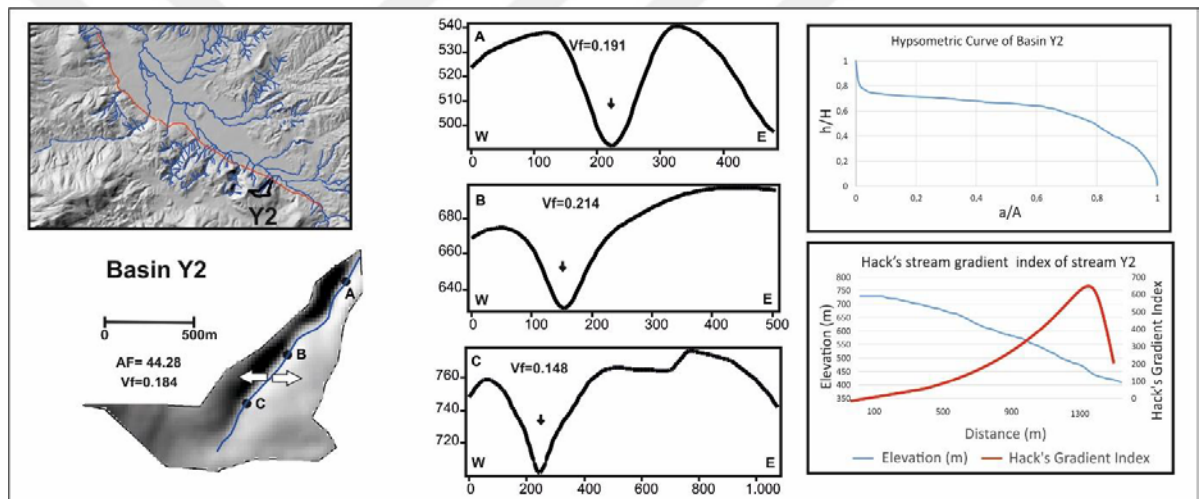


Figure 5. 14. Morphometric analysis of basin Y2. AF value does not show asymmetry. Vf values indicate that valley is V-shaped. Hypsometric curve shows that basin is young. Hack's stream gradient index indicate that fault is active.

Results

Size: The main stream channel of Y2 basin is 1.3 km long and drainage basin has an area of 0.64 km².

Asymmetry factor (AF): Downstream left side area of the basin is 0.28 km², compared to a total size of 0.64 km². AF of the basin is 44.28% and drainage flows almost middle of the basin.

Geology: Basin is entirely composed of limestone.

Hypsometric curve: Hypsometric curve of the basin shows convex shape.

Valley floor width to height ratio: Vf of the basin is 0.184. From bottom to top, Vf values are 0.191, 0.214 and 0.148.

Hack's stream gradient index: SL along the drainage shows peak downstream where the topographic profile of the channel instantly gets steeper; at a value of 664 gradient meters.

Evaluation

Drainage flows almost from the middle of the basin which means it does not show a distinct asymmetry towards that might indicate tilting.

Hypsometric curve has convex to sigmoidal shape indicating tectonic activity prevails against the erosional processes in the modification of landscape.

Values of valley floor width to height ratio (Vf) are low indicating V-shaped valleys which are the product of continuous uplift.

Because drainage flows in a single geologic formation, Hack's gradient index is directly linked with tectonic activity. According to Hack's gradient index the fault is active and according to Vf and hypsometric curve degree of activity of the fault is high.

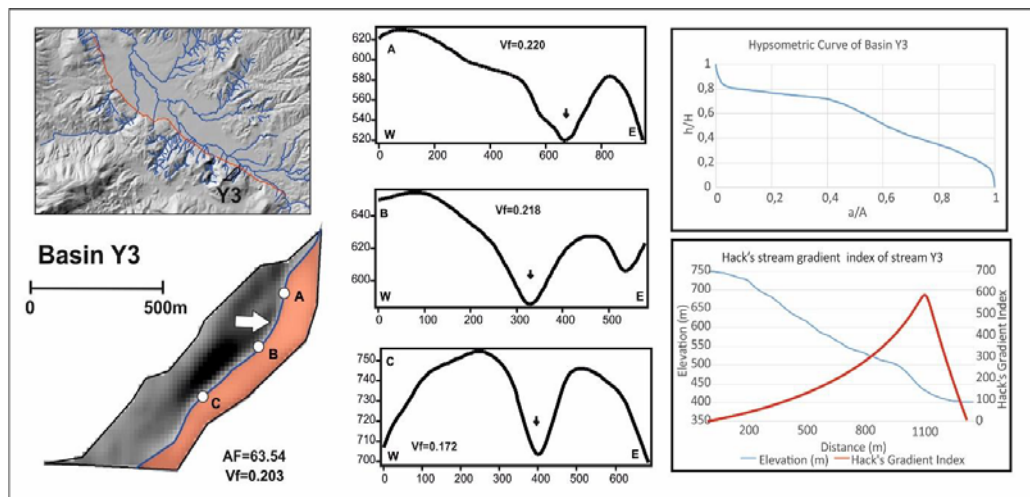


Figure 5. 15. Morphometric analysis of basin Y3. AF value shows asymmetry towards downstream right side of the basin. Vf values indicate that valley is V-shaped. Hypsometric curve shows that basin is young. Hack's stream gradient index indicate that fault is active.

Results

Size: The main stream channel of basin Y3 is 1 km long and drainage basin has an area of 0.45 km².

Asymmetry factor (AF): Downstream left side area of the basin is 0.29 km², compared to a total size. AF value of the basin is 63.54% and drainage flows from the right side of the basin.

Geology: Basin is entirely composed of limestone.

Hypsometric curve: Hypsometric curve of the basin shows convex profile.

Valley floor width to height ratio: Vf value of the basin is 0.203. From bottom to top, Vf values are 0.220, 0.218 and 0.172.

Hack's stream gradient index: SL along the drainage shows peak downstream where the topographic profile of the channel instantly gets steeper; at a value of 587 gradient meters.

Evaluation

Drainage flows almost from the downstream right side of the basin which means it shows a distinct asymmetry towards that might indicate tilting.

Hypsometric curve of the basin is typical for young basins which are influenced by tectonic uplift and are less affected from erosional processes.

Values of Valley floor width to height ratio (Vf) are low and indicating V-shaped valleys which are typical for tectonically uplifting area.

Because drainage flows in a single geologic formation, Hack's gradient index is directly linked with tectonic activity. According to Hack's gradient index the fault is active and according to Vf and shape of hypsometric curve degree of activity of the fault is high.

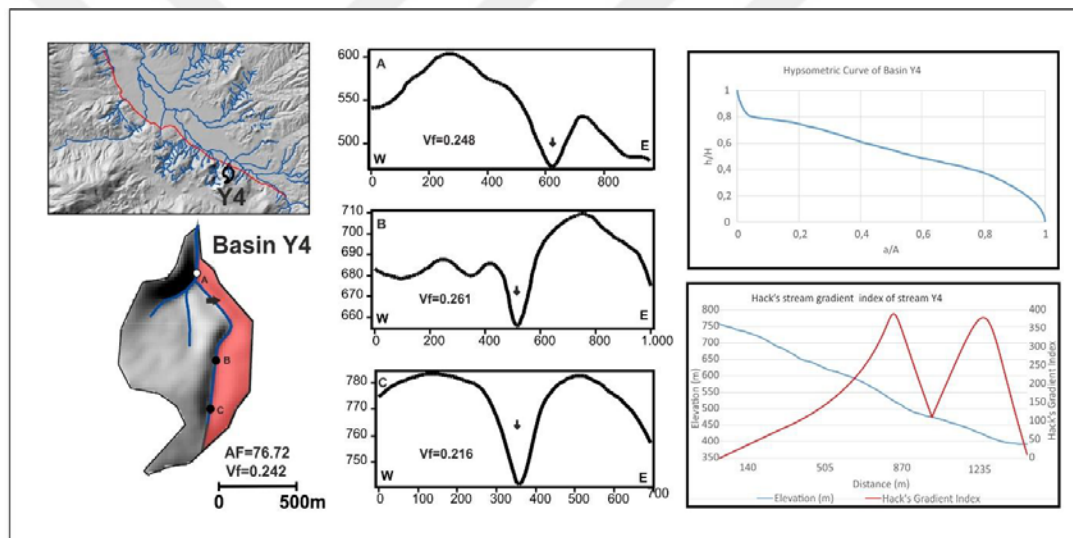


Figure 5. 16. Morphometric analysis of basin Y4. AF value shows asymmetry towards downstream right side of the basin. Vf values indicate that valley is V-shaped. Hypsometric curve shows that basin is young. Hack's stream gradient index indicate that faults are active.

Results

Size: The main stream channel of basin Y4 is 1.2 km long and drainage basin has an area of 0.72 km².

Asymmetry factor (AF): Downstream left side area of the basin is 0.55 km², compared to a total size of 0.72 km². AF value of the basin is 76.72% and drainage flows from the right side of the basin.

Geology: Basin is entirely composed of limestone.

Hypsometric curve: Hypsometric curve of the basin shows convex profile.

Valley floor width to height ratio: Vf value of the basin is 0.242. From bottom to top, Vf values are 0.248, 0.261 and 0.216.

Hack's stream gradient index: SL along the drainage show peaks along downstream where the profile of the stream changes instantly. The magnitudes of peaks are 387 and 366 gradient meters.

Evaluation

Drainage flows almost from the downstream right side of the basin which means it shows a distinct asymmetry towards that might indicate tilting.

Hypsometric curve of the basin is typical for young basins which are influenced by tectonic uplift and are less affected from erosional processes.

Values of Valley floor width to height ratio (Vf) are low and indicating V-shaped valleys which are typical for tectonically uplifting area.

Because drainage flows in a single geologic formation, Hack's gradient index is directly linked with tectonic activity. According to Hack's gradient index the fault is active and according to Vf and shape of hypsometric curve degree of activity of the fault is high.

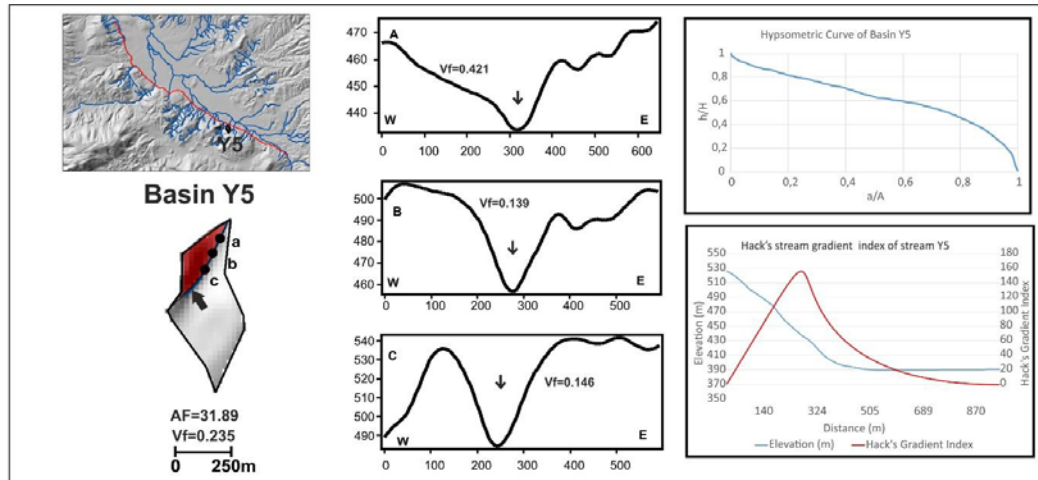


Figure 5. 17. Vf values indicate that valley is V-shaped. AF value shows asymmetry towards downstream left side of the basin. Hypsometric curve indicates that basin is young. Hack's stream gradient index implies that the fault is active.

Results

Size: Main stream channel of basin Y5 is 400 m long and drainage has an area of 0.13 km^2 .

Asymmetry factor (AF): Downstream left side area of the basin is 0.04 km^2 , compared to a total size of 0.13 km^2 . AF value of the basin is 31.89% and drainage flows from the left side of the basin.

Geology: Basin is entirely composed of limestone.

Hypsometric curve: Hypsometric curve of the basin shows perfect convex shape.

Valley floor width to height ratio: Vf value of the basin is 0.235. From bottom to top, Vf values are 0.421, 0.139 and 0.146.

Hack's stream gradient index: SL along the drainage shows peak downstream where the topographic profile of the channel instantly gets steeper; at a value of 152 gradient meters.

Evaluation

Drainage flows almost from the downstream left side of the basin which means it shows a distinct asymmetry towards that might indicate tilting.

Hypsometric curve of the basin is typical for young basins which are influenced by tectonic uplift and are less affected from erosional processes.

Values of Valley floor width to height ratio (Vf) are low and indicating V-shaped valleys which are typical for tectonically uplifting area.

Because drainage flows in a single geologic formation, Hack's gradient index is directly linked with tectonic activity. According to Hack's gradient index the fault is active and according to Vf and shape of hypsometric curve degree of activity of the fault is high.

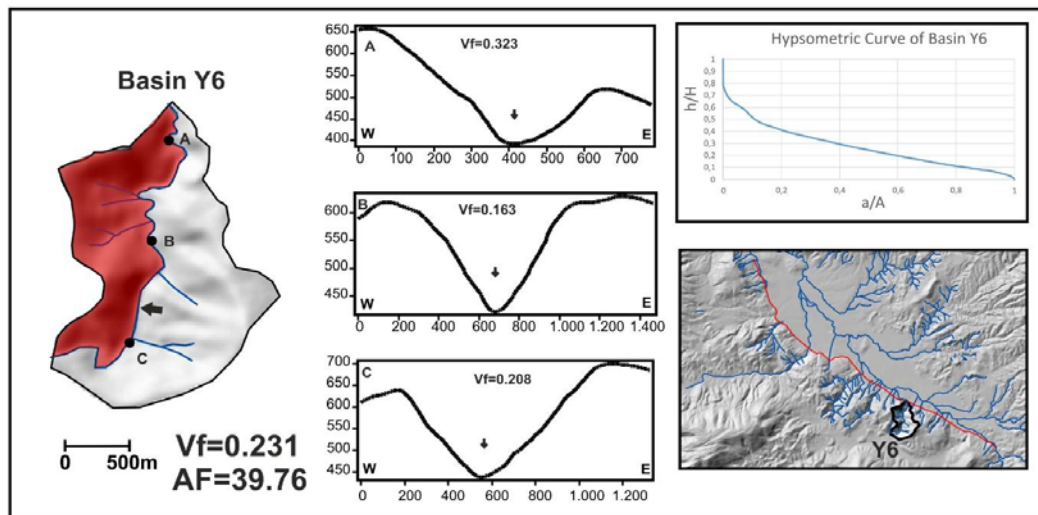


Figure 5. 18. Vf values indicate that valley is V-shaped. AF value shows asymmetry towards downstream left side of the basin. Hypsometric curve indicates that basin is old.

Results

Size: The main stream channel of basin Y6 is km long and drainage basin has an area of 2.57 km^2 .

Asymmetry factor (AF): Downstream left side area of the basin is 1.02 km^2 , compared to a total size of 2.57 km^2 . AF of the basin is 39.76% and drainage flows from the left side of the basin.

Geology: Basin is entirely composed of limestone.

Hypsometric curve: Hypsometric curve of the basin has concave shape.

Valley floor width to height ratio: Vf value of the basin is 0.231. From bottom to top, Vf values are 0.323, 0.163 and 0.208.

Hack's stream gradient index: SL analyse cannot be applied because stream flows between 2 segments of faults and it is not cut by fault.

Evaluation

Drainage flows almost from the downstream left side of the basin which means it shows a distinct asymmetry towards that might indicate tilting.

Hypsometric curve of the basin is typical for old basins whose landscape are modified by erosional processes and are less influenced by tectonic processes.

Values of Valley floor width to height ratio (Vf) are low and indicating V-shaped valleys which are typical for tectonically uplifting area.

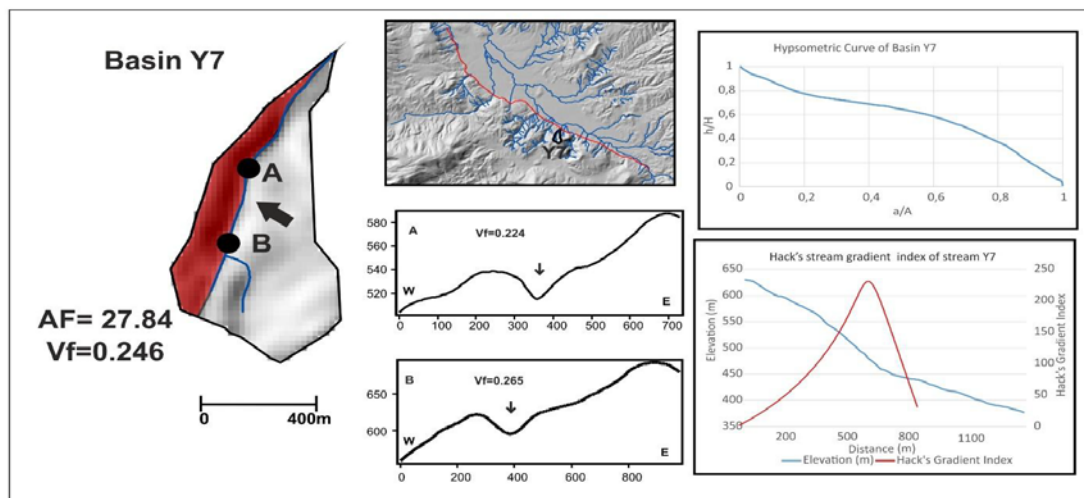


Figure 5. 19. Vf values indicate that valley is V-shaped. AF value shows asymmetry towards downstream left side of the basin. Hypsometric curve indicates that basin is young. Hack's stream gradient index implies that the fault is active.

Results

Size: Main stream channel of basin Y7 is 1.1 km long and drainage basin has an area of 0.42 km².

Asymmetry factor (AF): Downstream left side area of the basin is 0.12 km², compared to a total size of 0.42 km². AF value of the basin is 27.84% and drainage flows from the left side of the basin.

Geology: Basin is entirely composed of Phyllite.

Hypsometric curve: Hypsometric curve of the basin has ideal convex shape.

Valley floor width to height ratio: Vf value of the basin is 0.246. From bottom to top, Vf values are 0.224 and 0.265.

Hack's stream gradient index: SL along the drainage shows peak downstream where the topographic profile of the channel instantly gets steeper; at a value of 232 gradient meters.

Evaluation

Drainage flows from the downstream left side of the basin which means it shows a distinct asymmetry towards that might indicate tilting.

Hypsometric curve of the basin is typical for young basins which are influenced by tectonic uplift and are less affected from erosional processes.

Values of Valley floor width to height ratio (Vf) are low and indicating V-shaped valleys which are typical for tectonically uplifting area.

Because drainage flows in a single geologic formation, Hack's gradient index is directly linked with tectonic activity. According to Hack's gradient index the fault is active and according to Vf and shape of hypsometric curve degree of activity of the fault is high.

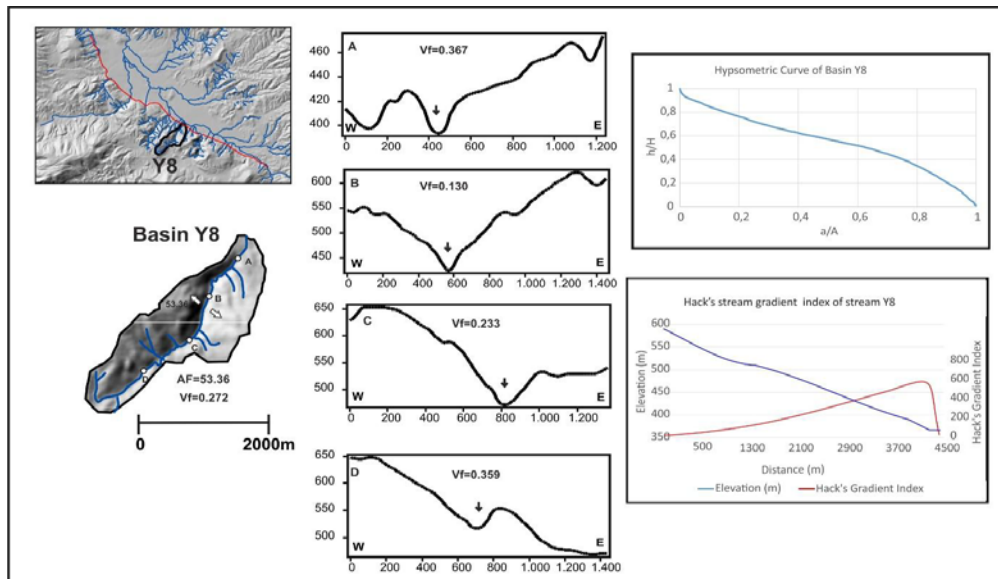


Figure 5. 20. Vf values indicate that valley is V-shaped. AF value does not show asymmetry. Hypsometric curve indicates that basin is young. Hack's stream gradient index implies that the fault is active.

Results

Size: Main stream channel of basin Y8 is km long and drainage basin has an area of 2.89 km².

Asymmetry factor (AF): Downstream left side area of the basin is 1.59 km², compared to a total size of 2.89 km². AF values of the basin is 53.36% and drainage flows almost from the middle of the basin.

Geology: Basin is entirely composed of Phyllite.

Hypsometric curve: Hypsometric curve of the basin shows convex profile.

Valley floor width to height ratio: Vf value of the basin is 0.272. From bottom to top, Vf values are 0.367, 0.130, 0.233 and 0.359.

Hack's stream gradient index: SL along the drainage shows peak downstream where the topographic profile of the channel instantly gets steeper; at a value of 500 gradient meters.

Evaluation

Drainage flows from almost the middle of the basin which means it does not show an asymmetry .

Hypsometric curve of the basin is typical for young basins which are influenced by tectonic uplift and are less affected from erosional processes.

Values of Valley floor width to height ratio (Vf) are low and indicating V-shaped valleys which are typical for tectonically uplifting area.

Because drainage flows in a single geologic formation, Hack's gradient index is directly linked with tectonic activity. According to Hack's gradient index the fault is active and according to Vf and shape of hypsometric curve degree of activity of the fault is high.

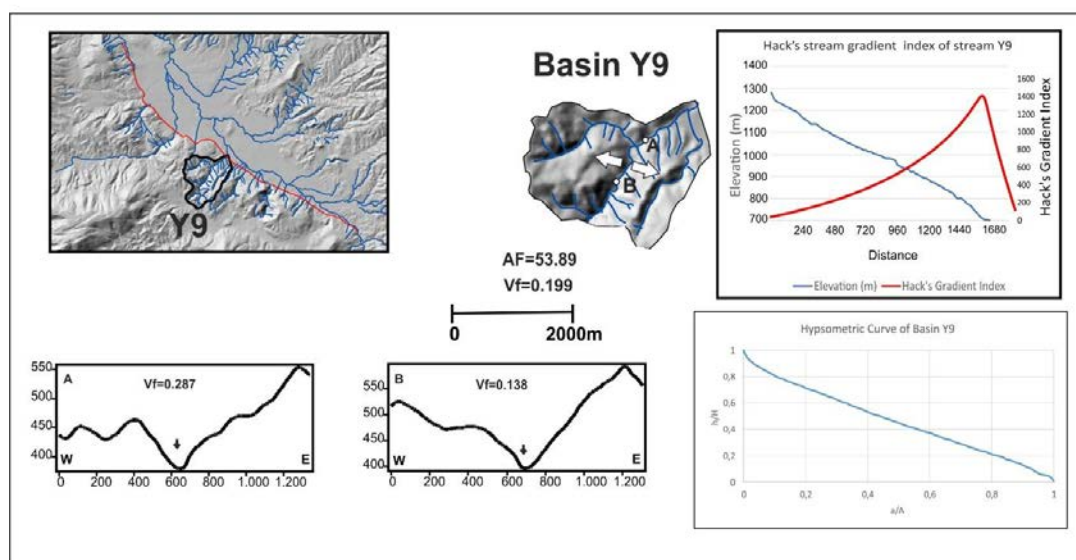


Figure 5. 21. Vf values indicate that valley is V-shaped. AF value does not show asymmetry. Hypsometric curve indicates that basin is mature. Hack's stream gradient index implies that the fault is active.

Results

Size: Main stream channel of basin Y9 is 4.25 km long and drainage basin has an area of 6.65 km².

Asymmetry factor (AF): Downstream left side area of the basin is 3.59 km², compared to a total size of 6.65 km². AF of the basin is 53.36% and drainage flows almost from the middle of the basin.

Geology: Basin is entirely composed of Phyllite.

Hypsometric curve: Hypsometric curve of the basin shows sigmoidal profile.

Valley floor width to height ratio: Vf value of the basin is 0.199. From bottom to top, Vf values are 0.287, 0.138, 0.155 and 0.216.

Hack's stream gradient index: SL along the drainage shows peak downstream where the topographic profile of the channel instantly gets steeper; at a value of 1350 gradient meters.

Evaluation

Drainage flows from almost the middle of the basin which means it does not show an asymmetry .

Hypsometric curve of the basin is typical for mature basins which are influenced by tectonic uplift and erosional processes equally.

Values of Valley floor width to height ratio (Vf) are low and indicating V-shaped valleys which are typical for tectonically uplifting area.

Because drainage flows in a single geologic formation, Hack's gradient index is directly linked with tectonic activity. According to Hack's gradient index the fault is active and according to Vf and shape of hypsometric curve degree of activity of the fault is high.

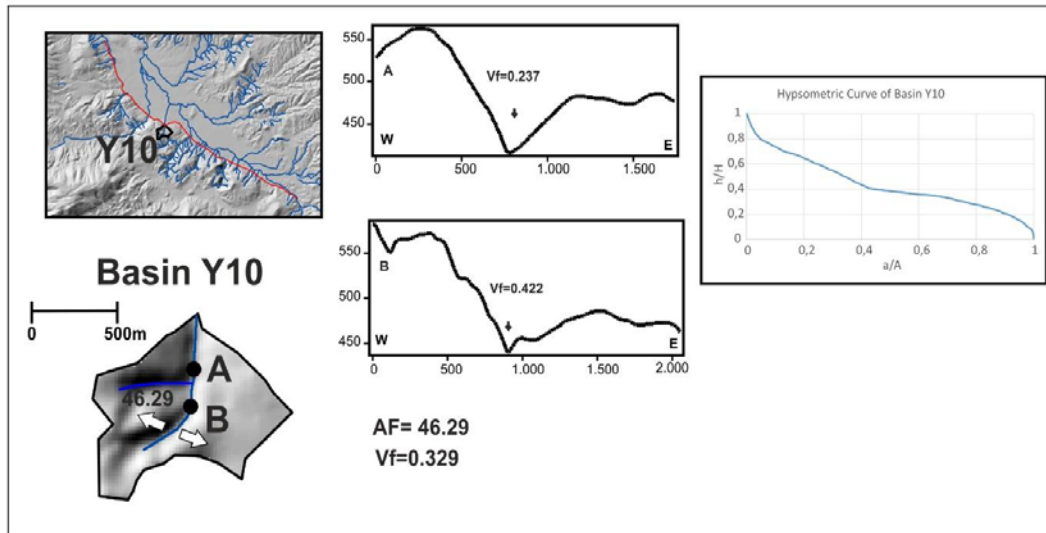


Figure 5. 22. Vf values indicate that valley is V-shaped. AF value does not show asymmetry. Hypsometric curve indicates that basin is mature.

Results

Size: Main stream channel of basin Y10 is 0.88 km long and drainage basin has an area of 0.69 km².

Asymmetry factor (AF): Downstream left side area of the basin is 0.32 km², compared to a total size of 0.69 km². AF value of the basin is 46.29% and drainage flows almost from the middle of the basin.

Geology: Basin is entirely composed of limestone.

Hypsometric curve: Hypsometric curve of the stream shows sigmoidal profile.

Valley floor width to height ratio: Vf value of the basin is 0.329. From bottom to top, Vf values are 0.237 and 0.422.

Hack's stream gradient index: Because stream flows between faults and isn't cut by them SL index cannot be applied.

Evaluation

Drainage flows from almost the middle of the basin which means it does not show an asymmetry .

Hypsometric curve of the basin is typical for mature basins which are influenced by tectonic uplift and erosional processes equally.

Values of Valley floor width to height ratio (Vf) are low and indicating V-shaped valleys which are typical for tectonically uplifting area.

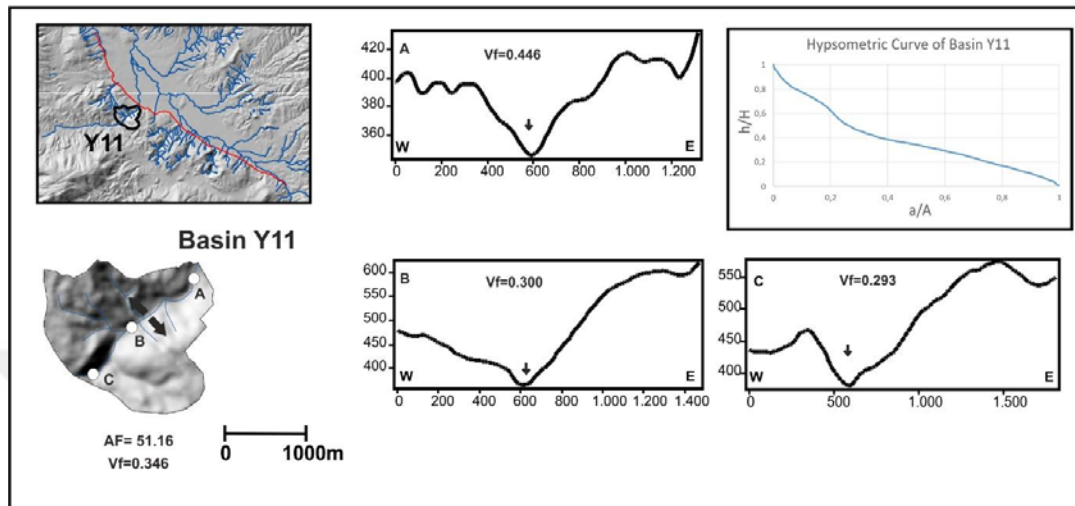


Figure 5. 23. Vf values indicate that valley is V-shaped. AF value does not show asymmetry. Hypsometric curve indicates that basin is old.

Results

Size: Main stream channel of basin Y11 is 2.15 km long and drainage basin has an area of 2.68 km².

Asymmetry factor (AF): Downstream left side area of the basin is 1.37 km², compare to a total size of 2.68 km². AF of the basin is 51.16% and drainage flows almost from the middle of the basin.

Geology: Basin is composed of limestone, Miocene clastics and phyllite.

Hypsometric curve: Hypsometric curve of the stream shows concave profile.

Valley floor width to height ratio: Vf value of the basin is 0.346. From bottom to top, Vf values are 0.446, 0.300 and 0.293.

Evaluation

Drainage flows from almost the middle of the basin which means it does not show an asymmetry.

Hypsometric curve of the basin is typical for old basins which are mostly influenced by erosional processes.

Values of Valley floor width to height ratio (Vf) are low and indicating V-shaped valleys which are typical for tectonically uplifting area.

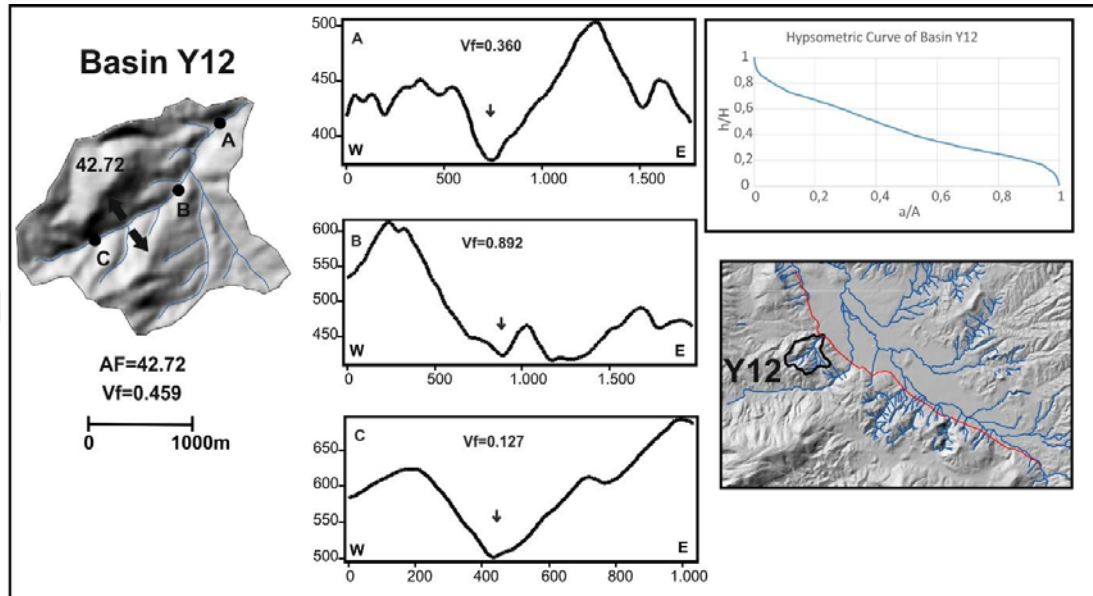


Figure 5. 24. Vf values indicate that valley is V-shaped. AF value does not show asymmetry. Hypsometric curve indicates that basin is mature.

Results

Size: Main stream channel of basin Y12 is 2.7 km long and drainage basin has an area of 4 km².

Asymmetry factor (AF): Downstream left side area of the basin is 1.7 km², compared to a total size of 4 km². AF of the basin is 42.72% and drainage flows almost from the middle of the basin.

Geology: Basin is composed of limestone, Miocene deposits and phyllite.

Hypsometric curve: Hypsometric curve of the stream shows sigmoidal profile.

Valley floor width to height ratio: Vf value of the basin is 0.459. From bottom to top, Vf values are 0.360, 0.892 and 0.127.

Evaluation

Drainage flows from almost the middle of the basin which means it does not show an asymmetry.

Hypsometric curve of the basin is typical for mature basins which are influenced by both tectonic and erosional processes in equal amount.

Values of Valley floor width to height ratio (V_f) are low and indicating V-shaped valleys which are typical for tectonically uplifting area.

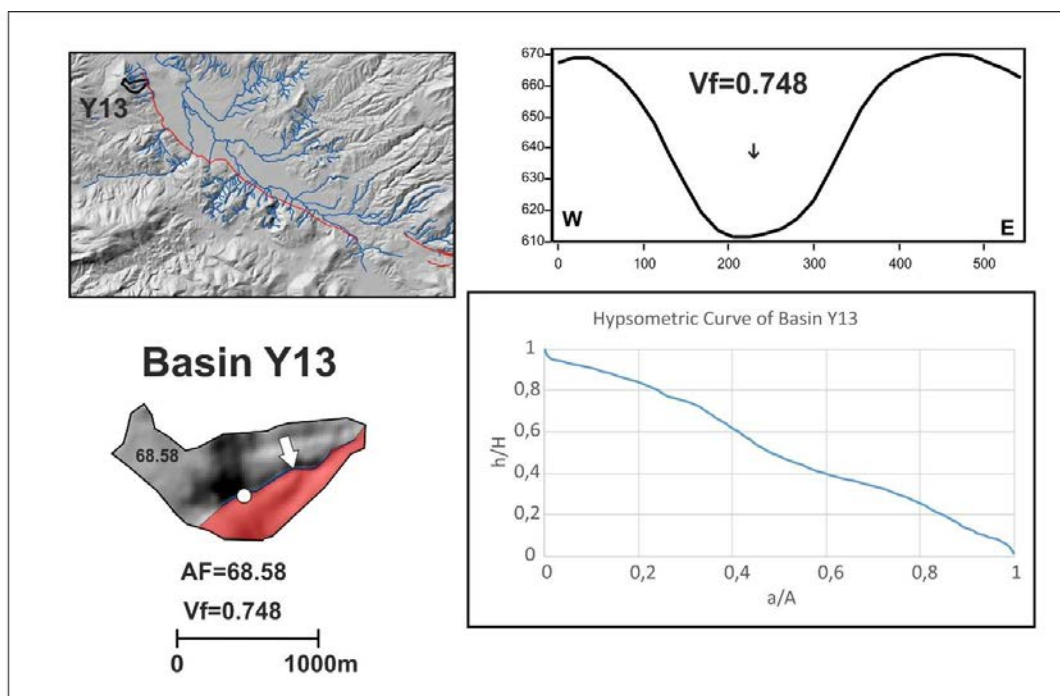


Figure 5. 25. V_f value indicate that valley is in the transition from V-shaped to U-shaped. AF value shows asymmetry towards downstream right side of the basin. Hypsometric curve indicates that basin is mature.

Results

Size: Main stream channel of basin Y11 is 1.1 km long and drainage basin has an area of 1 km².

Asymmetry factor (AF): Downstream left side area of the basin is 0.7 km², compared to a total size of 1km². AF of the basin is 68.58% and drainage flows from the right side of the basin.

Geology: Basin is composed of limestone and Miocene clastics.

Hypsometric curve: Hypsometric curve of the basin shows linear to sigmoidal profile.

Valley floor width to height ratio: Vf value of the basin is 0.748.

Evaluation

Drainage of this basin flows next to the downstream right divide of the valley and shows a distinct asymmetry towards that might indicate tilting.

Hypsometric curve of the basin is typical for mature basins which are influenced by both tectonic and erosional processes in equal amount.

Values of Valley floor width to height ratio (Vf) is moderate and indicating transition from V-shaped valley to U-shaped valley.

General evaluation of geomorphic indice results

Four indices have been used to evaluate the geomorphic reflection of tectonism for the two groups of drainage basins within the study area; Muğla drainage basins and Yatağan drainage basins. I calculated AF values to identify basin asymmetries that can be interpreted as tectonic tilting. Figure 5.26 shows the AF values for the Muğla and Yatağan regions. AF values represent the ratio of the area of the basin to the left (facing downstream) of the trunk stream, to the total area. In the Muğla region there are 4 streams with AF values > 50% and 6 values with AF values < 50%. Considering a $\pm 10\%$ zone as a symmetric basin, only 3 basins in Muğla and 6 in Yatağan region show asymmetric basins. However, the spatial distribution of asymmetric basins along the fault show no significant pattern that can be attributed to tilting. Instead adjacent basins on the same fault block show opposite asymmetry directions.

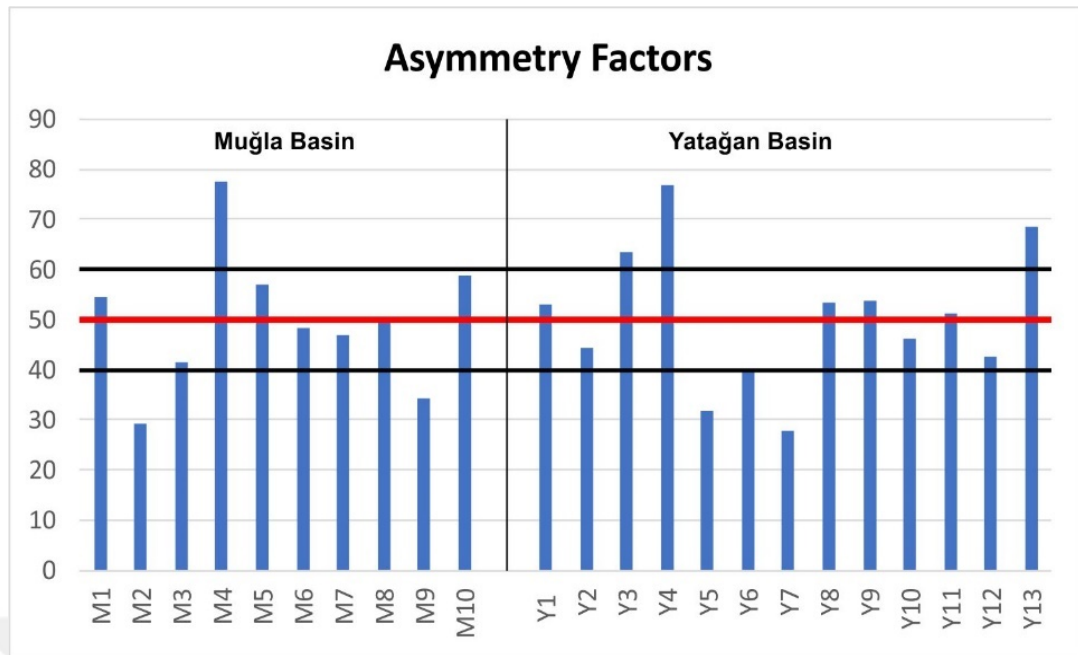


Figure 5. 26. Chart of the distribution of asymmetry factors of both Muğla and Yatağan drainage basins. Two horizontal black lines represent $\pm 10\%$ symmetry buffer. AF values exceeding this zone are considered to be asymmetric. A total of 9 basins are asymmetric.

Vf values represent whether a valley has a wide valley floor due to horizontal erosion and deposition or a narrow valley that due to a dominant vertical erosion that can be attributed to the result of tectonic uplift. In general Vf values in the study area show low Vf that indicate V-shaped valleys, particularly at sections close to the basin margin faults valleys have a very narrow floor and steep sides. At the Muğla section Vf profiles at the southern basin margin fault show values < 0.4 (Figure 5.27). However Vf values increase northwards away from the margin fault. The valleys north of the Aksivri Fault show the highest Vf values > 1 , which means that the tectonic activity decreases northward. Similar distribution is present at the Yatağan section (Fig 5.28). Vf values are minimum close to the basin margin fault, while values increase southward away from the fault. This means that sections of the drainage basin that are close to the main margin faults have a V-shaped valley profile, while the valley shapes transform into U-shaped valleys away from the fault.

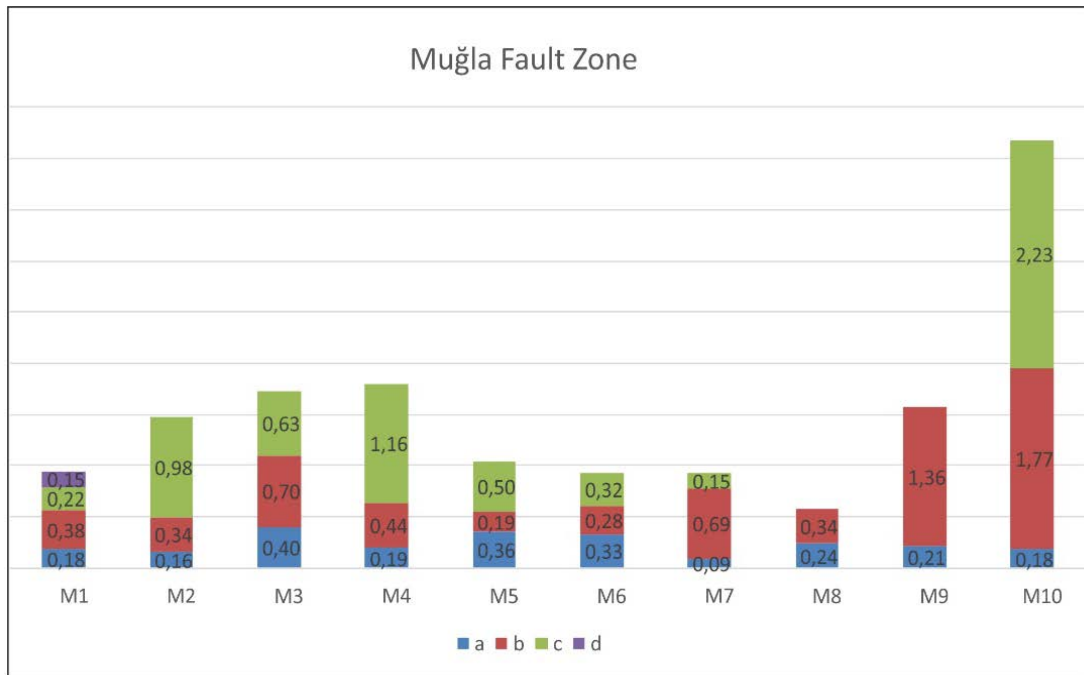


Figure 5. 27. Distribution of Vf values of the stream channel of Muğla section. In general Vf values in the study area show low Vf that indicate V-shaped valleys.

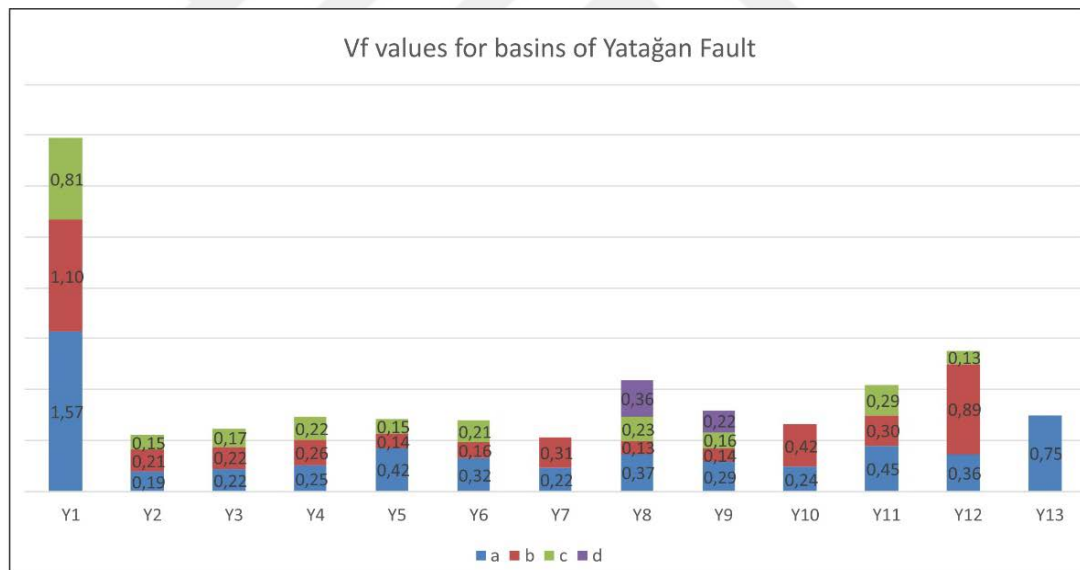


Figure 5. 28. Distribution of Vf values of the stream channel of Yatağan section. In general Vf values in the study area show low Vf that indicate V-shaped valleys.

Hypsometric curves of the basins in the region have all 3 types of profiles which are convex, sigmoidal and concave, which indicates young, mature and old basin morphologies, respectively. Convex shaped hypsometric curves are obtained for the

basins in the East of Muğla region and sigmoidal shaped curves are obtained for the basins in the West of the region (Figure 5.29). According to shapes of hypsometric curves at Mugla region it can be inferred that the basin morphologies are young to mature and are dominantly influenced by an ongoing (active) tectonic deformation. In the Yatağan region hypsometric curves are convex, sigmoidal and concave. Along the Yatağan fault, the central basins show convex hypsometric curves, pointing a young basin. The two basins at the tips of the Yatağan fault show sigmoidal to concave shape which illustrates a mature to old morphology that are less controlled by fault activity (Figure 5.30.).

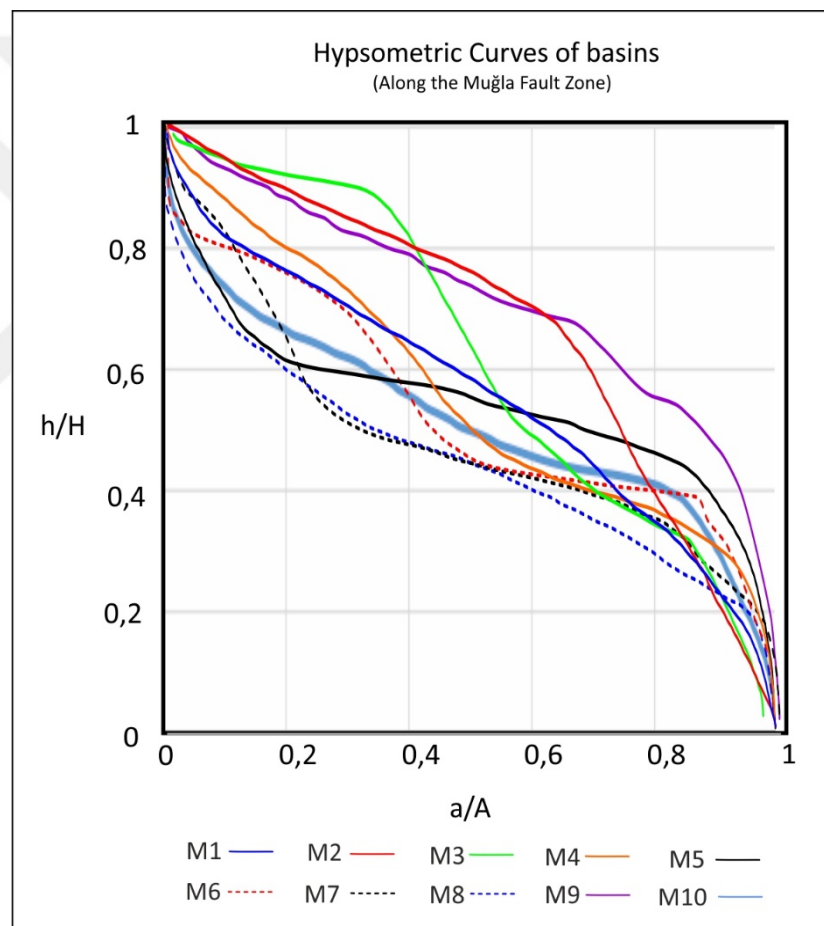


Figure 5. 29. Hypsometric curves of drainage basins in the Muğla section. Convex to sigmoidal shaped curves are observed in the drainage basins.

The Hack's index or stream length gradient index marks instant increases of slope angle along the Thalweg of the stream. In Muğla area the fault is highly segmented

because of it is branching. Hack's index analyses in the Muğla region are characterized by peaks with high magnitudes on the basin margin faults and peaks with low magnitudes on the second branch. Changes in the geological units have not affected the SL values in both areas, therefore instant increases in the SL values are directly linked with an active fault scarp. In the Yatağan region all of the peaks are above the basin margin fault except Y4. This second peak in the basin Y4 may be related with

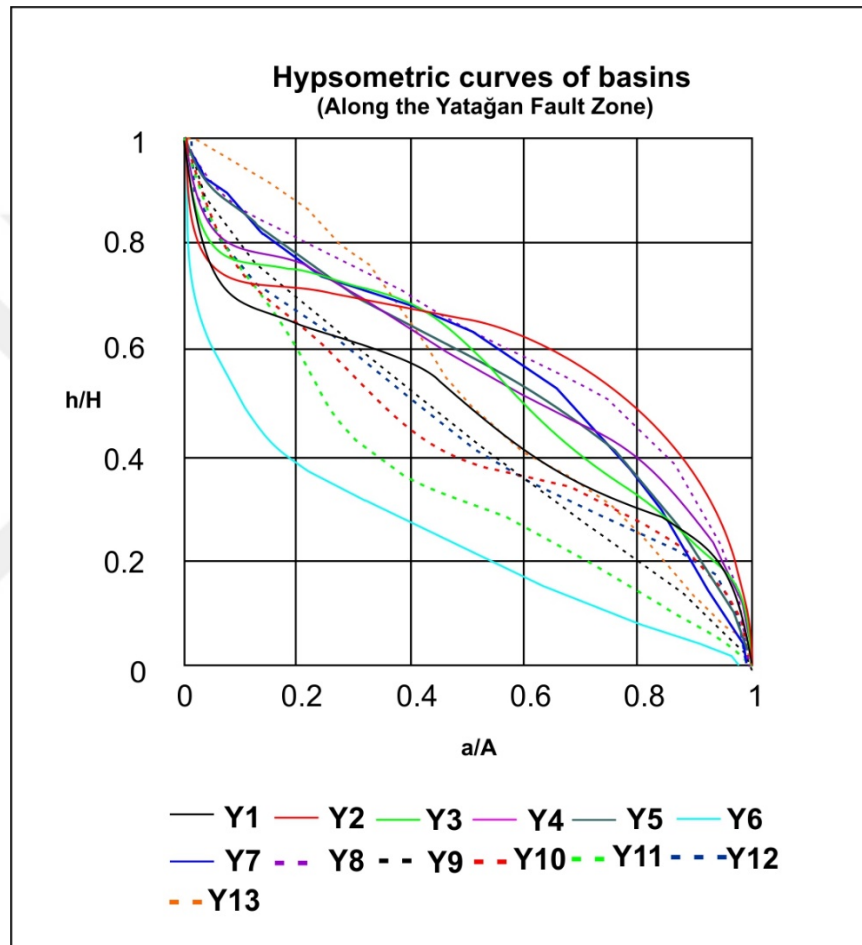


Figure 5. 30. Hypsometric curves of drainage basins in the Yatağan section. Sigmoidal to concave shaped curves are observed in the drainage basins.

another escarpment, however this finding has not been verified in the field. The SL profiles of the drainage basins of Muğla and Yatağan basins are given in the Figures 5.31 and 5.32 respectively.

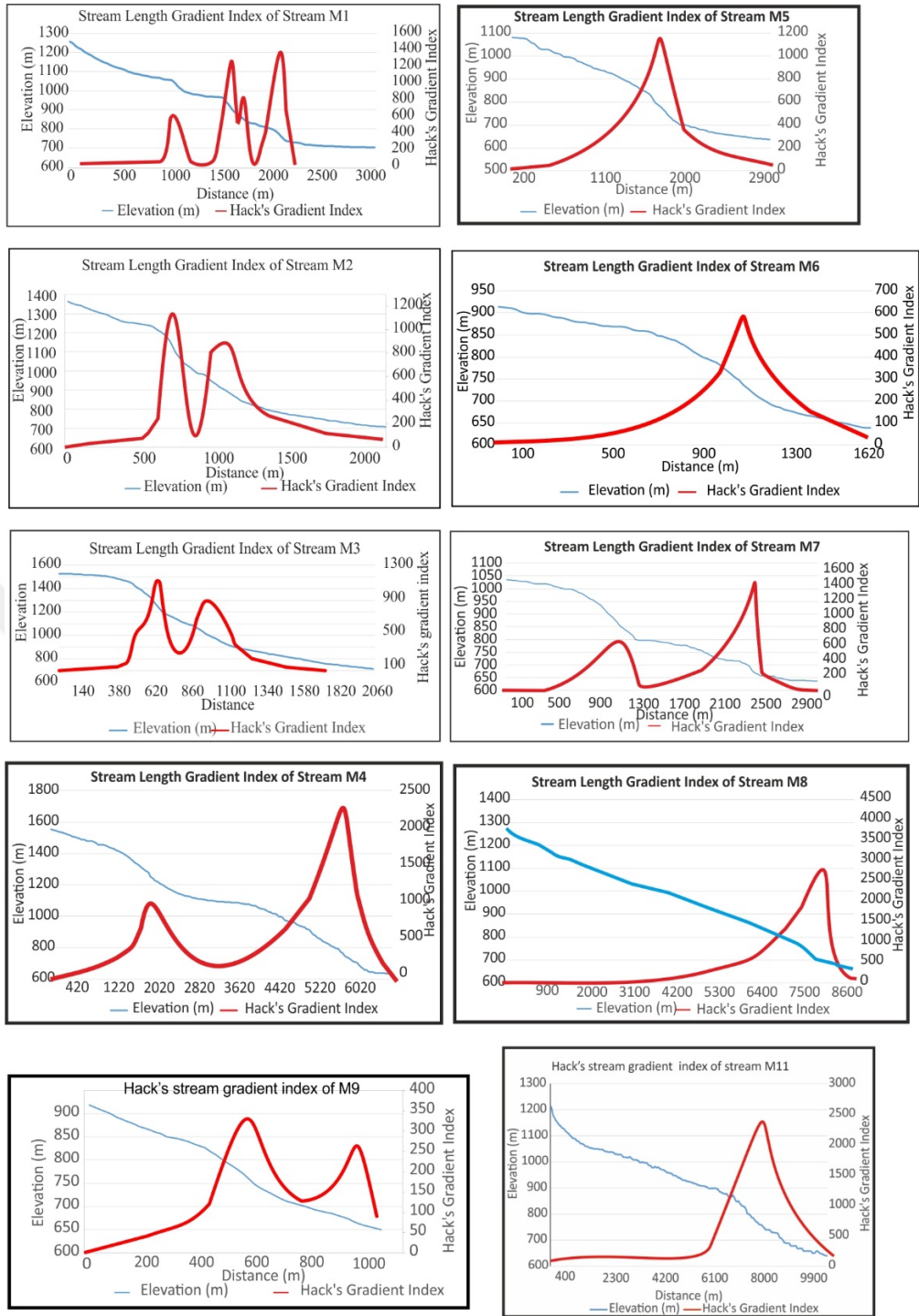


Figure 5. 31. Hack’s index analyses in the Muğla region are characterized by peaks with high magnitudes on the basin margin faults and peaks with low magnitudes on the second branch.

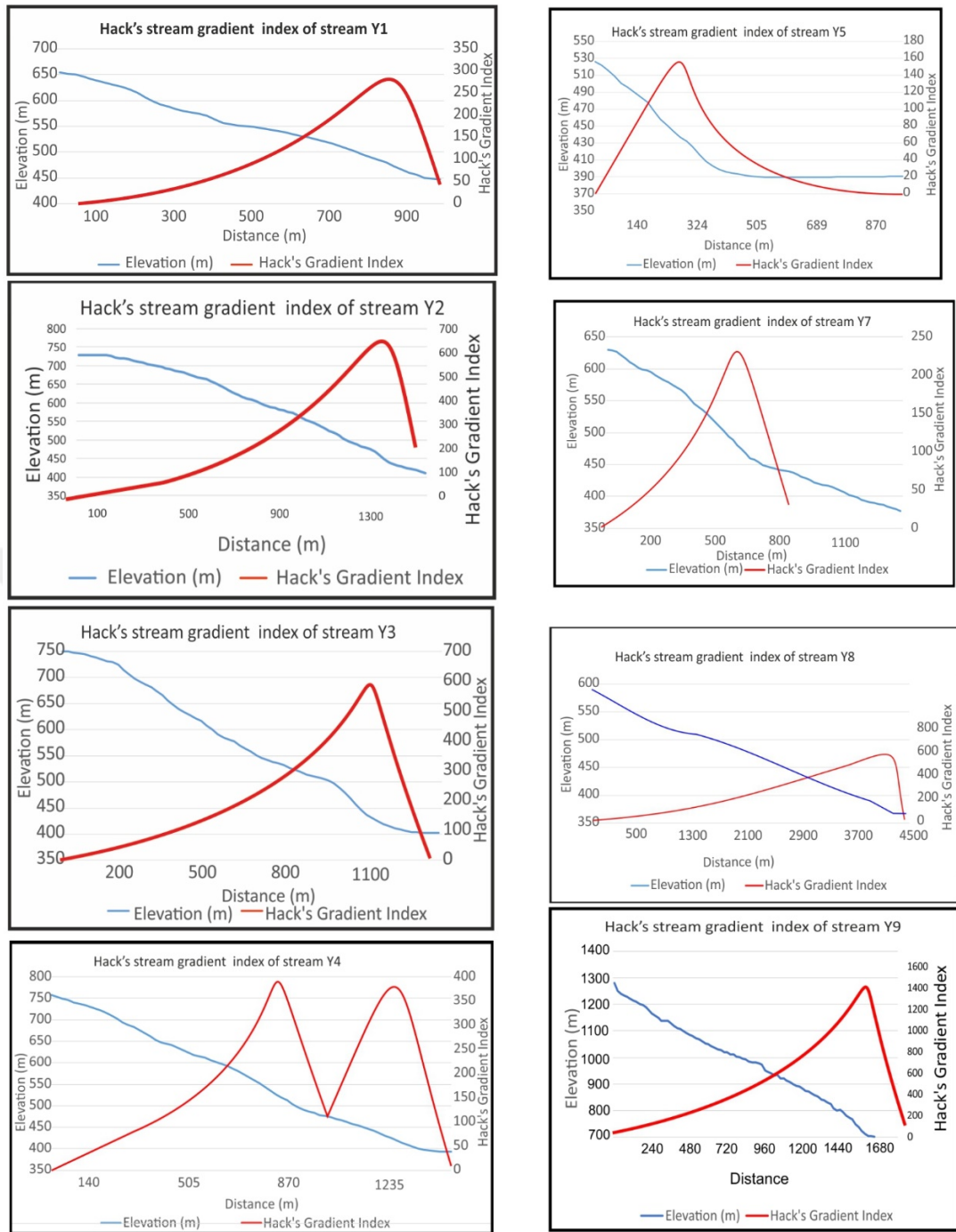


Figure 5.32. In the Yatağan region all of the peaks are above the basin margin fault except Y4. This second peak in the basin Y4 may be related with another escarpment, however this finding has not been verified in the field.

Overall, the studied indices document that the drainage basins of Muğla and Yatağan are highly influenced by the basin margin faults. The tectonic activity decreases away from the fault as has been exposed by the Vf indices and V-shaped valleyse

turn into U-shaped valleys. There is no distinct asymmetry pattern in the basins, therefore we consider there is no tectonic tilting in the area, except for the Muğla and Yatağan basins its self (half grabens). Finally the hysometric curves demonstrate that the drainage basins in both areas are relatively young and are influence by tectonic uplift.



6. CONCLUSION

The result of this thesis can be summarized as:

- 1- Muğla-Gökova region is characterized by four types of basins with different ages and orientations as NE trending Kale-Tavas Basin filled by Late Oligocene-Early Miocene deposits, NE-SW trending Eskihisar-Tınaz Basins filled by Middle Miocene deposits, NW-SE trending Yatağan basin filled by Upper Miocene-Pliocene deposits and Paşapınarı-Muğla-Yeşilyurt, Ula and Gökova basins formed by the faults and Filled by Plio-Quaternary deposits (Gürer et al., 2011). Study area comprises Yatağan, Paşapınarı and Muğla basins. Paşapınarı basin forms the lowermost part of Yatağan basin and discussed as Yatağan basin in this study.
- 2- Basement of the Muğla-Yatağan region is characterized by Menderes Massif and it is overlain by Lycian Nappes with thrust faults. Neogene deposits at the region are Turgut Formation, Sekköy Formation and Yatağan formation. Turgut Formation is conformably overlain by Sekköy Formation. Yatağan Formation unconformably overlies Sekköy Formation. Plio-Quaternary deposits are located at the top unconformably.
- 3- The seismic history marks several damaging earthquakes in the region with destructive intensities such as the AD 142 or the Bayır 1941 earthquake M:6.1. Even if not belongs to these earthquakes, geologic evidences of recent earthquake faulting have been observed at two localities within the Holocene colluviums in Menteşe and Düğerek, as back-tilting and 50 cm offset layers in Menteşe and as highly inclined layers in Düğerek. New trenches will be opened in the future studies in order to investigate the earthquake history of the region. Historical and present-day earthquake records show that moderate to large shocks are followed by an earthquake swarm, where even aftershocks

can have destructive effects. Kavakçalı earthquake swarm is the best example of earthquake swarm in present seismicity of the area.

- 4- The tectonic activity of the region is imprinted in the morphology of the area. Steep fault escarpments, iron-flats, hanging valleys, and V-shaped valleys have been documented along the Muğla and Yatağan faults. Both, the Yatağan basin and the Muğla basin show asymmetric characteristics. In Muğla, the northern margin of the basin is composed of steep high mountain fronts, while the southern margin shows a smooth topography. Similarly the southern margin of the Yatağan basin is represented with steep high escarpments and high hills, while the northern margin has a gentle topography. In both basin, rivers in the alluvium flow close the steeper margins, indicating that the basin is tilted towards the basin margin faults as expected in half grabens.
- 5- The analysis of four geomorphic indices yield results that signify the ongoing tectonic activity in the region. The low Vf values (< 0.4) mark V-shaped valleys at proximal to the faults which turn to U-shape valleys away from the fault. Hypsometric curves point moderate to young drainage basins that are influenced by tectonic processes. The peaks in the SL indices are directly linked with active fault escarpments observed in the field because drainages flow in a single geological formation. AF analysis yield no specific pattern of tectonic tilting in the area.
- 6- Our mapping showed that the Muğla fault is approximately 30 km long and consist of several sub-segments and branches. The Yatağan fault is 25 km long and consist also of sub-segments. Using the seismic moment and moment magnitude scale of Hanks and Kanamori (1979) we calculate that the Muğla-Yatağan region prone to earthquakes M 5.7 to 6.6 assuming 6 km fault width, 25-55 km fault length and 10-80 cm average displacement.

REFERENCES

- Akbay, S. (2011) *Geology and petrography of rocks cropping out northeast of Ula district (Muğla)*, Undergraduate thesis, Muğla Sıtkı Koçman University, Muğla.
- Aksoy, M. E. (2009) *Active tectonics and paleoseismology of the Ganos fault segment and seismic characteristics of the 9 August 1912 Mürefte Earthquake of the North Anatolian Fault (Western Turkey)*, phd thesis, University of Strasbourg & İstanbul Technical University.
- Aktimur, H., Sarıaslan, M., Sönmez, M., Keçer, M., Uysal, Ş. and Özmutaf, M. (1996) *Land use potential of Muğla city (central town)*, MTA Report.
- Alçıçek, H. (2010) *Stratigraphic correlation of the Neogene basins in southwestern Anatolia: regional palaeogeographical, palaeoclimatic and tectonic implications*, Palaeogeography, Palaeoclimatology, Palaeoecology 291(3): 297-318.
- Anderson, E. M. (1942) *The Dynamics of Faulting and Dyke Formation with Application to Britain*. Edinburgh: Oliver and Boyd.
- Atalay, Z. (1980) *Stratigraphy of continental Neogene in the region of Muğla-Yatağan, Turkey*, Bull. Geol. Soc. Turkey 23: 93-99.
- Barka, A. (1992) *The north Anatolian fault zone*, Annales tectonicae, 6:164-195.
- Barka, A., Altunel, E., Akyüz, S., Şaroğlu, F., Emre, Ö. and Kuşçu, İ. (1996) *Güneybatı Anadolu'nun aktif fayları ve kireçtaşı fay şevlerinin incelenmesi (Investigations of active faults and limestone scarps in SW Anatolia)*, Ankara (In Turkish).
- Barka, A., Altunel, E., Akyüz, S., Şaroğlu, F., Emre, Ö. and Kuşçu, İ. (1996) *Gökova ve Saroz Körfezi çevresindeki aktif fayların deprem aktivitelerinin jeolojik. Jeomorfolojik ve paleosismolojik yöntemlerle belirlenmesi ve 1995 Dinar depremi*, YDABÇAG 237-G TÜBİTAK Project (In Turkish), Ankara, 102p.

- Barka A.A. and Reilinger R., (1997) *Active tectonics of the Mediterranean region: deduced from GPS, neotectonic and seismicity data*, *Annali di Geophys.* XI:587-610.
- Barut, İ. F. and Gürpınar, O. (2005) *An approach to the hydrogeological circulation model of the salty karstic springs in the Milas (Muğla) Basin*. 18:1-22.
- Becker-Platen, J. D. (1970) *Lithostratigraphische Untersuchungen im Känozoikum-Südwest-Anatoliens (Türkei)*. - (Känozoikum und Braunkohlen der Türkei. 2.), *Beih. Geol. Jb.*, 97, 244 s.
- Bozkurt, E. (2001) *Neotectonics of Turkey—a synthesis*, *Geodinamica acta* 14(1-3): 3-30.
- Bozkurt, E. & Rojay, B. (2005), *Episodic, two-stage Neogene extension and short-term intervening compression in Western Turkey: field evidence from the Kiraz Basin and Bozdağ Horst*, *Geodinamica acta*, 18: 3-4, 299-316, DOI: 10.3166/ga.18.299-316.
- Collins, A. S. and Robertson, A. H. (1997) *Lycian melange, southwestern Turkey: an emplaced Late Cretaceous accretionary complex*, *Geology* 25(3): 255-258.
- Collins, A. S. and Robertson, A. H. (1998) *Processes of Late Cretaceous to Late Miocene episodic thrust-sheet translation in the Lycian Taurides, SW Turkey*, *Journal of the Geological Society* 155(5): 759-772.
- Collins, A. S. and Robertson, A. H. (1999) *Evolution of the Lycian Allochthon, western Turkey, as a north-facing Late Palaeozoic to Mesozoic rift and passive continental margin*, *Geological Journal* 34(12): 107-138.
- dePolo, C. M., Clark, D. G., Slemmons, D. B., and Aymand, W. H. (1989). *Historical Basin and Range Province surface faulting and fault segmentation*. In *Fault Segmentation and Controls of Rupture Initiation and Termination* (D. P. Schwartz, and R. H. Sibson, Eds.), U.S. Geol. Surv. Open File Rep. 89–315, pp. 131–162.
- dePolo, C. M., Clark, D. G., Slemmons, D. B., and Ramelli, A. R. (1991). *Historical surface faulting in the Basin and Range Province, western North America—Implications for fault segmentation*. *J. Struct. Geol.* 13, 123–136.

- Doglioni, C., Carminati, E., Petricca, P. and Riguzzi, F. (2015) *Normal fault earthquakes or graviquakes*, Sci. Rep. 5, 12110; doi: 10.1038/srep12110
- Duman, T. Y., Emre, Ö., Özalp, S. and Elmacı, H. (2011) 1:250.000 scale active fault map series of Turkey, Aydın (NJ 35–11) Quadrangle, General Directorate of Mineral Research and Exploration, Ankara, Ankara-Turkey, Serial Number: 7.
- Ersoy, E., Çemen, İ., Helvacı, C. and Billor, Z. (2014) *Tectono-stratigraphy of the Neogene basins in Western Turkey: Implications for tectonic evolution of the Aegean Extended Region*, Tectonophysics 635: 33-58.
- Eyidoğan, H., Akıncı, A., Gündoğdu, O., Polat, O. and Kaypak, B. (1996) *Gökova Havzasının güncel depremselliğinin incelenmesi (Investigation of recent seismicity of Gökova Basin)*, Ankara.
- Fidolini, F., Ghinassi, M., Aldinucci, M., Billi, P., Boaga, J., Deiana, R. and Brivio, L. (2013) *Fault-sourced alluvial fans and their interaction with axial fluvial drainage: An example from the Plio-Pleistocene Upper Valdarno Basin (Tuscany, Italy)*, Sedimentary Geology 289: 19-39.
- Folk, L. (1974) *Petrology of Sedimentary Rocks*, The Walter Geology Library - The University of Texas at Austin: Austin, US (TX)
- Goldsworthy, M. and Jackson, J. (2000) *Active normal fault evolution in Greece revealed by geomorphology and drainage patterns*, Journal of the Geological Society 157(5): 967-981.
- Görür, N., Şengör, A.M.C., Sakıncı, M. et. al. (1995) *Rift formation in the Gökova region, southwest Anatolia: implications for the opening of the Aegean Sea*. Geological Magazine. 132:637-650.
- Gül, M. (2015) *Lithological properties and environmental importance of the Quaternary colluviums (Muğla, SW Turkey)*, Environmental Earth Sciences 74(5): 4089-4108.

- Gül, M., Karacan, E. and Aksoy, M. E. (2013) *Muğla kenti yerleşim alanı ve yakın çevresinin Genel Jeolojik ve mühendislik jeolojisi özelliklerinin araştırılması (An investigation of general geologic and engineering geological properties of Muğla and surroundings)*, Muğla Sıtkı Koçman University, Research Fund Project, BAP 12-54: 28 (Unpublished, in Turkish).
- Gürer, F. Ö. and Yılmaz, Y. (2002) *Geology of the Ören and surrounding areas, SW Anatolia*, Turkish Journal of Earth Sciences, Vol 11, pp 1-13.
- Gürer, Ö. F., Özburun, M., Sangu, E. and Gürbüz, A. Y. (2011) *Muğla Yatağan Havzası ve Çevresinin Neotektonik İncelenmesi (Neotectonic investigation of the Muğla-Yatağan Basins and surrounding area)*, Ankara, TUBITAK (108Y277) Project Report
- Gürer, Ö. F., Sanğu, E., Özburan, M., Gürbüz, A. and Filoreau, N. S. (2013) *Complex basin evolution in the Gökova Gulf Region: implications on the Late Cenozoic tectonics of southwest Turkey*, International Journal of Earth Sciences, 102:2199-2221, DOI 10.1007/s00531-013-0909-1.
- Işık, V., Uysal, I. T., Caglayan, A. and Seyitoglu, G. (2014) *The evolution of intraplate fault systems in central Turkey: Structural evidence and Ar-Ar and Rb-Sr age constraints for the Savcili Fault Zone*, Tectonics 33(10): 1875-1899.
- Kahraman, B., Dirik, K., Özsayın, E. and Kutluay, A. (2011) *Tectonics of the Yatağan - Eskişehir Basin, western Anatolia, Turkey, 64th Geological Congress of Turkey*, Abstract Book, p. 4.
- Kalafat, D. (2016) *statistical evaluation of Turkey earthquake data (1900-2015): A case study*, 2:14-36.
- Kanamori, H. (1977) *The energy release in great earthquakes*, Journal of geophysical research 82(20): 2981-2987.
- Karabacak, V. (2015) *Seismic damage in the Lagina sacred area on the Muğla Fault: a key point for the understanding of the obliquely situated faults of western Anatolia*, Journal of Seismology 20(1): 277-289.

- Kaya, T. T., Mayda, S., Kostopoulos, D. S., Alcicek, M. C., Merceron, G., Tan, A., Karakutuk, S., Giesler, A. K. and Scott, R. S. (2012) *Şerefköy-2, a new late Miocene mammal locality from the Yatağan Formation, Muğla, SW Turkey*, *Comptes Rendus Palevol* 11(1): 5-12.
- Kayan, İ. (1979) *Geomorphology of Muğla-Yatağan Neogene basins*, TUBITAK, Temel bilimler araştırma grubu TBAG-189 no Project, Ankara: 272.
- Keller, E. A. and Pinter, N. (1996) *Active tectonics: earthquakes, uplift and landscape*, Prentice Hall Upper Seddle River, NJ, USA,
- Keller, E. A. and Pinter, N. (2002) *Active tectonics: earthquakes, uplift and landscape*, Prentice Hall Upper Seddle River, NJ, USA, 362p.
- McCalpin, J. (2009) *Paleoseismology*, Academic Press, San Diego
- McKenzie, D. (1978) *Active tectonics of the Alpine—Himalayan belt: the Aegean Sea and surrounding regions*, *Geophysical Journal International* 55(1): 217-254.
- Meghraoui, M. and Crone, A. J. (2001) *Earthquakes and their preservation in the geological record*, *Journal of Seismology* 5(3): 281-285.
- Okay, A. I. (2008) *Geology of Turkey: a synopsis*, *Anschnitt* 21: 19-42.
- Okay, A. I. and Tüysüz, O. (1999) *Tethyan sutures of northern Turkey*, *Geological Society, London, Special Publications* 156(1): 475-515.
- Oral M.B., Reilinger R. E., Toksoz M., Kong R.W., Barka A.A., Kınık İ. and Lenk, O., (1995) *Global positioning system offers evidence of plate motions in eastern Mediterranean*, *EOS Transac.* 76 (9).
- Özkaymak, Ç. (2014) *Tectonic analysis of the Honaz Fault (western Anatolia) using geomorphic indices and the regional implications*, *Geodinamica Acta* 27(2-3): 110-129.
- Özkaymak, Ç. and Sözbilir, H. (2012) *Tectonic geomorphology of the Spildağı high ranges, western Anatolia*, *Geomorphology* 173: 128-140.

- Peacock, D., Knipe, R. and Sanderson, D. (2000) *Glossary of normal faults*, Journal of Structural Geology 22(3): 291-305.
- Reid, H. F. and Commission, S. E. I. (1910) *The California earthquake of April 18, 1906*, Report of the State Earthquake Investigation Commission. 2. The mechanics of the earthquake, Carnegie Inst. of Washington.
- Robertson, A.H.F (2000) Mesozoic-Tertiary tectonic-sedimentary evolution of a south Tethyan oceanic basin and its margins in southern Turkey. In: Bozkurt, E., Winchester, J.A. and Piper, J.D.A. (eds) *Tectonics and Magmatism in Turkey and the Surrounding Area*. Geological Society, London, Special Publications 173, 353- 384.
- Schorlemmer, D., Wiemer, S. and Wyss, M. (2005) *Variations in earthquake-size distribution across different stress regimes*, Nature, 437(7058): 539-542.
- Schuiling, R. (1962) *On petrology, age and structure of the Menderes migmatite complex (SW-Turkey)*, Bulletin of the Mineral Research and Exploration Institute of Turkey 58: 71-84.
- Schwartz, D. and Sibson, R. (1989) *Fault Segmentation and Controls of Rupture Initiation and Termination*, Proc. of Conf. XLV.
- Seyitođlu, G. and Scott, B. (1991) *Late Cenozoic crustal extension and basin formation in west Turkey*, Geological Magazine 128(02): 155-166.
- Seyitođlu, G., Scott, B. and Rundle, C. (1992) *Timing of Cenozoic extensional tectonics in west Turkey*, Journal of the Geological Society 149(4): 533-538.
- Slemmons, D. B. and Depolo, C. M. (1986) *Evaluation of active faulting and associated hazards*, Active Tectonics: 45-62.
- Şarođlu, F., Emre, Ö. and Boray, A. (1987) *Türkiye'nin diri fayları ve deprensellikleri (In Turkish)*, MTA Report (8174): 394.
- Şenel, M. (2007) Characteristic features of the Lycian Nappes and their evolution, *Turkish Geological Congress, 2007, İzmir*.

- Şengör, A., Görür, N. and Şaroğlu, F. (1985) *Strike-slip faulting and related basin formation in zones of tectonic escape: Turkey as a case study.*
- Şengör, A. and Kidd, W. (1979) *Post-collisional tectonics of the Turkish-Iranian plateau and a comparison with Tibet*, Tectonophysics 55(3): 361-376.
- Tan, O., Tapırdamaz, C., and Yörük, A. (2008) *The Earthquake Catalogues for Turkey* Turkish Journal of Earth Sciences 17: 405-418.
- Van Hinsbergen, D. J., Dekkers, M. J., Bozkurt, E. and Koopman, M. (2010) *Exhumation with a twist: paleomagnetic constraints on the evolution of the Menderes metamorphic core complex, western Turkey*, Tectonics 29(3).
- Wiemer, S., Baer M. (2000) *Mapping and removing quarry blast events from seismicity catalogs.*, Bull. Seism. Soc. Am. 90(2), p.525-530.
- Wells, D. L. and Coppersmith, K. J. (1994) *New empirical relationships among magnitude, rupture length, rupture width, rupture area, and surface displacement*, Bulletin of the seismological Society of America 84(4): 974-1002.
- Wheeler, R. L. (1989). Persistent segment boundaries on basin-range normal faults. In Fault Segmentation and Controls of Rupture Initiation and Termination (D. P. Schwartz, and R. H. Sibson, Eds.), U.S. Geol. Surv. Open File Rep. 89–315, pp. 432–444.
- Wyss, M. (1979) *Earthquake Prediction and Seismicity Pattern, Contributions to Current Research in Geophysics*, Birkhauser, Basel, 238.
- Yıldırım, C. (2014) *Relative tectonic activity assessment of the Tuz Gölü fault zone; Central Anatolia, Turkey*, Tectonophysics 630: 183-192.
- Yilmaz, Y. (1993) *New evidence and model on the evolution of the southeast Anatolian orogen*, Geological Society of America Bulletin 105(2): 251-271.

Yılmaz Y, Genç, S. C., Gürer, Ö. F., Bozcu, M., Yılmaz, K., Karacık, Z., Altunkaynak, S. and Elmas, A. (2000) When did the western Anatolian grabens begin to develop? In: Bozkurt, E., Winchester, J.A., Piper JDA (eds) *Tectonics and Magmatism in Turkey and the Surrounding Area*. Geological Society of London, Special Publication, 173:353–384.

Yılmaz, Y. and Polat, A. (1998) *Geology and evolution of the Thrace volcanics, Turkey*, *Acta Volcanologica* 10, 293-303.

Zhang, P., Mao, F. and Slemmons, D. (1999) *Rupture terminations and size of segment boundaries from historical earthquake ruptures in the Basin and Range Province*, *Tectonophysics* 308(1): 37-52.



CIRRICULUM VITAE

Name Surname : ORKUN TÜRE
Birth Date : 12.12.1989
Title : Research Assistant
Phone : 05536106256
E-mail : orkunture@mu.edu.tr

Education

Degree	University	Department	Year
Bachelor's Degree	Muğla Sıtkı Koçman University	<u>Geological Engineering</u>	2013
Master of Science	Muğla Sıtkı Koçman University	<u>Geological Engineering</u>	2013 -

Language

- English ÜDS (73.75)

Publications

International congress, symposium, etc.

- Türe, O., Ersen, M. A. (2016) *Tectonic geomorphology of Muğla-Yatağan fault* TURQUA. Avrasya Yer Bilimleri Enstitüsü. 9-11 Mayıs 2016.
- Türe, O., Aksoy, M. E. (2016) *Muğla fayı ve Yatağan fayının Kuvaterner aktivitesinin arazi gözlemleri ve jeomorfolojik indislerle yorumlanması: Muğla/Türkiye*. 20. Aktif Tektonik Araştırma Grubu Çalıştayı (ATAG 20) Pamukkale Üniversitesi.

- Ersen M. A, Yıldırım C., Türe, O., Yılmaz, Ö., Doksanaltı E. M., Şahin, S., Sarıkaya M. A., Akkaya, G. (2016) *Datça-Knidos fayında paleosismolojik bulgular*, 20. Aktif Tektonik Araştırma Grubu Çalıştayı (ATAG 20) Pamukkale Üniversitesi.
- Ersen M. A, Yıldırım C., Türe, O., Yılmaz, Ö., Akkaya, G., Doksanaltı E. M., Şahin, S., Sarıkaya M. A. (2016) *Datça-Knidos fayı paleosismolojisi üzerine ön bulgular*, Türkiye Kuvaterner Sempozyumu. Avrasya Yer Bilimleri Enstitüsü. 9-11 Mayıs 2016.
- Avşar, Ö., Uslular, G., Türe, O., (2015) *Web-based Computer Application for Assessment of Hydrogeochemistry Data of Geothermal Sites of Turkey: Muğla (SW Turkey) Example*, Proceedings World Geothermal Congress 2015 Melbourne, Australia, 19-25 April 2015.
- Avşar, Ö., Avşar, U., Arslan, Ş., Kurtuluş, B., Türe, O., Güleç, N. (2014) *Discovery of a subaqueous hot spring by a new method in Fethiye-Göcek Bay, (SW Turkey)* 8. International Symposium of Eastern Mediterranean Geology: Muğla Sıtkı Koçman Üniversitesi/Türkiye. 13-17 Ekim 2014.
- Avşar, Ö., Türe, O., (2014) *Water chemistry of hot waters of Umut geothermal field (SW Turkey)*, European Geoscience Union 2014, 27 Nisan-2 May 2014, Viyana. – 2014.

Awards

- ATAG 20. Best paper